# Topological analysis of visual and auditory perception


Yifei Zhu

Southern University of Science and Technology

2026.5.15

## Motivation: topology of population activity in visual cortex

In collaboration with mathematicians working in the emerging field of topological data analysis (TDA), Ringach and colleagues gave a topological characterization of population activity in primary visual cortex (V1).

*Singh et al., Topological analysis of population activity in visual cortex,* ***Journal of Vision*** *2008.*

## Motivation: topology of population activity in visual cortex

In collaboration with mathematicians working in the emerging field of topological data analysis (TDA), Ringach and colleagues gave a topological characterization of population activity in primary visual cortex (V1).

*Singh et al., Topological analysis of population activity in visual cortex,* ***Journal of Vision*** *2008.*

**Basic question.** How sensory input and ongoing cortical activity combine to generate a response to a given stimulus?

## Motivation: topology of population activity in visual cortex

In collaboration with mathematicians working in the emerging field of topological data analysis (TDA), Ringach and colleagues gave a topological characterization of population activity in primary visual cortex (V1).

*Singh et al., Topological analysis of population activity in visual cortex,* ***Journal of Vision*** *2008.*

**Basic question.** How sensory input and ongoing cortical activity combine to generate a response to a given stimulus?

**Key hypothesis.** Natural signals shape the architecture and dynamics of V1.

## Motivation: topology of population activity in visual cortex

In collaboration with mathematicians working in the emerging field of topological data analysis (TDA), Ringach and colleagues gave a topological characterization of population activity in primary visual cortex (V1).

*Singh et al., Topological analysis of population activity in visual cortex,* ***Journal of Vision*** *2008.*

**Basic question.** How sensory input and ongoing cortical activity combine to generate a response to a given stimulus?

**Key hypothesis.** Natural signals shape the architecture and dynamics of V1.

**Computational model.** A relatively weak input effectively serves to push the patterns of activity around in a low-dimensional manifold.

## Motivation: topology of population activity in visual cortex

In collaboration with mathematicians working in the emerging field of topological data analysis (TDA), Ringach and colleagues gave a topological characterization of population activity in primary visual cortex (V1).

*Singh et al., Topological analysis of population activity in visual cortex,* ***Journal of Vision*** *2008.*

**Basic question.** How sensory input and ongoing cortical activity combine to generate a response to a given stimulus?

**Key hypothesis.** Natural signals shape the architecture and dynamics of V1.

**Computational model.** A relatively weak input effectively serves to push the patterns of activity around in a low-dimensional manifold. It is possible that the structure of this manifold is linked to the structure of the signals one naturally encounters in the environment.

## Motivation: topology of population activity in visual cortex

In collaboration with mathematicians working in the emerging field of topological data analysis (TDA), Ringach and colleagues gave a topological characterization of population activity in primary visual cortex (V1).

*Singh et al., Topological analysis of population activity in visual cortex,* ***Journal of Vision*** *2008.*

**Basic question.** How sensory input and ongoing cortical activity combine to generate a response to a given stimulus?

**Key hypothesis.** Natural signals shape the architecture and dynamics of V1.

**Computational model.** A relatively weak input effectively serves to push the patterns of activity around in a low-dimensional manifold. It is possible that the structure of this manifold is linked to the structure of the signals one naturally encounters in the environment.

*Carlsson, Ishkhanov, de Silva, & Zomorodian, On the local behavior of spaces of natural images,* ***International Journal of Computer Vision*** *2008.*

## Motivation: topology of population activity in visual cortex

In collaboration with mathematicians working in the emerging field of topological data analysis (TDA), Ringach and colleagues gave a topological characterization of population activity in primary visual cortex (V1).

*Singh et al., Topological analysis of population activity in visual cortex,* ***Journal of Vision*** *2008.*

**Basic question.** How sensory input and ongoing cortical activity combine to generate a response to a given stimulus?

**Key hypothesis.** Natural signals shape the architecture and dynamics of V1.

**Computational model.** A relatively weak input effectively serves to push the patterns of activity around in a low-dimensional manifold. It is possible that the structure of this manifold is linked to the structure of the signals one naturally encounters in the environment.

*Carlsson, Ishkhanov, de Silva, & Zomorodian, On the local behavior of spaces of natural images,* ***International Journal of Computer Vision*** *2008.*

## Motivation: topology of population activity in visual cortex

In collaboration with mathematicians working in the emerging field of topological data analysis (TDA), Ringach and colleagues gave a topological characterization of population activity in primary visual cortex (V1).

*Singh et al., Topological analysis of population activity in visual cortex,* ***Journal of Vision*** *2008.*

**Basic question.** How sensory input and ongoing cortical activity combine to generate a response to a given stimulus?

**Key hypothesis.** Natural signals shape the architecture and dynamics of V1.

**Computational model.** A relatively weak input effectively serves to push the patterns of activity around in a low-dimensional manifold. It is possible that the structure of this manifold is linked to the structure of the signals one naturally encounters in the environment.

*Carlsson, Ishkhanov, de Silva, & Zomorodian, On the local behavior of spaces of natural images,* ***International Journal of Computer Vision*** *2008.*

We will see analogues of such links in machine learning of visual signals.

## Motivation: topology of population activity in visual cortex

How to experimentally and computationally detect topological structure in the architecture and dynamics of V1?

# Motivation: topology of population activity in visual cortex

How to experimentally and computationally detect topological structure in the architecture and dynamics of V1?

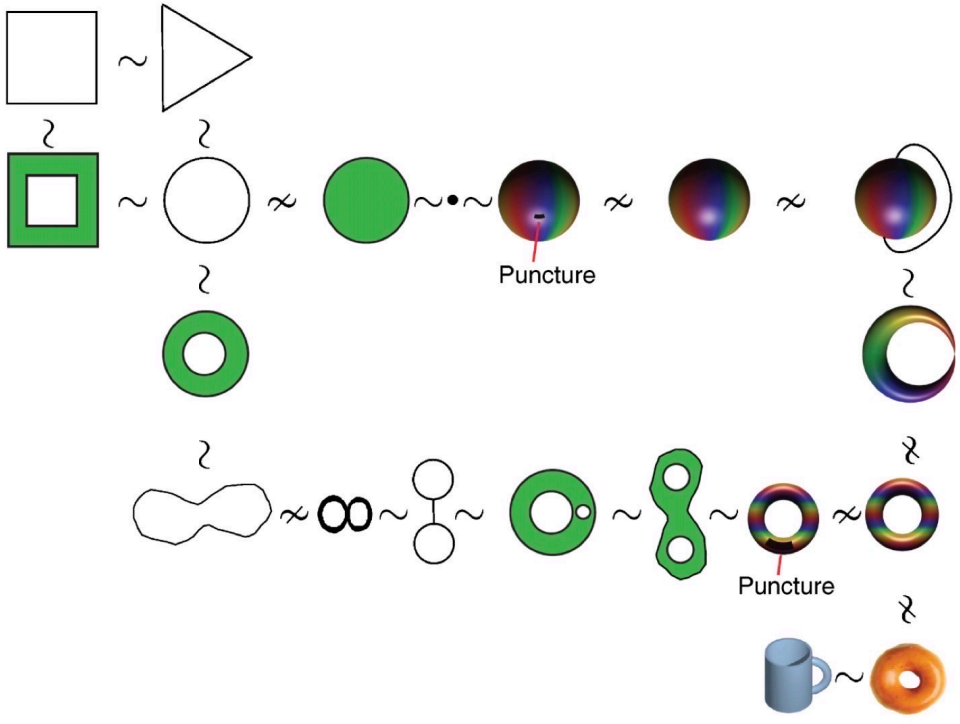


Figure 1. Topological equivalence in rubber-world. The figure illustrates the notion of equivalence by showing several objects (topological spaces) connected by the symbols $\sim$ when they are equivalent or by $\nsim$ when they are not. The reader should think that all the objects shown are made of an elastic material and visualize the equivalence of two spaces by imagining a deformation between to objects.

*From Singh et al., 2008.*

## Motivation: topology of population activity in visual cortex

How to experimentally and computationally detect topological structure in the architecture and dynamics of V1?

Visual stimulation (electrophysiology)

## Motivation: topology of population activity in visual cortex

How to experimentally and computationally detect topological structure in the architecture and dynamics of V1?

Visual stimulation (electrophysiology)

- *Spontaneous condition*

## Motivation: topology of population activity in visual cortex

How to experimentally and computationally detect topological structure in the architecture and dynamics of V1?

Visual stimulation (electrophysiology)

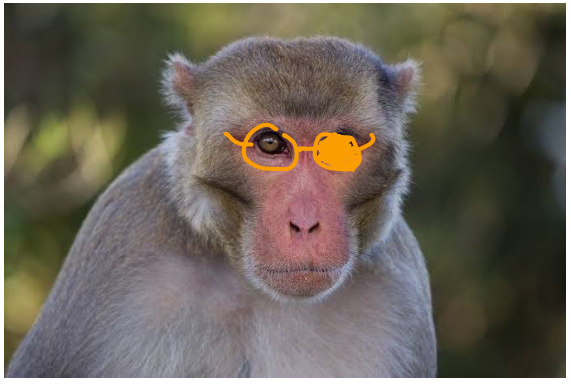

- *Spontaneous condition*
- *Evoked condition*

## Motivation: topology of population activity in visual cortex

How to experimentally and computationally detect topological structure in the architecture and dynamics of V1?

Visual stimulation (electrophysiology)

↓

Construction of point clouds

- *Collect spontaneous and evoked activity segments in lengths of 10 s each*

## Motivation: topology of population activity in visual cortex

How to experimentally and computationally detect topological structure in the architecture and dynamics of V1?

Visual stimulation (electrophysiology)

↓

Construction of point clouds

- *Collect spontaneous and evoked activity segments in lengths of 10 s each*
- *Spike-sort signals from each electrode*
- *Sub-select a group of 5 neurons that showed the highest firing rates*

## Motivation: topology of population activity in visual cortex

How to experimentally and computationally detect topological structure in the architecture and dynamics of V1?

Visual stimulation (electrophysiology)

↓

Construction of point clouds

- *Collect spontaneous and evoked activity segments in lengths of 10 s each*
- *Spike-sort signals from each electrode*
- *Sub-select a group of 5 neurons that showed the highest firing rates*
- *Bin spikes in 50-ms windows*
- *Obtain from each segment 200 points in* $\mathbb{R}^5$

## Motivation: topology of population activity in visual cortex

How to experimentally and computationally detect topological structure in the architecture and dynamics of V1?

Visual stimulation (electrophysiology)

↓

Construction of point clouds

- *Collect spontaneous and evoked activity segments in lengths of 10 s each*
- *Spike-sort signals from each electrode*
- *Sub-select a group of 5 neurons that showed the highest firing rates*
- *Bin spikes in 50-ms windows*
- *Obtain from each segment 200 points in* $\mathbb{R}^5$

# Motivation: topology of population activity in visual cortex

How to experimentally and computationally detect topological structure in the architecture and dynamics of V1?

Visual stimulation (electrophysiology)

↓

Construction of point clouds

- *Collect spontaneous and evoked activity segments in lengths of 10 s each*
- *Spike-sort signals from each electrode*
- *Sub-select a group of 5 neurons that showed the highest firing rates*
- *Bin spikes in 50-ms windows*
- *Obtain from each segment 200 points in $\mathbb{R}^5$*

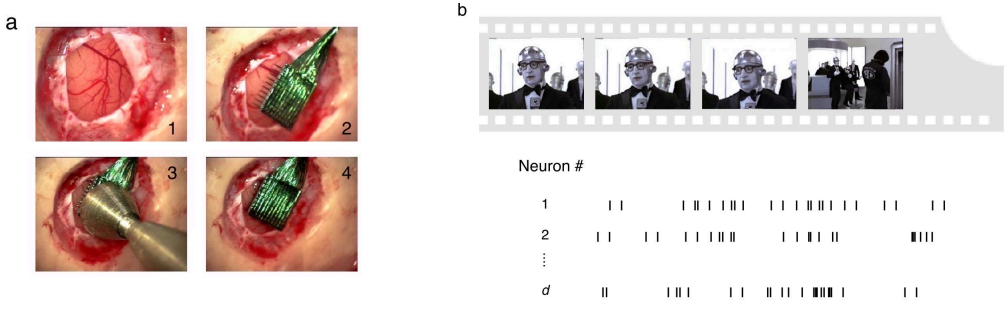


Figure 8. Experimental recordings in primary visual cortex. (a) Insertion sequence of a multi-electrode array into primary visual cortex (Nauhaus & Ringach, 2007). (b) Natural image sequences, sampled from commercial movies, were used to stimulate all receptive fields of neurons isolated by the array. In the spontaneous condition, activity was recorded while both eyes were occluded.

# Motivation: topology of population activity in visual cortex

How to experimentally and computationally detect topological structure in the architecture and dynamics of V1?

Visual stimulation (electrophysiology)

↓

Construction of point clouds

↓

Topological feature extraction (persistent homology)

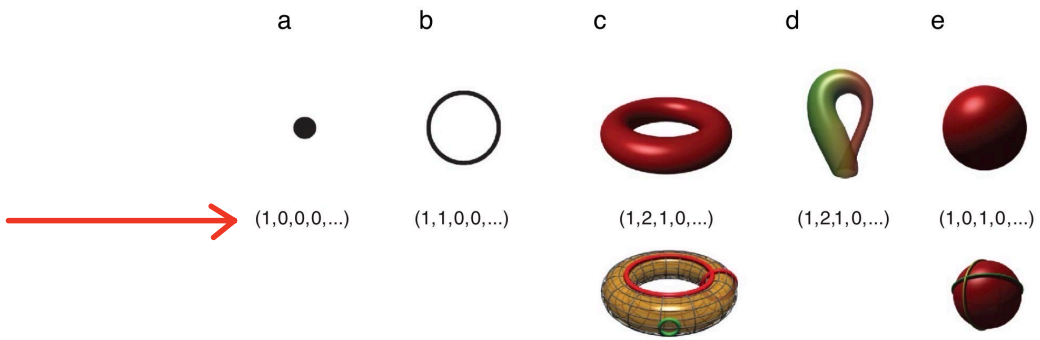


Figure 2. Betti numbers provide a signature of the underlying topology. Illustrated in the figure are five simple objects (topological spaces) together with their Betti number signatures: (a) a point, (b) a circle, (c) a hollow torus, (d) a Klein bottle, and (e) a hollow sphere. For the case of the torus (c), the figure shows three loops on its surface. The red loops are "essential" in that they cannot be shrunk to a point, nor can they be deformed one into the other without tearing the loop. The green loop, on the other hand, can be deformed to a point without any obstruction. For the torus, therefore, we have $b_1 = 2$. For the case of the sphere, the loops shown (and actually all loops on the sphere) can be contracted to points, which is reflected by the fact that $b_1 = 0$. Both the sphere and the torus have $b_2 = 1$, this is due to the fact both surfaces enclose a part of space (a void).

# Motivation: topology of population activity in visual cortex

How to experimentally and computationally detect topological structure in the architecture and dynamics of V1?

Visual stimulation (electrophysiology)

↓

Construction of point clouds

↓

Topological feature extraction (persistent homology)

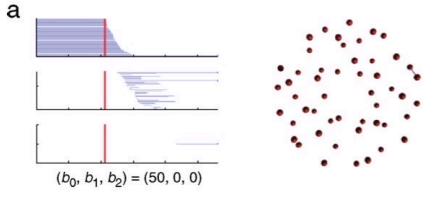


Figure 3. Barcodes and Rips complexes. The figure illustrates the construction of the Rips complex and the generation of barcodes (only the first three Betti numbers are displayed) for 50 points randomly sampled from the surface of a torus. Panels a to d show the barcode "sliced" at different values of $\varepsilon$ (the horizontal axis) with the corresponding Rips complexes shown to the right. The corresponding Betti numbers for each level of $\varepsilon$ can be obtained by counting the number of horizontal lines crossed by the vertical red line in each graph.

# Motivation: topology of population activity in visual cortex

How to experimentally and computationally detect topological structure in the architecture and dynamics of V1?

Visual stimulation (electrophysiology)

↓

Construction of point clouds

↓

Topological feature extraction (persistent homology)

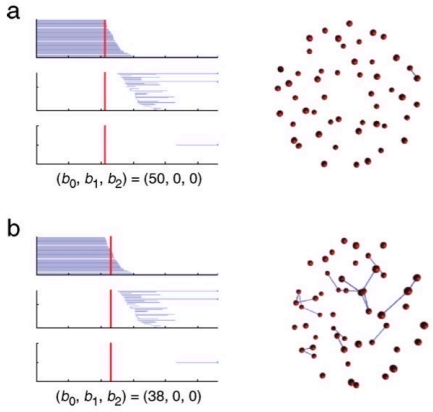


Figure 3. Barcodes and Rips complexes. The figure illustrates the construction of the Rips complex and the generation of barcodes (only the first three Betti numbers are displayed) for 50 points randomly sampled from the surface of a torus. Panels a to d show the barcode "sliced" at different values of $\varepsilon$ (the horizontal axis) with the corresponding Rips complexes shown to the right. The corresponding Betti numbers for each level of $\varepsilon$ can be obtained by counting the number of horizontal lines crossed by the vertical red line in each graph.

*ε = measure of closeness (for "clustering")*

# Motivation: topology of population activity in visual cortex

How to experimentally and computationally detect topological structure in the architecture and dynamics of V1?

Visual stimulation (electrophysiology)

↓

Construction of point clouds

↓

Topological feature extraction (persistent homology)

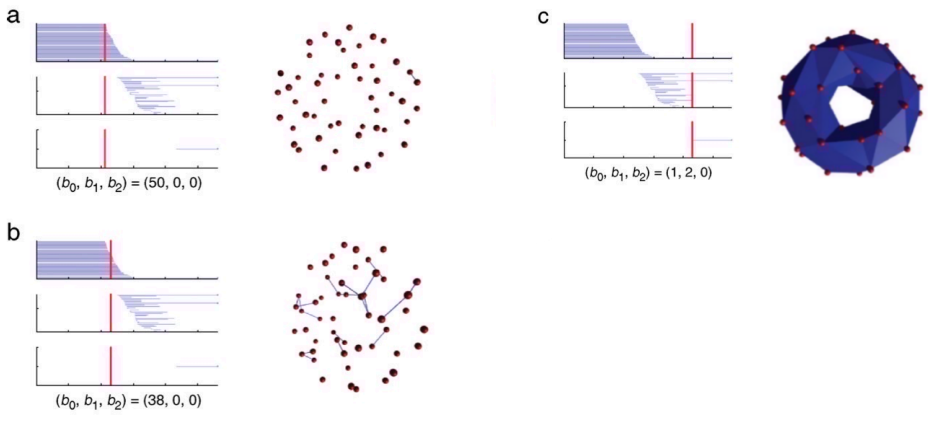


Figure 3. Barcodes and Rips complexes. The figure illustrates the construction of the Rips complex and the generation of barcodes (only the first three Betti numbers are displayed) for 50 points randomly sampled from the surface of a torus. Panels a to d show the barcode "sliced" at different values of $\varepsilon$ (the horizontal axis) with the corresponding Rips complexes shown to the right. The corresponding Betti numbers for each level of $\varepsilon$ can be obtained by counting the number of horizontal lines crossed by the vertical red line in each graph.

# Motivation: topology of population activity in visual cortex

How to experimentally and computationally detect topological structure in the architecture and dynamics of V1?

Visual stimulation (electrophysiology)

↓

Construction of point clouds

↓

Topological feature extraction (persistent homology)

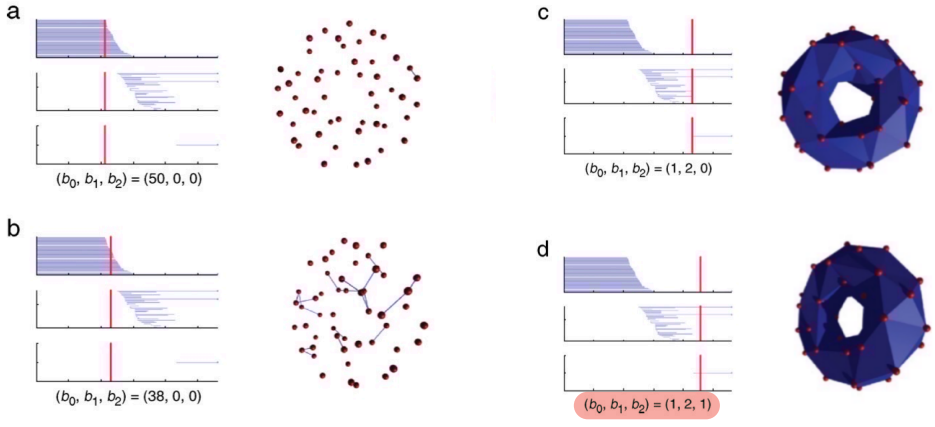


Figure 3. Barcodes and Rips complexes. The figure illustrates the construction of the Rips complex and the generation of barcodes (only the first three Betti numbers are displayed) for 50 points randomly sampled from the surface of a torus. Panels a to d show the barcode "sliced" at different values of $\varepsilon$ (the horizontal axis) with the corresponding Rips complexes shown to the right. The corresponding Betti numbers for each level of $\varepsilon$ can be obtained by counting the number of horizontal lines crossed by the vertical red line in each graph.

# Motivation: topology of population activity in visual cortex

How to experimentally and computationally detect topological structure in the architecture and dynamics of V1?

Visual stimulation (electrophysiology)

↓

Construction of point clouds

↓

Topological feature extraction (persistent homology)

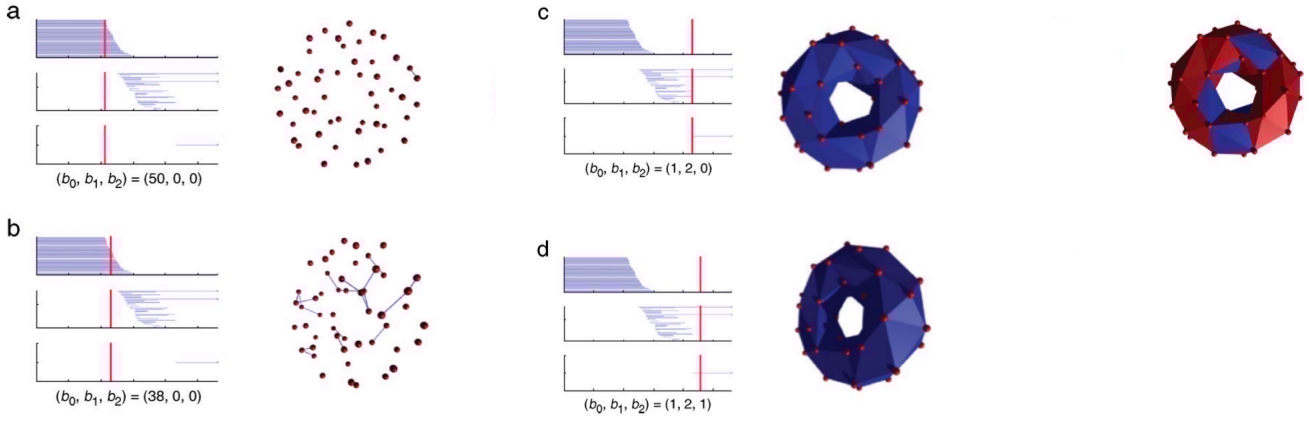


Figure 3. Barcodes and Rips complexes. The figure illustrates the construction of the Rips complex and the generation of barcodes (only the first three Betti numbers are displayed) for 50 points randomly sampled from the surface of a torus. Panels a to d show the barcode "sliced" at different values of $\varepsilon$ (the horizontal axis) with the corresponding Rips complexes shown to the right. The corresponding Betti numbers for each level of $\varepsilon$ can be obtained by counting the number of horizontal lines crossed by the vertical red line in each graph.

# Motivation: topology of population activity in visual cortex

How to experimentally and computationally detect topological structure in the architecture and dynamics of V1?

Visual stimulation (electrophysiology)

↓

Construction of point clouds

↓

Topological feature extraction (persistent homology)

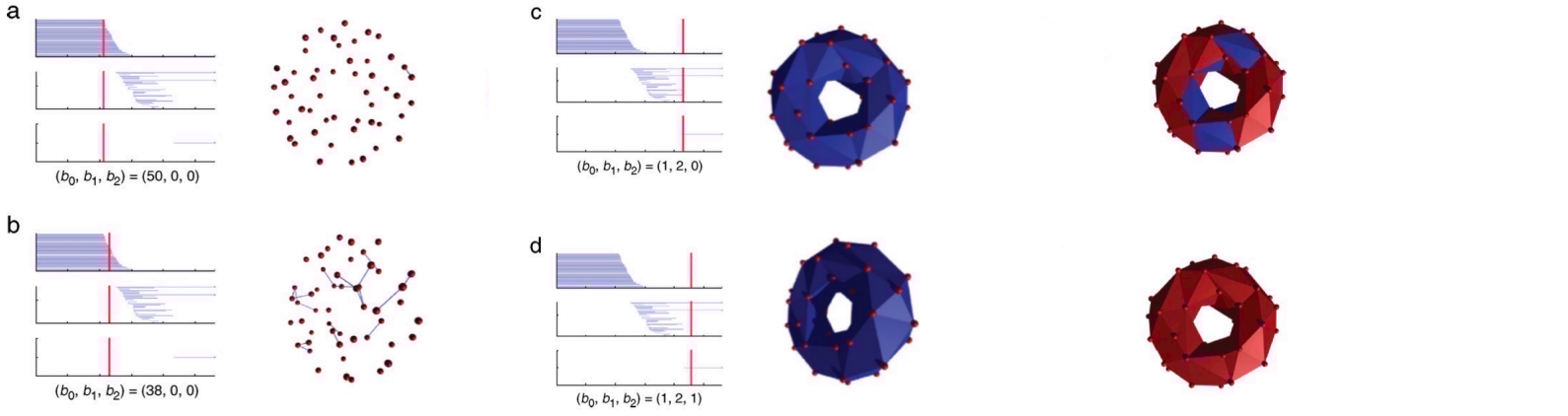


Figure 3. Barcodes and Rips complexes. The figure illustrates the construction of the Rips complex and the generation of barcodes (only the first three Betti numbers are displayed) for 50 points randomly sampled from the surface of a torus. Panels a to d show the barcode "sliced" at different values of $\varepsilon$ (the horizontal axis) with the corresponding Rips complexes shown to the right. The corresponding Betti numbers for each level of $\varepsilon$ can be obtained by counting the number of horizontal lines crossed by the vertical red line in each graph.

# Motivation: topology of population activity in visual cortex

How to experimentally and computationally detect topological structure in the architecture and dynamics of V1?

Visual stimulation (electrophysiology)

↓

Construction of point clouds

↓

Topological feature extraction (persistent homology)

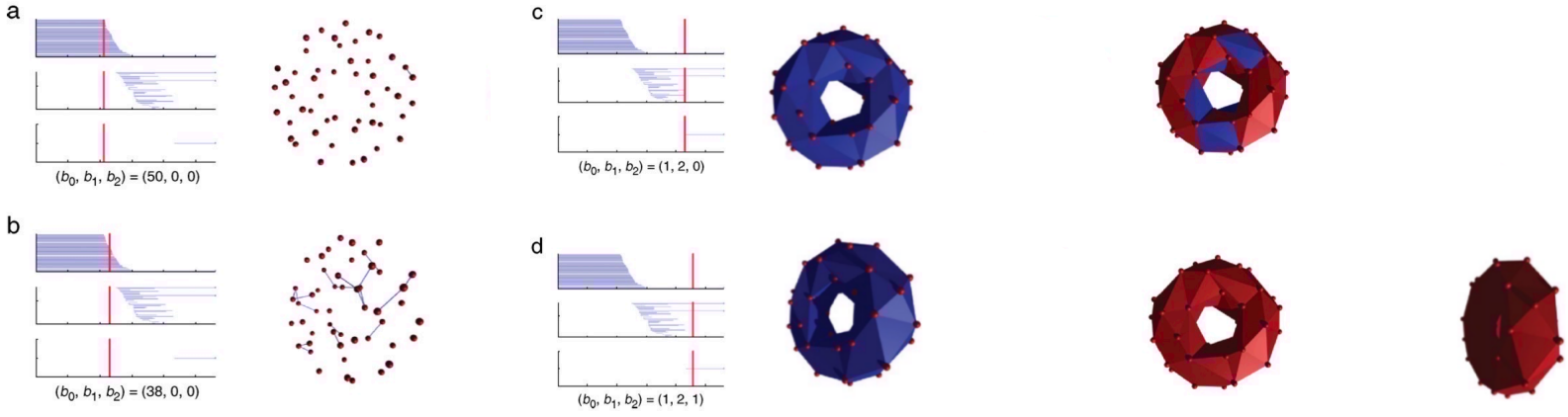


Figure 3. Barcodes and Rips complexes. The figure illustrates the construction of the Rips complex and the generation of barcodes (only the first three Betti numbers are displayed) for 50 points randomly sampled from the surface of a torus. Panels a to d show the barcode "sliced" at different values of $\varepsilon$ (the horizontal axis) with the corresponding Rips complexes shown to the right. The corresponding Betti numbers for each level of $\varepsilon$ can be obtained by counting the number of horizontal lines crossed by the vertical red line in each graph.

## Motivation: topology of population activity in visual cortex

How to experimentally and computationally detect topological structure in the architecture and dynamics of V1?

Visual stimulation (electrophysiology)

↓

Construction of point clouds

↓

Topological feature extraction (persistent homology)

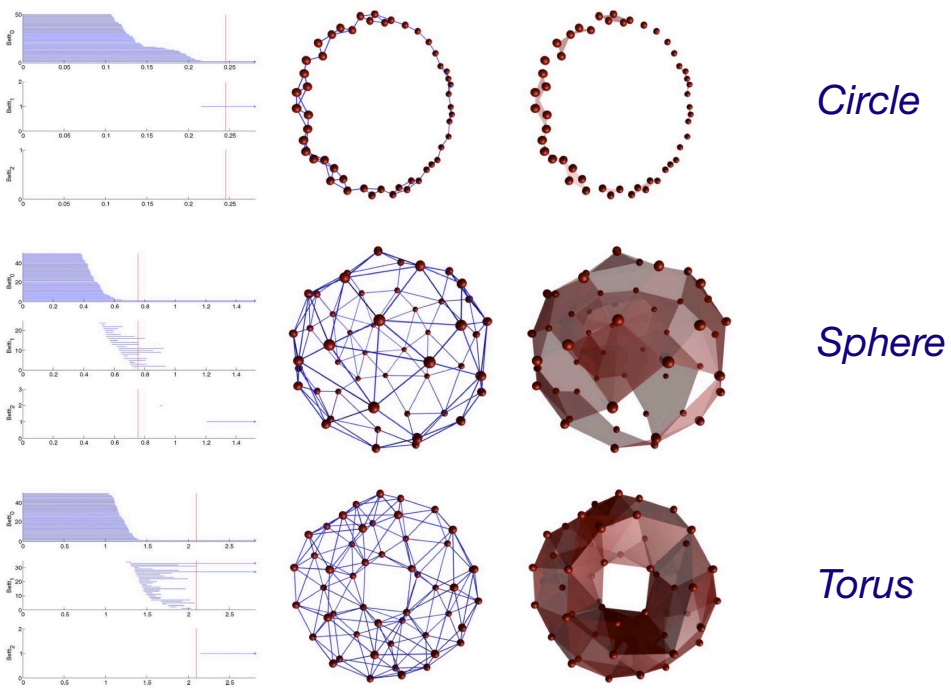

*Circle*

*Sphere*

*Torus*

# Motivation: topology of population activity in visual cortex

How to experimentally and computationally detect topological structure in the architecture and dynamics of V1?

Visual stimulation (electrophysiology)

↓

Construction of point clouds

↓

Topological feature extraction (persistent homology)

↓

**Results!**

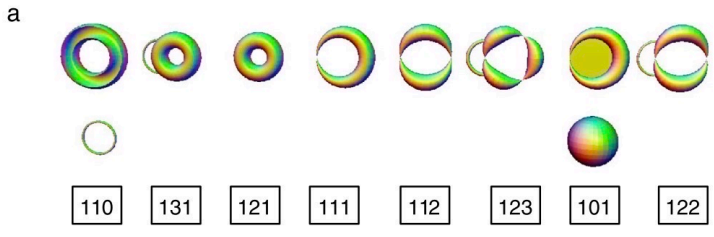


Figure 9. Estimation of topological structure in driven and spontaneous conditions. (a) Ordering of topological signatures observed in our experiments. Each triplet ($b_0$, $b_1$, $b_2$) is shown along an illustration of objects consistent with these signature. (b) Distribution of topological signatures in the spontaneous and natural image stimulation conditions pooled across the three experiments performed. Each row correspond to signatures with a minimum interval length (denoted as the threshold) expressed as a fraction of the covering radius of the data cloud (see Appendix A for the definition of the covering radius).

# Motivation: topology of population activity in visual cortex

How to experimentally and computationally detect topological structure in the architecture and dynamics of V1?

Visual stimulation (electrophysiology)

↓

Construction of point clouds

↓

Topological feature extraction (persistent homology)

↓

**Results!**

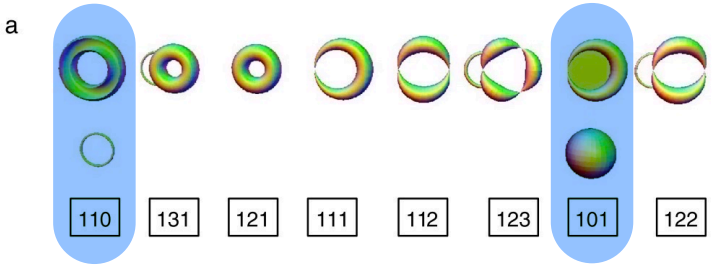


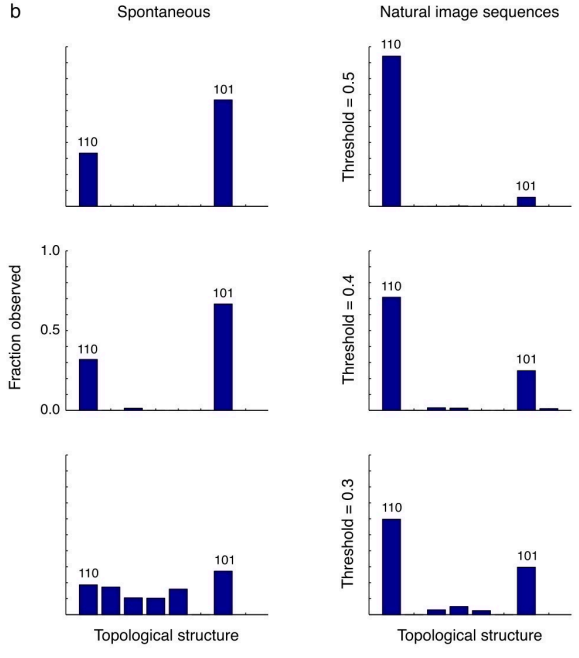


Figure 9. Estimation of topological structure in driven and spontaneous conditions. (a) Ordering of topological signatures observed in our experiments. Each triplet ($b_0$, $b_1$, $b_2$) is shown along an illustration of objects consistent with these signature. (b) Distribution of topological signatures in the spontaneous and natural image stimulation conditions pooled across the three experiments performed. Each row correspond to signatures with a minimum interval length (denoted as the threshold) expressed as a fraction of the covering radius of the data cloud (see Appendix A for the definition of the covering radius).

## Motivation: topology of population activity in visual cortex

How to experimentally and computationally detect topological structure in the architecture and dynamics of V1?

Visual stimulation (electrophysiology)

↓

Construction of point clouds

↓

Topological feature extraction (persistent homology)

↓

**Results!**

Also validation experiments with simulated signals, robustness, model explanation, etc.

## Motivation: topology of population activity in visual cortex

How to experimentally and computationally detect topological structure in the architecture and dynamics of V1?

Visual stimulation (electrophysiology)

↓

Construction of point clouds

↓

Topological feature extraction (persistent homology)

↓

**Results!**

Also validation experiments with simulated signals, robustness, model explanation, etc.

**Questions:**

- Why does a circle emerge as the topological structure of population activity in V1? Why a sphere?

## Motivation: topology of population activity in visual cortex

How to experimentally and computationally detect topological structure in the architecture and dynamics of V1?

Visual stimulation (electrophysiology)

↓

Construction of point clouds

↓

Topological feature extraction (persistent homology)

↓

**Results!**

Also validation experiments with simulated signals, robustness, model explanation, etc.

**Questions:**

- Why does a circle emerge as the topological structure of population activity in V1? Why a sphere?
- What about auditory signals? Architecture and dynamics of A1? Analogy or contrast?

# Tracing back from perception to signals: natural image statistics

- *Lee, Pedersen, & Mumford, The nonlinear statistics of high-contrast patches in natural images,* ***International Journal of Computer Vision*** *2003.*
- *Carlsson, Ishkhanov, de Silva, & Zomorodian, On the local behavior of  spaces of natural images,* ***International Journal of Computer Vision*** *2008.*

# Tracing back from perception to signals: natural image statistics

- *Lee, Pedersen, & Mumford, The nonlinear statistics of high-contrast patches in natural images,* ***International Journal of Computer Vision*** *2003.*
- *Carlsson, Ishkhanov, de Silva, & Zomorodian, On the local behavior of  spaces of natural images,* ***International Journal of Computer Vision*** *2008.*

An image taken by black and white digital camera can be viewed as a vector, with one coordinate for each pixel.

## Tracing back from perception to signals: natural image statistics

- *Lee, Pedersen, & Mumford, The nonlinear statistics of high-contrast patches in natural images,* ***International Journal of Computer Vision*** *2003.*
- *Carlsson, Ishkhanov, de Silva, & Zomorodian, On the local behavior of  spaces of natural images,* ***International Journal of Computer Vision*** *2008.*

An image taken by black and white digital camera can be viewed as a vector, with one coordinate for each pixel.

Each pixel has a “grayscale” value, can be thought of as a real number (in reality, takes one of 256 values).

## Tracing back from perception to signals: natural image statistics

- *Lee, Pedersen, & Mumford, The nonlinear statistics of high-contrast patches in natural images,* ***International Journal of Computer Vision*** *2003.*
- *Carlsson, Ishkhanov, de Silva, & Zomorodian, On the local behavior of spaces of natural images,* ***International Journal of Computer Vision*** *2008.*

An image taken by black and white digital camera can be viewed as a vector, with one coordinate for each pixel.

Each pixel has a “grayscale” value, can be thought of as a real number (in reality, takes one of 256 values).

Typical camera uses tens of thousands of pixels, so images lie in a very high-dimensional space, call it pixel space, ***P***.

## Tracing back from perception to signals: natural image statistics

- *Lee, Pedersen, & Mumford, The nonlinear statistics of high-contrast patches in natural images,* ***International Journal of Computer Vision*** *2003.*
- *Carlsson, Ishkhanov, de Silva, & Zomorodian, On the local behavior of spaces of natural images,* ***International Journal of Computer Vision*** *2008.*

An image taken by black and white digital camera can be viewed as a vector, with one coordinate for each pixel.

Each pixel has a "grayscale" value, can be thought of as a real number (in reality, takes one of 256 values).

Typical camera uses tens of thousands of pixels, so images lie in a very high-dimensional space, call it pixel space, $\boldsymbol{P}$.

Mumford asks: What can be said about the set of images $\boldsymbol{I} \subset \boldsymbol{P}$ one obtains when one takes many images with a digital camera?

## Tracing back from perception to signals: natural image statistics

Lee, Mumford, Pedersen: Useful to study *local* structure of images statistically.

## Tracing back from perception to signals: natural image statistics

Lee, Mumford, Pedersen: Useful to study *local* structure of images statistically.

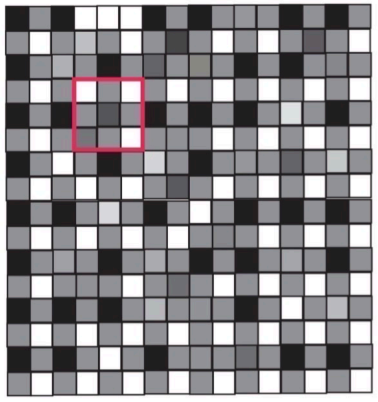

3 x 3 patches in images

## Tracing back from perception to signals: natural image statistics

Lee, Mumford, Pedersen: Useful to study *local* structure of images statistically.

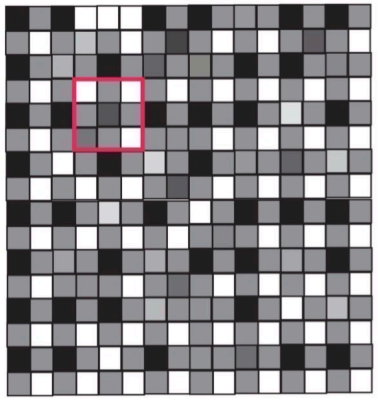

3 x 3 patches in images

**Observations**:

1. Each patch gives a vector in $\mathbb{R}^9$.

## Tracing back from perception to signals: natural image statistics

Lee, Mumford, Pedersen: Useful to study *local* structure of images statistically.

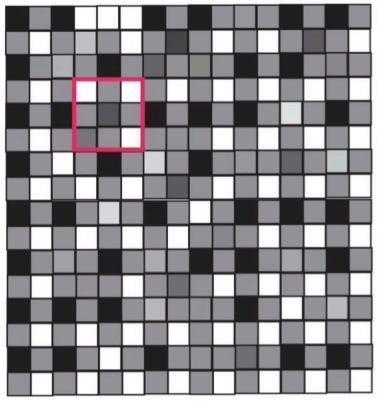

3 x 3 patches in images

**Observations**:

1. Each patch gives a vector in $\mathbb{R}^9$.
2. Most patches will be nearly constant, or *low* contrast, because of the presence of regions of solid shading in most images.

## Tracing back from perception to signals: natural image statistics

Lee, Mumford, Pedersen: Useful to study *local* structure of images statistically.

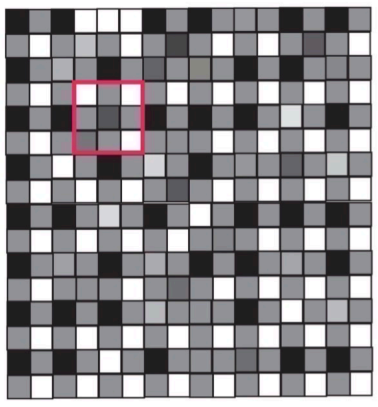

3 x 3 patches in images

**Observations**:

1. Each patch gives a vector in $\mathbb{R}^9$.
2. Most patches will be nearly constant, or *low* contrast, because of the presence of regions of solid shading in most images.

## Tracing back from perception to signals: natural image statistics

Lee, Mumford, Pedersen: Useful to study *local* structure of images statistically.

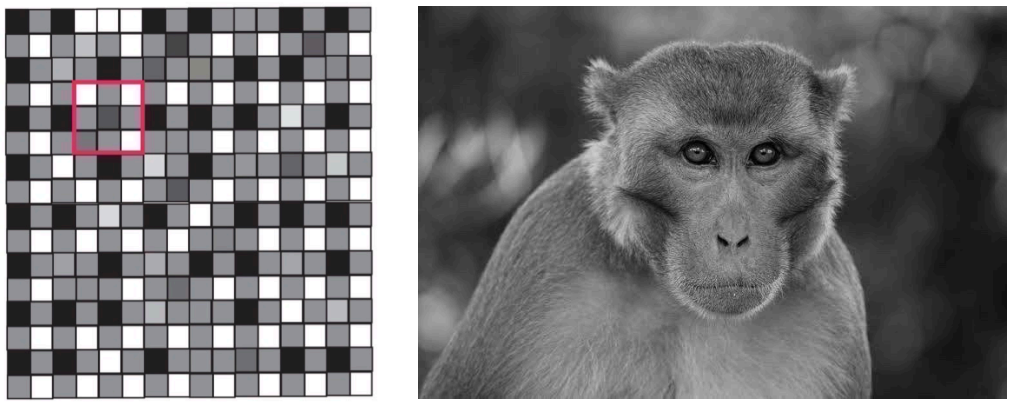

3 x 3 patches in images

**Observations**:

1. Each patch gives a vector in $\mathbb{R}^9$.
2. Most patches will be nearly constant, or *low* contrast, because of the presence of regions of solid shading in most images.
3. Low contrast will dominate statistics, not interesting. *High* contrast patches delineate profiles.

## Tracing back from perception to signals: natural image statistics

Lee, Mumford, & Pedersen study only high contrast patches:

## Tracing back from perception to signals: natural image statistics

Lee, Mumford, & Pedersen study only high contrast patches:

- Collect approximately $4.5 \times 10^6$ high contrast patches from a collection of images obtained by van Hateren and van der Schaaf.

## Tracing back from perception to signals: natural image statistics

Lee, Mumford, & Pedersen study only high contrast patches:

- Collect approximately $4.5 \times 10^6$ high contrast patches from a collection of images obtained by van Hateren and van der Schaaf.

- Normalize mean intensity by subtracting mean from each pixel value to obtain patches with mean intensity = 0.

## Tracing back from perception to signals: natural image statistics

Lee, Mumford, & Pedersen study only high contrast patches:

- Collect approximately $4.5 \times 10^6$ high contrast patches from a collection of images obtained by van Hateren and van der Schaaf.
- Normalize mean intensity by subtracting mean from each pixel value to obtain patches with mean intensity = 0.
- Puts data on an 8-dimensional hyperplane, $\cong \mathbb{R}^8$.

## Tracing back from perception to signals: natural image statistics

Lee, Mumford, & Pedersen study only high contrast patches:

- Collect approximately $4.5 \times 10^6$ high contrast patches from a collection of images obtained by van Hateren and van der Schaaf.
- Normalize mean intensity by subtracting mean from each pixel value to obtain patches with mean intensity = 0.
- Puts data on an 8-dimensional hyperplane, $\cong \mathbb{R}^8$.
- Normalize contrast by dividing by the norm, so obtain patches with norm = 1.

## Tracing back from perception to signals: natural image statistics

Lee, Mumford, & Pedersen study only high contrast patches:

- Collect approximately $4.5 \times 10^6$ high contrast patches from a collection of images obtained by van Hateren and van der Schaaf.
- Normalize mean intensity by subtracting mean from each pixel value to obtain patches with mean intensity = 0.
- Puts data on an 8-dimensional hyperplane, $\cong \mathbb{R}^8$.
- Normalize contrast by dividing by the norm, so obtain patches with norm = 1.
- So, data now lie on a 7-dimensional sphere, $\cong S^7$.

## Tracing back from perception to signals: natural image statistics

Lee, Mumford, & Pedersen study only high contrast patches:

- Collect approximately $4.5 \times 10^6$ high contrast patches from a collection of images obtained by van Hateren and van der Schaaf.
- Normalize mean intensity by subtracting mean from each pixel value to obtain patches with mean intensity = 0.
- Puts data on an 8-dimensional hyperplane, $\cong \mathbb{R}^8$.
- Normalize contrast by dividing by the norm, so obtain patches with norm = 1.
- So, data now lie on a 7-dimensional sphere, $\cong S^7$.

**Result**: Point cloud data $M$ lying on a sphere in $\mathbb{R}^8$.

## Tracing back from perception to signals: natural image statistics

Carlsson, Ishkhanov, de Silva, & Zomorodian analyze it with persistent homology to understand it qualitatively.

## Tracing back from perception to signals: natural image statistics

Carlsson, Ishkhanov, de Silva, & Zomorodian analyze it with persistent homology to understand it qualitatively.

**First observation**: The points fill out $S^7$ in the sense that every point in $S^7$ is "close" to a point in $M$.

## Tracing back from perception to signals: natural image statistics

Carlsson, Ishkhanov, de Silva, & Zomorodian analyze it with persistent homology to understand it qualitatively.

**First observation**: The points fill out $S^7$ in the sense that every point in $S^7$ is "close" to a point in $M$. However, density of points varies a great deal from region to region.

How to analyze?

## Tracing back from perception to signals: natural image statistics

Carlsson, Ishkhanov, de Silva, & Zomorodian analyze it with persistent homology to understand it qualitatively.

**First observation**: The points fill out $S^7$ in the sense that every point in $S^7$ is "close" to a point in $M$. However, density of points varies a great deal from region to region.

How to analyze? Set *thresholds* for $M$.

## Tracing back from perception to signals: natural image statistics

Carlsson, Ishkhanov, de Silva, & Zomorodian analyze it with persistent homology to understand it qualitatively.

**First observation**: The points fill out $S^7$ in the sense that every point in $S^7$ is "close" to a point in $M$. However, density of points varies a great deal from region to region.

How to analyze? Set *thresholds* for $M$. Define $M[T] \subset M$ by

$$M[T] = \{x \mid x \text{ is in } T\text{-th percentile of densest points}\}$$

## Tracing back from perception to signals: natural image statistics

Carlsson, Ishkhanov, de Silva, & Zomorodian analyze it with persistent homology to understand it qualitatively.

**First observation**: The points fill out $S^7$ in the sense that every point in $S^7$ is "close" to a point in $M$. However, density of points varies a great deal from region to region.

How to analyze? Set *thresholds* for $M$. Define $M[T] \subset M$ by

$$M[T] = \{x \mid x \text{ is in } T\text{-th percentile of densest points}\}$$

By computing the persistent homology of these $M[T]$'s, they reveal

## Tracing back from perception to signals: natural image statistics

Carlsson, Ishkhanov, de Silva, & Zomorodian analyze it with persistent homology to understand it qualitatively.

**First observation**: The points fill out $S^7$ in the sense that every point in $S^7$ is "close" to a point in $M$. However, density of points varies a great deal from region to region.

How to analyze? Set *thresholds* for $M$. Define $M[T] \subset M$ by

$$M[T] = \{x \mid x \text{ is in } T\text{-th percentile of densest points}\}$$

By computing the persistent homology of these $M[T]$'s, they reveal

1. $5 \times 10^4$ points, $T = 25$:
   There are 5 independent 1-dimensional cycles on $M[T]$.
   Red and green circles don't touch, each touches black circle.

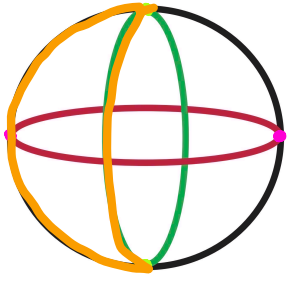

THREE CIRCLE MODEL

## Tracing back from perception to signals: natural image statistics

Carlsson, Ishkhanov, de Silva, & Zomorodian analyze it with persistent homology to understand it qualitatively.

**First observation**: The points fill out $S^7$ in the sense that every point in $S^7$ is "close" to a point in $M$. However, density of points varies a great deal from region to region.

How to analyze? Set *thresholds* for $M$. Define $M[T] \subset M$ by

$$M[T] = \{x \mid x \text{ is in } T\text{-th percentile of densest points}\}$$

By computing the persistent homology of these $M[T]$'s, they reveal

1. $5 \times 10^4$ points, $T = 25$:
   There are 5 independent 1-dimensional cycles on $M[T]$.
   Red and green circles don't touch, each touches black circle.

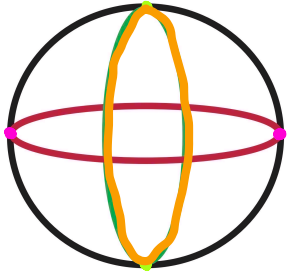

THREE CIRCLE MODEL

## Tracing back from perception to signals: natural image statistics

Carlsson, Ishkhanov, de Silva, & Zomorodian analyze it with persistent homology to understand it qualitatively.

**First observation**: The points fill out $S^7$ in the sense that every point in $S^7$ is "close" to a point in $M$. However, density of points varies a great deal from region to region.

How to analyze? Set *thresholds* for $M$. Define $M[T] \subset M$ by

$$M[T] = \{x \mid x \text{ is in } T\text{-th percentile of densest points}\}$$

By computing the persistent homology of these $M[T]$'s, they reveal

1. $5 \times 10^4$ points, $T = 25$:
   There are 5 independent 1-dimensional cycles on $M[T]$.
   Red and green circles don't touch, each touches black circle.

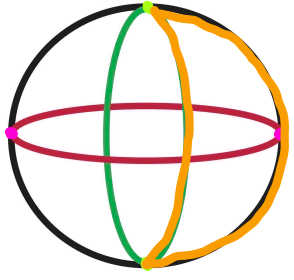

THREE CIRCLE MODEL

## Tracing back from perception to signals: natural image statistics

Carlsson, Ishkhanov, de Silva, & Zomorodian analyze it with persistent homology to understand it qualitatively.

**First observation**: The points fill out $S^7$ in the sense that every point in $S^7$ is "close" to a point in $M$. However, density of points varies a great deal from region to region.

How to analyze? Set *thresholds* for $M$. Define $M[T] \subset M$ by

$$M[T] = \{x \mid x \text{ is in } T\text{-th percentile of densest points}\}$$

By computing the persistent homology of these $M[T]$'s, they reveal

1. $5 \times 10^4$ points, $T = 25$:
   There are 5 independent 1-dimensional cycles on $M[T]$.
   Red and green circles don't touch, each touches black circle.

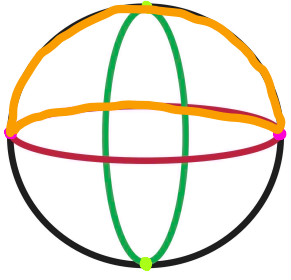

THREE CIRCLE MODEL

## Tracing back from perception to signals: natural image statistics

Carlsson, Ishkhanov, de Silva, & Zomorodian analyze it with persistent homology to understand it qualitatively.

**First observation**: The points fill out $S^7$ in the sense that every point in $S^7$ is "close" to a point in $M$. However, density of points varies a great deal from region to region.

How to analyze? Set *thresholds* for $M$. Define $M[T] \subset M$ by

$$M[T] = \{x \mid x \text{ is in } T\text{-th percentile of densest points}\}$$

By computing the persistent homology of these $M[T]$'s, they reveal

1. $5 \times 10^4$ points, $T = 25$:
   There are 5 independent 1-dimensional cycles on $M[T]$.
   Red and green circles don't touch, each touches black circle.

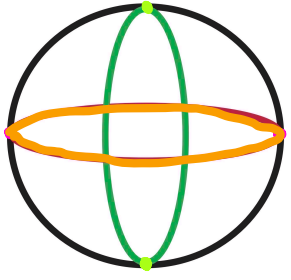

THREE CIRCLE MODEL

## Tracing back from perception to signals: natural image statistics

Carlsson, Ishkhanov, de Silva, & Zomorodian analyze it with persistent homology to understand it qualitatively.

**First observation**: The points fill out $S^7$ in the sense that every point in $S^7$ is "close" to a point in $M$. However, density of points varies a great deal from region to region.

How to analyze? Set *thresholds* for $M$. Define $M[T] \subset M$ by

$$M[T] = \{x \mid x \text{ is in } T\text{-th percentile of densest points}\}$$

By computing the persistent homology of these $M[T]$'s, they reveal

1. $5 \times 10^4$ points, $T = 25$:
   There are 5 independent 1-dimensional cycles on $M[T]$.
   Red and green circles don't touch, each touches black circle.

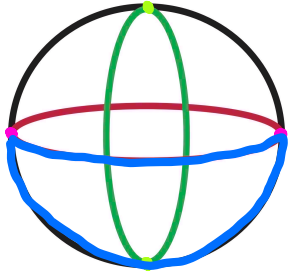

THREE CIRCLE MODEL

## Tracing back from perception to signals: natural image statistics

Carlsson, Ishkhanov, de Silva, & Zomorodian analyze it with persistent homology to understand it qualitatively.

**First observation**: The points fill out $S^7$ in the sense that every point in $S^7$ is "close" to a point in $M$. However, density of points varies a great deal from region to region.

How to analyze? Set *thresholds* for $M$. Define $M[T] \subset M$ by

$$M[T] = \{x \mid x \text{ is in } T\text{-th percentile of densest points}\}$$

By computing the persistent homology of these $M[T]$'s, they reveal

1. $5 \times 10^4$ points, $T = 25$:
   There are 5 independent 1-dimensional cycles on $M[T]$.
   Red and green circles don't touch, each touches black circle.
   ***Is there a surface in which this picture fits?***

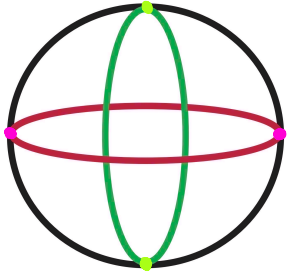

THREE CIRCLE MODEL

## Tracing back from perception to signals: natural image statistics

Carlsson, Ishkhanov, de Silva, & Zomorodian analyze it with persistent homology to understand it qualitatively.

**First observation**: The points fill out $S^7$ in the sense that every point in $S^7$ is "close" to a point in $M$. However, density of points varies a great deal from region to region.

How to analyze? Set *thresholds* for $M$. Define $M[T] \subset M$ by

$$M[T] = \{x \mid x \text{ is in } T\text{-th percentile of densest points}\}$$

By computing the persistent homology of these $M[T]$'s, they reveal

1. $5 \times 10^4$ points, $T = 25$:
   There are 5 independent 1-dimensional cycles on $M[T]$.
   Red and green circles don't touch, each touches black circle.
   ***Is there a surface in which this picture fits?***
2. $4.5 \times 10^6$ points, $T = 10$:
   There are one 0D cycle (connected), two 1D cycles (loops),
   and one 2D cycle (surface), i.e., topological signature = (1, 2, 1).

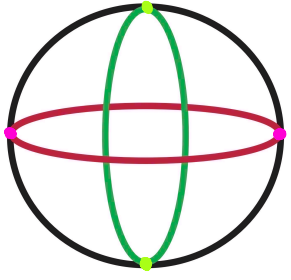

THREE CIRCLE MODEL

## Tracing back from perception to signals: natural image statistics

## Klein bottle!

# Tracing back from perception to signals: natural image statistics

**Klein bottle!**

Visualization:

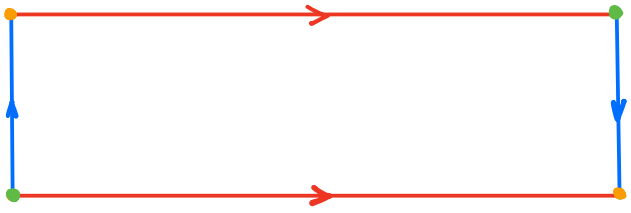

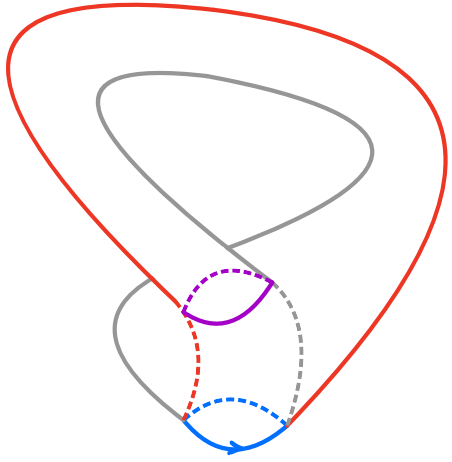

# Tracing back from perception to signals: natural image statistics

**Klein bottle!**

Visualization:

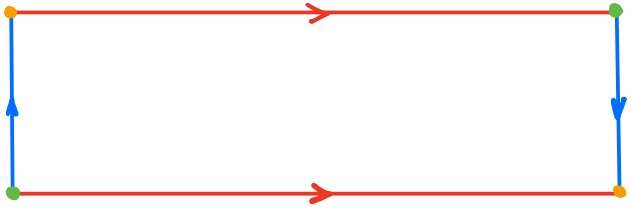

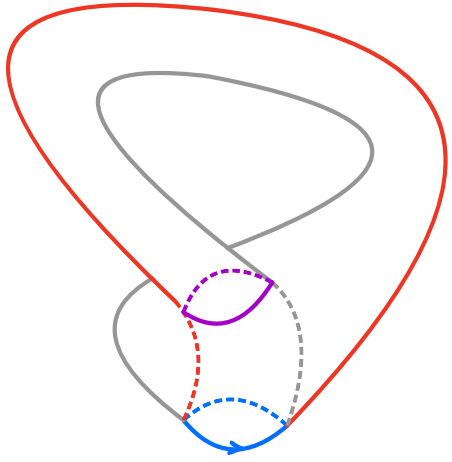

Three circles fit naturally inside the Klein bottle?

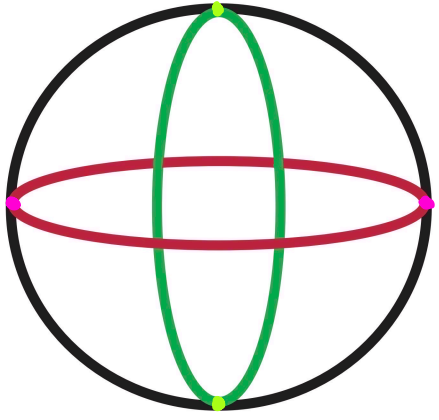

# Tracing back from perception to signals: natural image statistics

## Klein bottle!

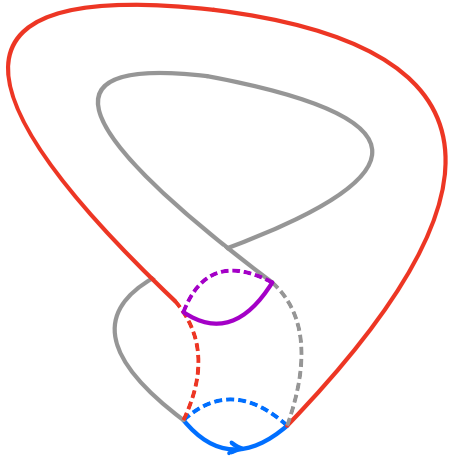

Visualization:

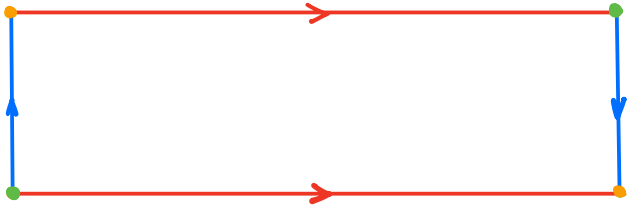

Three circles fit naturally inside the Klein bottle?

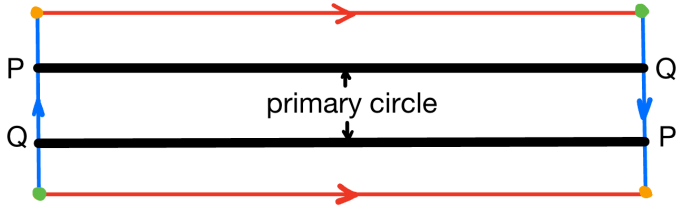


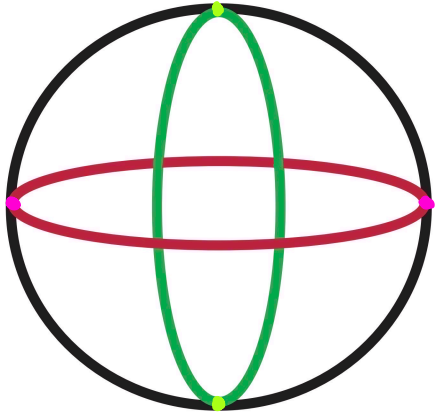

# Tracing back from perception to signals: natural image statistics

## Klein bottle!

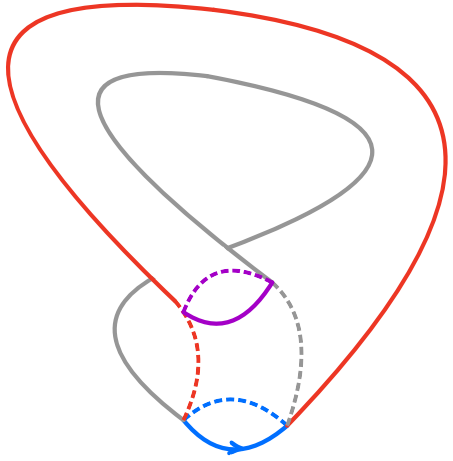

Visualization:

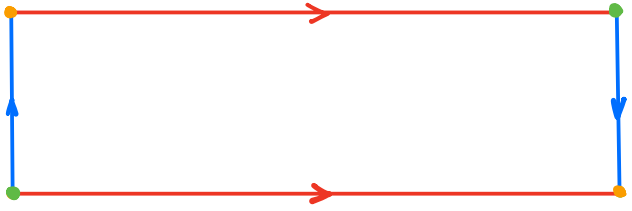

Three circles fit naturally inside the Klein bottle?

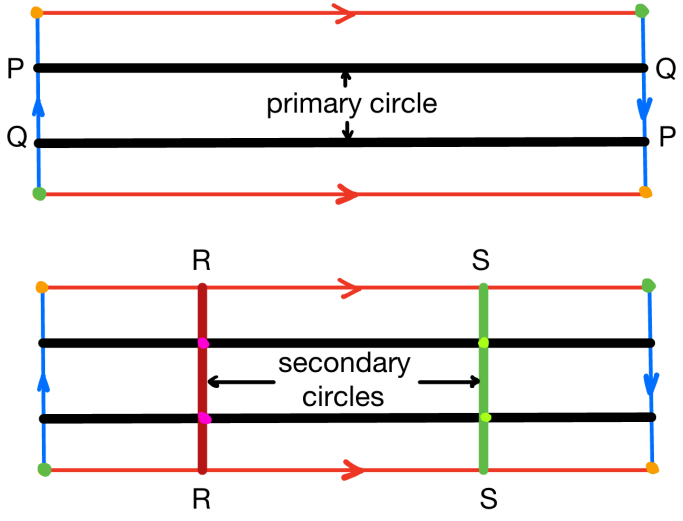


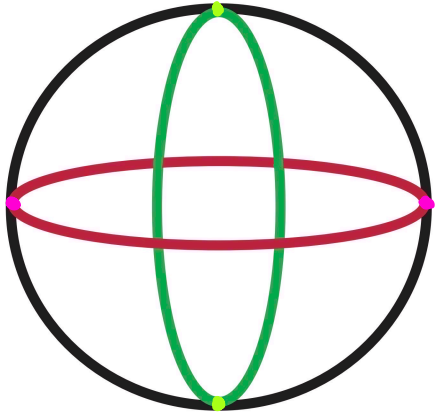

# Tracing back from perception to signals: natural image statistics

## Klein bottle!

Visualization:

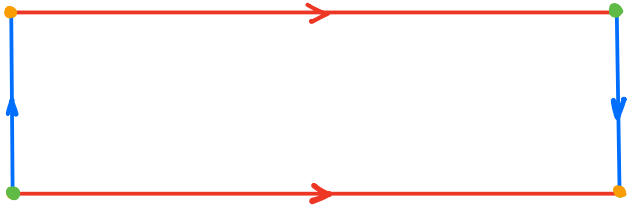

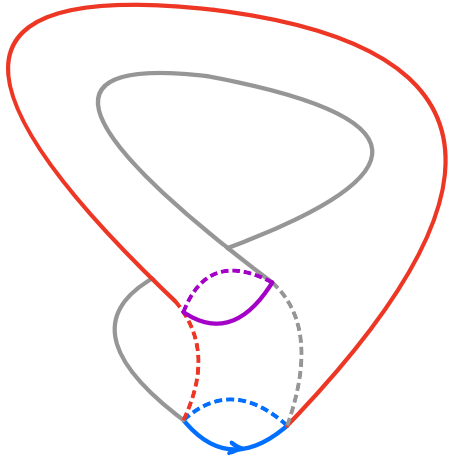

Three circles fit naturally inside the Klein bottle?

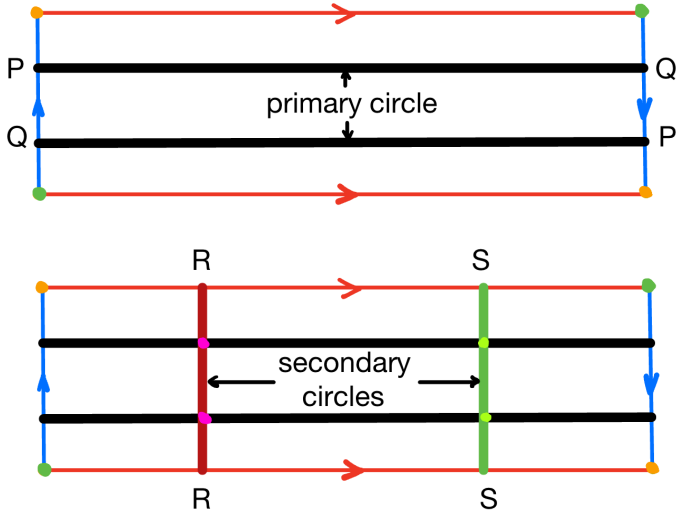


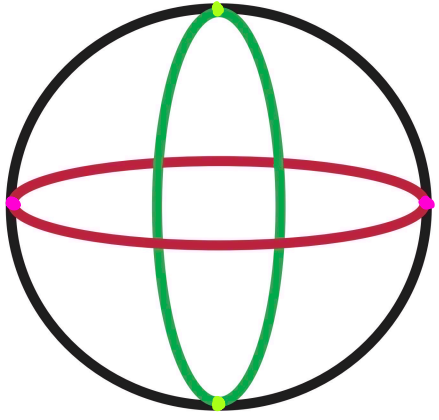

Klein bottle emerges as where local data from digital camera images distribute.

# Tracing back from perception to signals: natural image statistics

## Klein bottle!

Visualization:

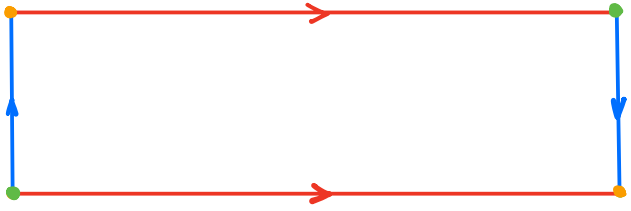

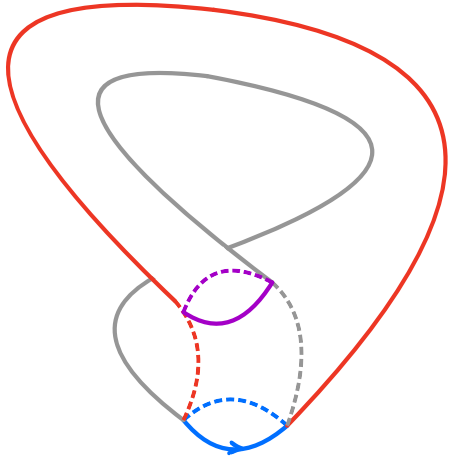

Three circles fit naturally inside the Klein bottle?

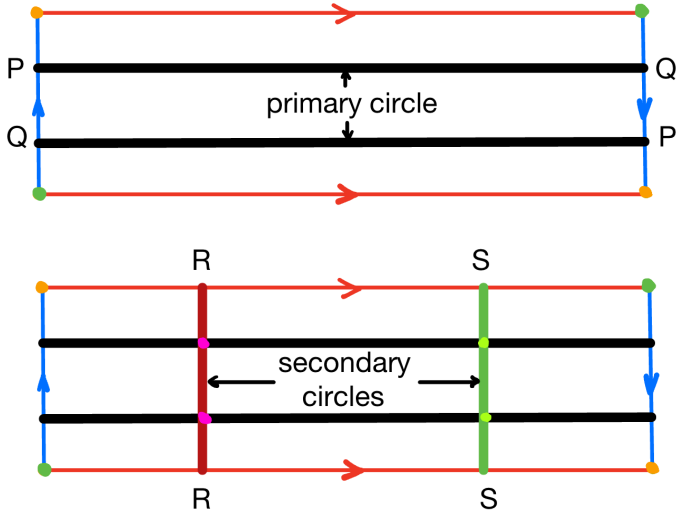


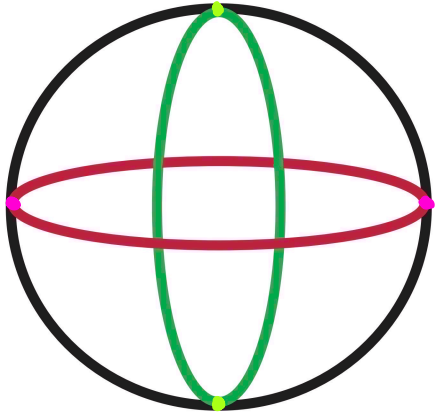

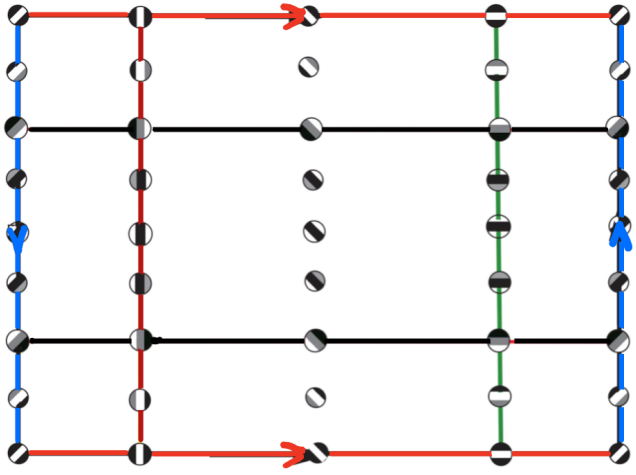

Klein bottle emerges as where local data from digital camera images distribute.

# Tracing back from perception to signals: natural image statistics

## Klein bottle!

Visualization:

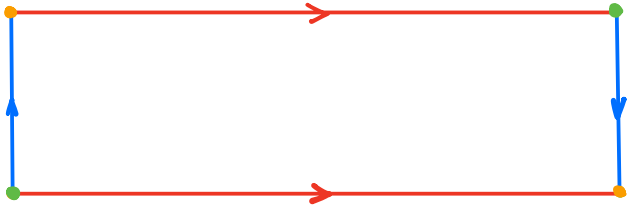

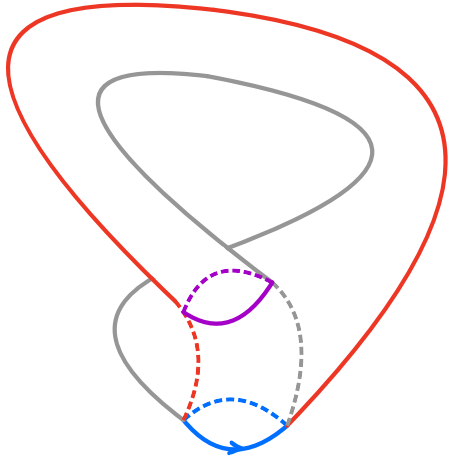

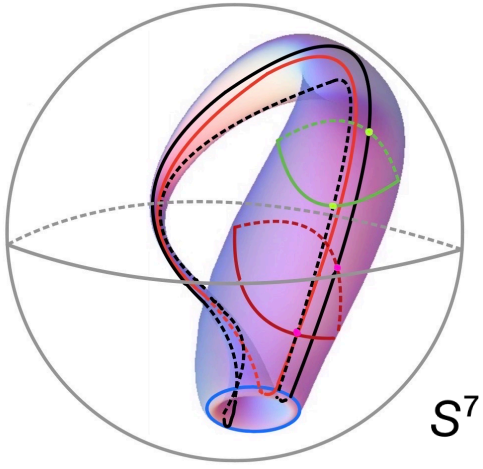


Three circles fit naturally inside the Klein bottle?

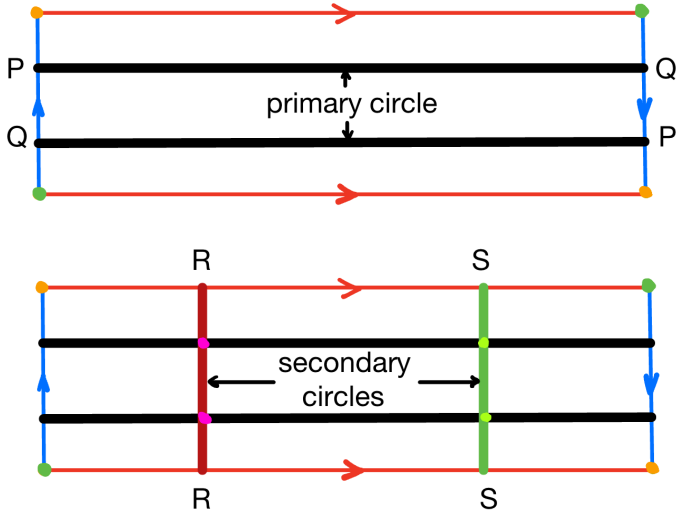


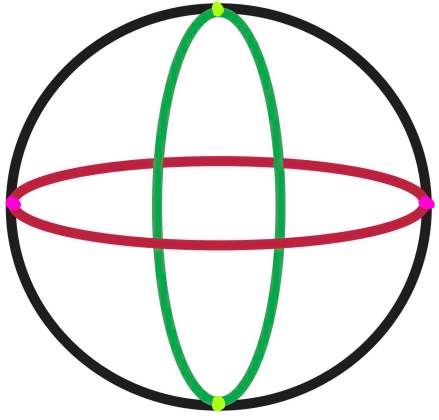

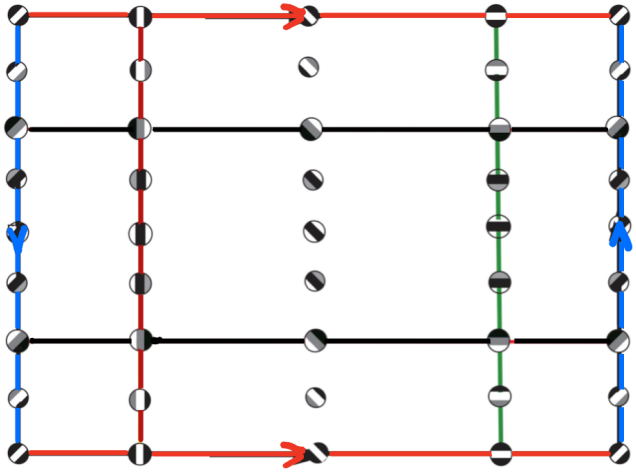

Klein bottle emerges as where local data from digital camera images distribute.

## From visual perception to image data analysis, then to deep learning

A decade later, Love, Filippenko, Maroulas, & Carlsson have made the Klein bottle as a topological input for designing convolutional layers in neural networks that learn image data.

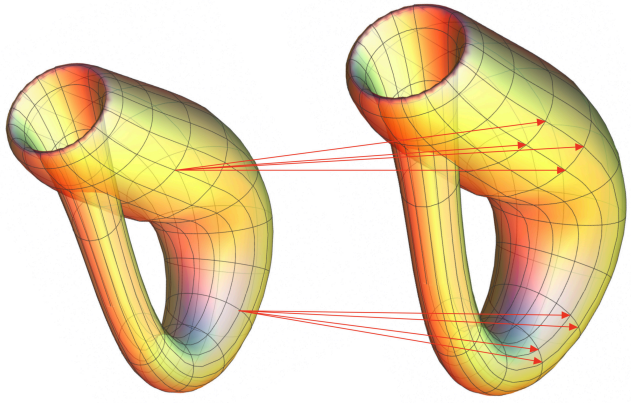

## From visual perception to image data analysis, then to deep learning

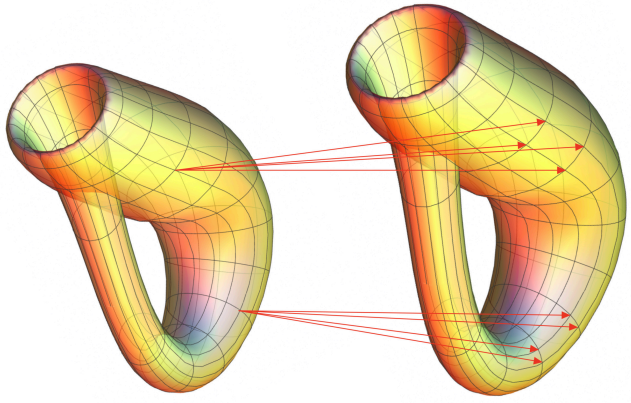

A decade later, Love, Filippenko, Maroulas, & Carlsson have made the Klein bottle as a topological input for designing convolutional layers in neural networks that learn image data.

Moreover, they have incorporated the tangent bundle of a Klein bottle into TCNNs for learning video data.

## From visual perception to image data analysis, then to deep learning

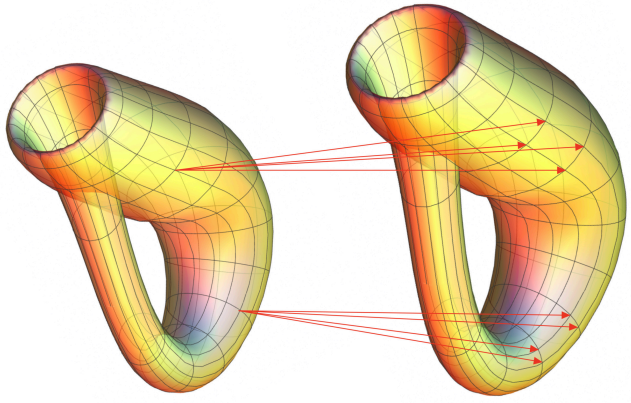

A decade later, Love, Filippenko, Maroulas, & Carlsson have made the Klein bottle as a topological input for designing convolutional layers in neural networks that learn image data.

Moreover, they have incorporated the tangent bundle of a Klein bottle into TCNNs for learning video data.

Both learnings achieved higher accuracies with smaller training sets.

- *Love, Filippenko, Maroulas, & Carlsson, Topological convolutional layers for deep learning,* ***Journal of Machine Learning Research****, 2023.*

## From visual perception to image data analysis, then to deep learning

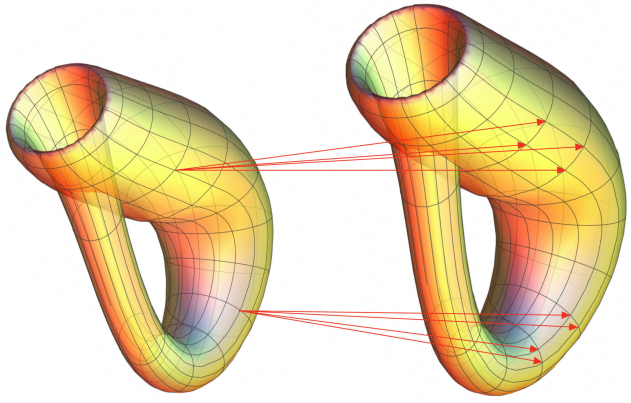

A decade later, Love, Filippenko, Maroulas, & Carlsson have made the Klein bottle as a topological input for designing convolutional layers in neural networks that learn image data.

Moreover, they have incorporated the tangent bundle of a Klein bottle into TCNNs for learning video data.

Both learnings achieved higher accuracies with smaller training sets.

- *Love, Filippenko, Maroulas, & Carlsson, Topological convolutional layers for deep learning,* ***Journal of Machine Learning Research****, 2023.*
- *Carlsson & Gabrielsson, Topological approaches to deep learning,* ***Topological Data Analysis: The Abel Symposium****, 2018.*

# From visual perception to image data analysis, then to deep learning

Topology of convolutional neural networks: Emergence of cycles during a training process

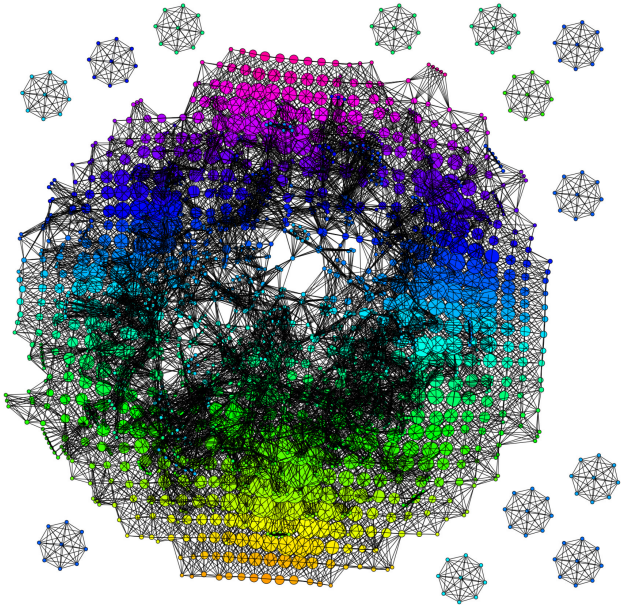

Untrained

Reproduced by Haiyu Zhang using GUDHI, after Carlsson & Gabrielsson

# From visual perception to image data analysis, then to deep learning

Topology of convolutional neural networks: Emergence of cycles during a training process

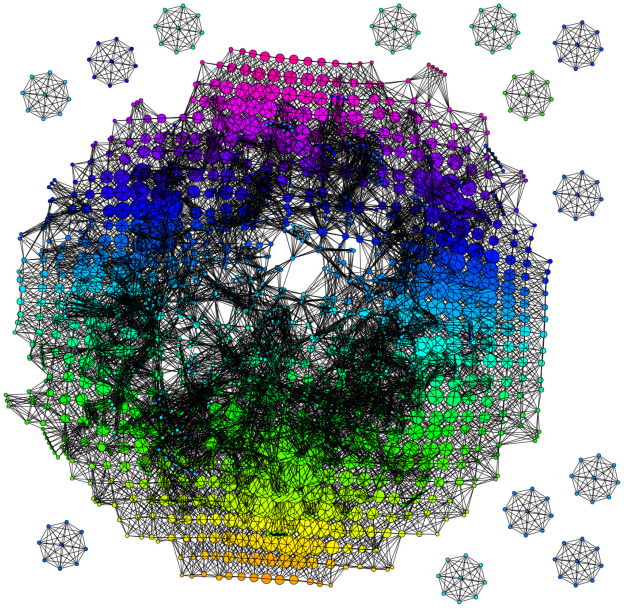

Untrained

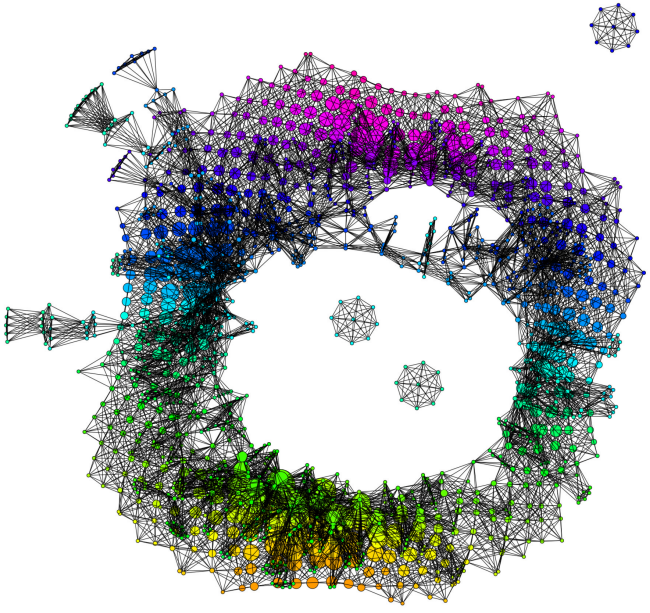

After 5 epochs

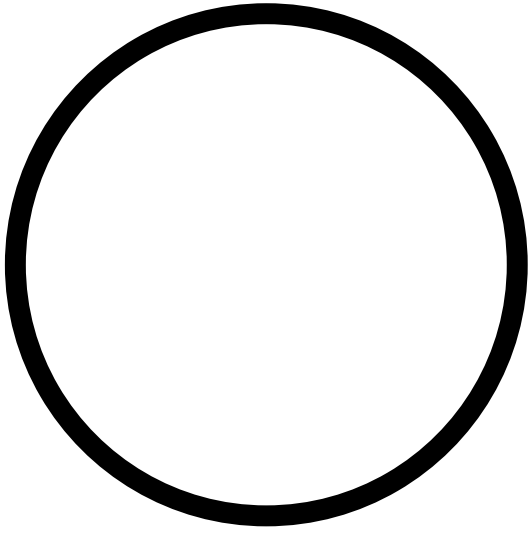

Reproduced by Haiyu Zhang using GUDHI, after Carlsson & Gabrielsson

# From visual perception to image data analysis, then to deep learning

Topology of convolutional neural networks: Emergence of cycles during a training process

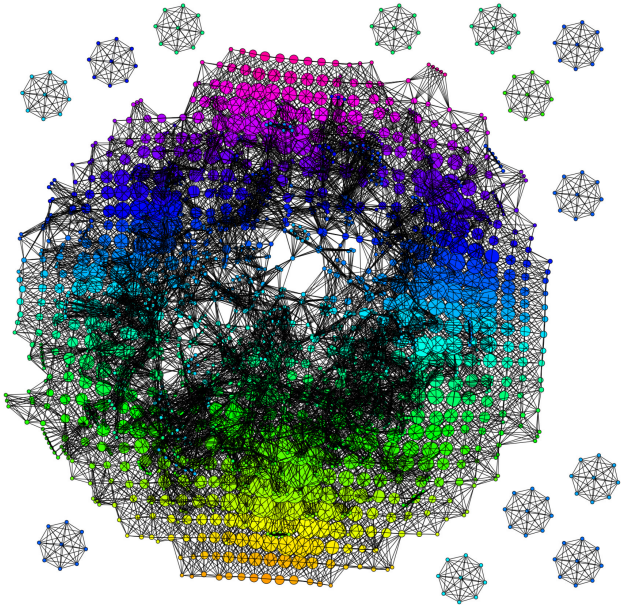

Untrained

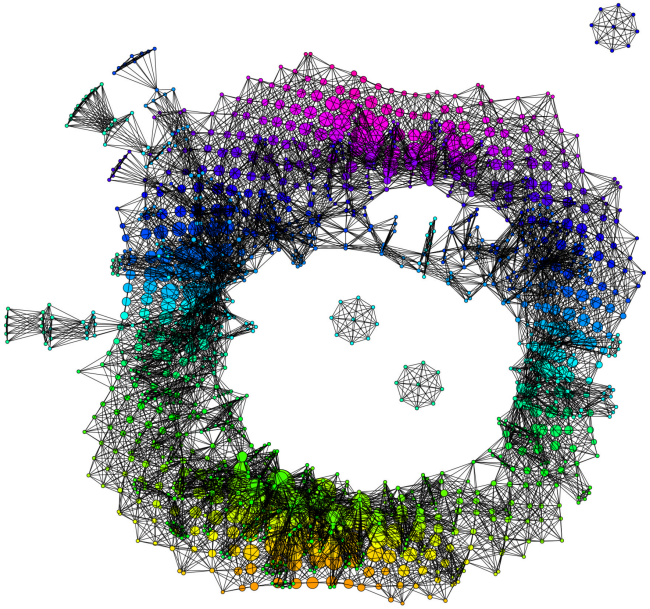

After 5 epochs

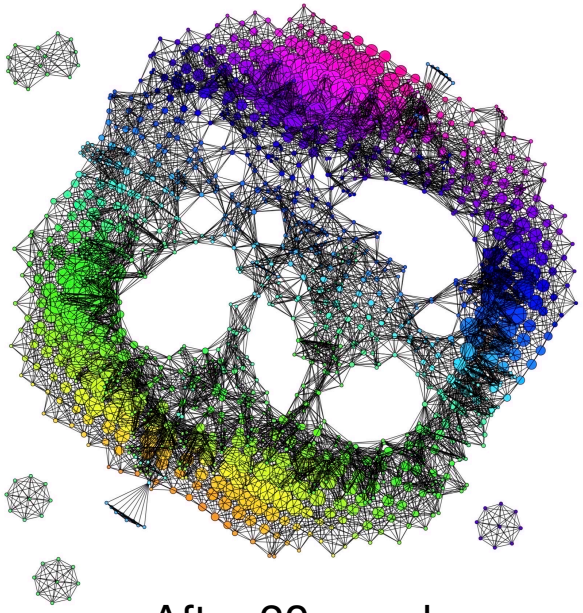

After 20 epochs

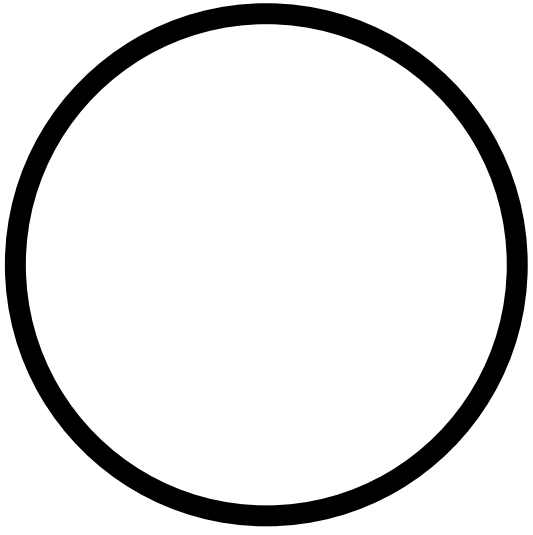

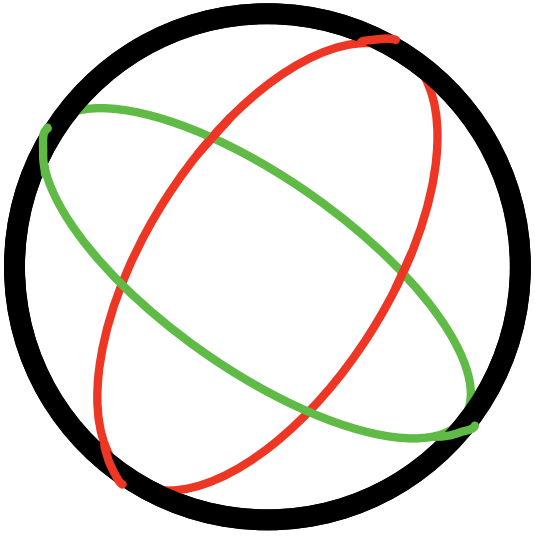

Reproduced by Haiyu Zhang using GUDHI, after Carlsson & Gabrielsson

## From visual to auditory perception

In 1966, Mark Kac asked the famous question:

**Can you hear the shape of a drum?**

## From visual to auditory perception

In 1966, Mark Kac asked the famous question:

**Can you hear the shape of a drum?**

To hear the shape of a drum is to deduce information about the shape of the drumhead from the sound it makes, using mathematical theory.

## From visual to auditory perception

In 1966, Mark Kac asked the famous question:

**Can you hear the shape of a drum?**

To hear the shape of a drum is to deduce information about the shape of the drumhead from the sound it makes, using mathematical theory.

Now, we mirror the question across senses and address instead:

## From visual to auditory perception

In 1966, Mark Kac asked the famous question:

**Can you hear the shape of a drum?**

To hear the shape of a drum is to deduce information about the shape of the drumhead from the sound it makes, using mathematical theory.

Now, we mirror the question across senses and address instead:

**Can you see the sound of a human speech?**

## From visual to auditory perception

In 1966, Mark Kac asked the famous question:

**Can you hear the shape of a drum?**

To hear the shape of a drum is to deduce information about the shape of the drumhead from the sound it makes, using mathematical theory.

Now, we mirror the question across senses and address instead:

**Can you see the sound of a human speech?**

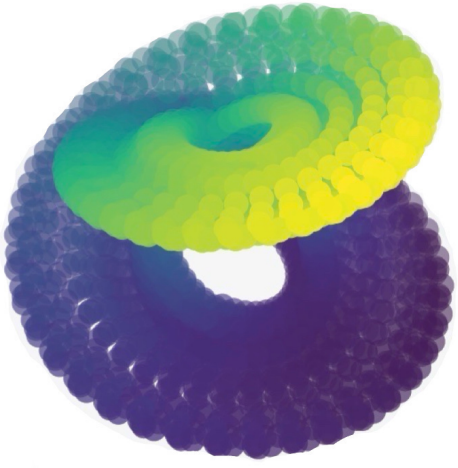

## Overview: context & summary

Topological speech (and audio) signal processing

## Overview: context & summary

Topological speech (and audio) signal processing

*time series data*

## Overview: context & summary

Topological speech (and audio) signal processing

*time series data*

*one of the essential components of AI*

## Overview: context & summary

Topological speech (and audio) signal processing, beyond direct biomimetic engineering

# Overview: context & summary

Topological speech (and audio) signal processing, beyond direct biomimetic engineering:

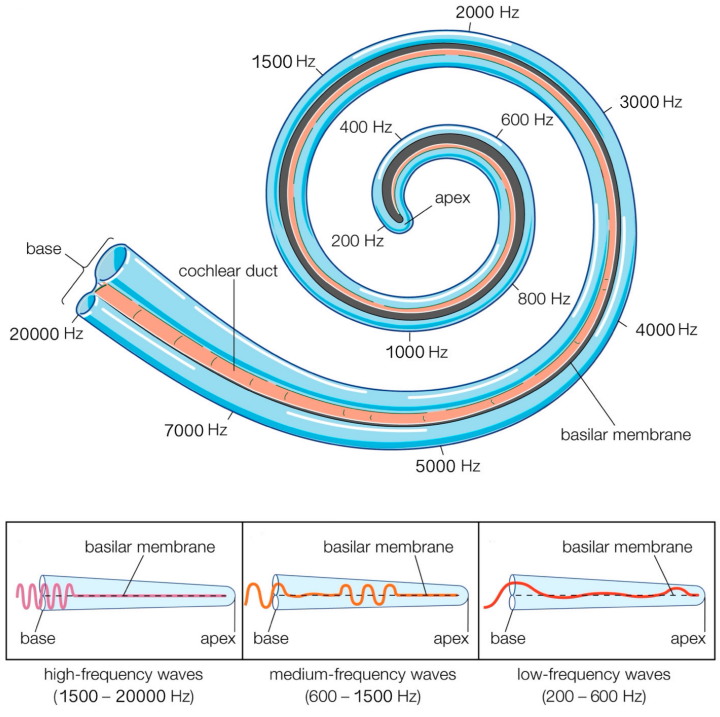


*Adapted from Encyclopædia Britannica*

Distribution of frequencies along the basilar membrane of the cochlea, which functions as a natural Fourier analysis device

# Overview: context & summary

Topological speech (and audio) signal processing, beyond direct biomimetic engineering: topological features vs. STFT

*short-time Fourier transform*

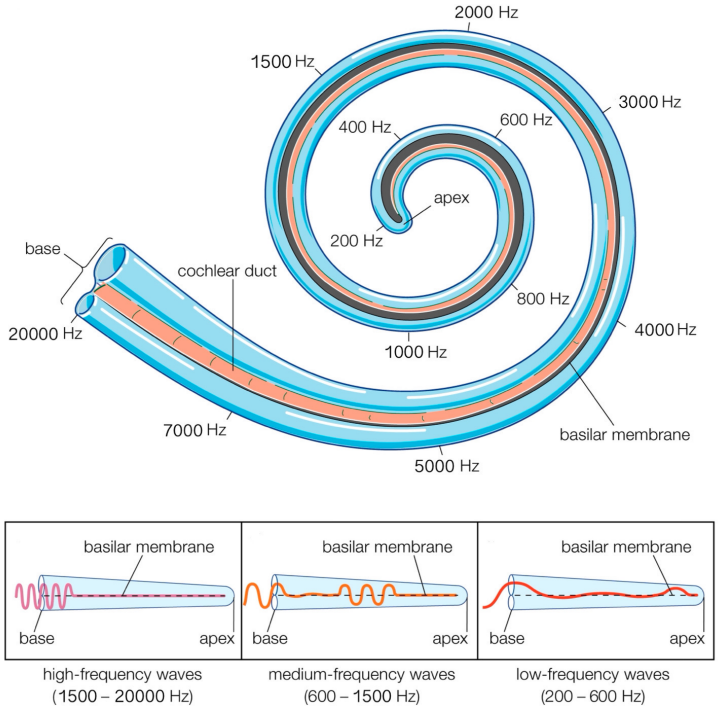


*Adapted from Encyclopædia Britannica*

Distribution of frequencies along the basilar membrane of the cochlea, which functions as a natural Fourier analysis device

# Overview: context & summary

Topological speech (and audio) signal processing, beyond direct biomimetic engineering: topological features vs. STFT/MFCC *mel-frequency cepstral coefficients*

*short-time Fourier transform*

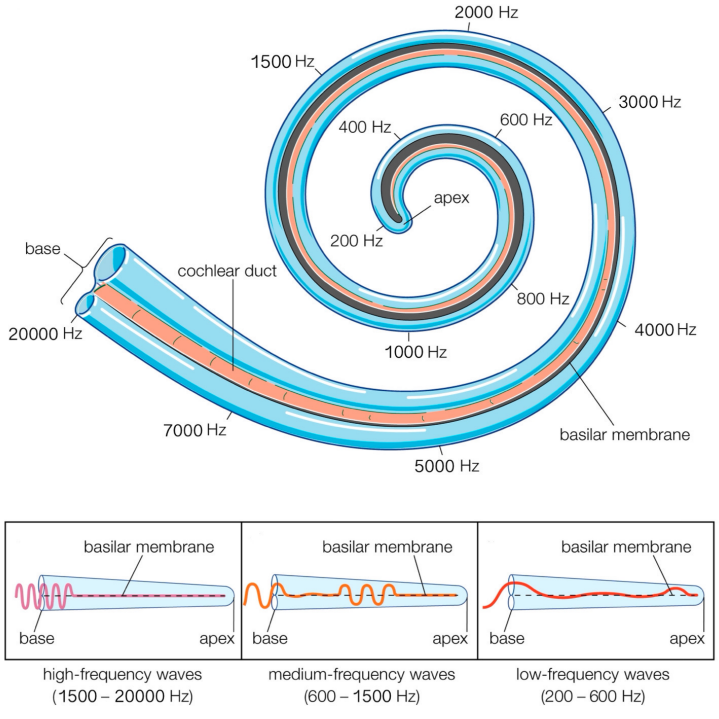


*Adapted from Encyclopædia Britannica*

Distribution of frequencies along the basilar membrane of the cochlea, which functions as a natural Fourier analysis device

## Overview: context & summary

Topological speech (and audio) signal processing, beyond direct biomimetic engineering: topological features vs. STFT/MFCC

Combination of TDA to ML *machine learning*

*topological data analysis*

## Overview: context & summary

Topological speech (and audio) signal processing, beyond direct biomimetic engineering: topological features vs. STFT/MFCC

Combination of TDA to ML:

1. TopCap
2. TopNN
3. TopKer

## Overview: context & summary

Topological speech (and audio) signal processing, beyond direct biomimetic engineering: topological features vs. STFT/MFCC

Combination of TDA to ML:

1. TopCap *capability of capturing topological structures of data*
2. TopNN
3. TopKer

## Overview: context & summary

Topological speech (and audio) signal processing, beyond direct biomimetic engineering: topological features vs. STFT/MFCC

Combination of TDA to ML:

1. TopCap *capability of capturing topological structures of data*
2. TopNN *topology-enhanced neural network*
3. TopKer

## Overview: context & summary

Topological speech (and audio) signal processing, beyond direct biomimetic engineering: topological features vs. STFT/MFCC

Combination of TDA to ML:

1. TopCap *capability of capturing topological structures of data*
2. TopNN *topology-enhanced neural network*
3. TopKer *topology-informed convolution kernel*

## Overview: context & summary

Topological speech (and audio) signal processing, beyond direct biomimetic engineering: topological features vs. STFT/MFCC

Combination of TDA to ML:

1. TopCap: stands in comparison, datasets + models
2. TopNN
3. TopKer

## Overview: context & summary

Topological speech (and audio) signal processing, beyond direct biomimetic engineering: topological features vs. STFT/MFCC

Combination of TDA to ML:

1. TopCap: stands in comparison, datasets + models
2. TopNN
3. TopKer

## Overview: context & summary

Topological speech (and audio) signal processing, beyond direct biomimetic engineering: topological features vs. STFT/MFCC

Combination of TDA to ML:

1. TopCap: stands in comparison, datasets + models
2. TopNN
3. TopKer

## Overview: context & summary

Topological speech (and audio) signal processing, beyond direct biomimetic engineering: topological features vs. STFT/MFCC

Combination of TDA to ML:

1. TopCap: stands in comparison, datasets + models
2. TopNN: outperforms, accuracy + convergence of loss function + steadiness + robustness against noise
3. TopKer

## Overview: context & summary

Topological speech (and audio) signal processing, beyond direct biomimetic engineering: topological features vs. STFT/MFCC

Combination of TDA to ML:

1. TopCap: stands in comparison, datasets + models
2. TopNN: outperforms, accuracy + convergence of loss function + steadiness + robustness against noise
3. TopKer

## Overview: context & summary

Topological speech (and audio) signal processing, beyond direct biomimetic engineering: topological features vs. STFT/MFCC

Combination of TDA to ML:

1. TopCap: stands in comparison, datasets + models
2. TopNN: outperforms, accuracy + convergence of loss function + steadiness + robustness against noise
3. TopKer: superior performance + cross-domain adaptability

*phoneme recognition*

## Overview: context & summary

Topological speech (and audio) signal processing, beyond direct biomimetic engineering: topological features vs. STFT/MFCC

Combination of TDA to ML:

1. TopCap: stands in comparison, datasets + models
2. TopNN: outperforms, accuracy + convergence of loss function + steadiness + robustness against noise
3. TopKer: superior performance + cross-domain adaptability

*phoneme recognition* *other audio and visual recognition tasks*

## Periodic phenomena: a motivating example

Let $T^2 = (\mathbb{R}/\mathbb{Z})^2$ be the 2D torus. Consider the dynamical system given by

$$\begin{aligned} \Phi_\sigma \colon T^2 \times \mathbb{R} &\to T^2 \\ \big((a,b),t\big) &\mapsto (a+t, b+\sigma t) \end{aligned}$$

## Periodic phenomena: a motivating example

Let $T^2 = (\mathbb{R}/\mathbb{Z})^2$ be the 2D torus. Consider the dynamical system given by

$$\Phi_\sigma : T^2 \times \mathbb{R} \to T^2$$
$$\big((a, b), t\big) \mapsto (a + t, b + \sigma t)$$

If $\sigma$ is rational, then every orbit is periodic.

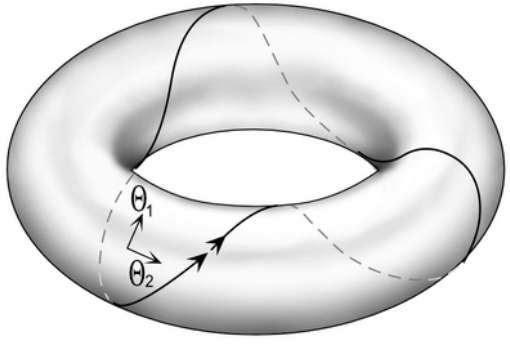

## Periodic phenomena: a motivating example

Let $T^2 = (\mathbb{R}/\mathbb{Z})^2$ be the 2D torus. Consider the dynamical system given by

$$\Phi_\sigma : T^2 \times \mathbb{R} \to T^2$$
$$\big((a, b), t\big) \mapsto (a + t, b + \sigma t)$$

If $\sigma$ is rational, then every orbit is periodic. Otherwise every orbit is dense in $T^2$.

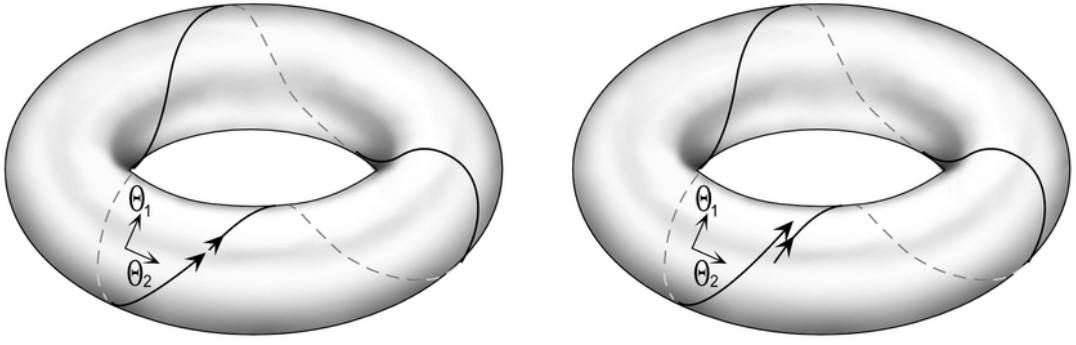


*rational σ* *irrational σ*

## Periodic phenomena: a motivating example

Let $T^2 = (\mathbb{R}/\mathbb{Z})^2$ be the 2D torus. Consider the dynamical system given by

$$\Phi_\sigma \colon T^2 \times \mathbb{R} \to T^2$$
$$\big((a,b),t\big) \mapsto (a+t, b+\sigma t)$$

If $\sigma$ is rational, then every orbit is periodic. Otherwise every orbit is dense in $T^2$.

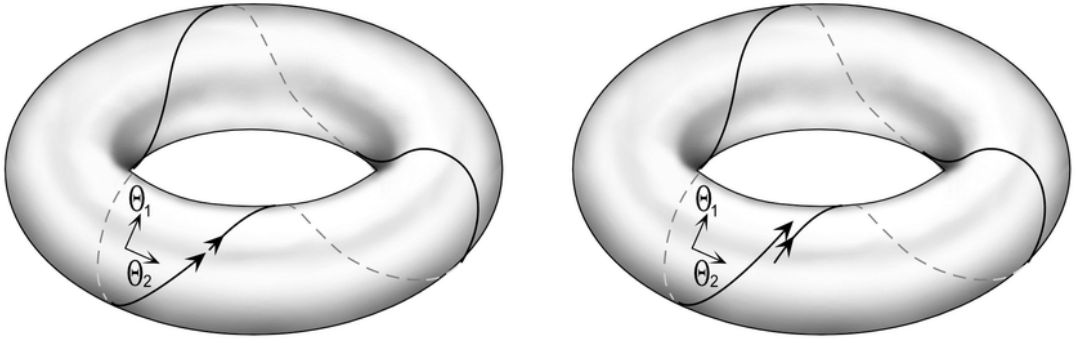


*rational σ* *irrational σ*

## From time series to topological shapes

Most periodic time series can be realized by a topological circle $S^1$ embedded in a Euclidean space of higher dimension.

## Topological time series analysis

Let us make the assumption that sampled signals are distributed over a manifold (!)

## Topological time series analysis

Let us make the assumption that sampled signals are distributed over a manifold (!) To topologically analyze time series, we then proceed as follows:

Step 1 Embed the data into a Euclidean space of suitable dimension

## Topological time series analysis

Let us make the assumption that sampled signals are distributed over a manifold (!) To topologically analyze time series, we then proceed as follows:

Step 1 Embed the data into a Euclidean space of suitable dimension;

Step 2 Compute the algebraic invariants for statistical inference.

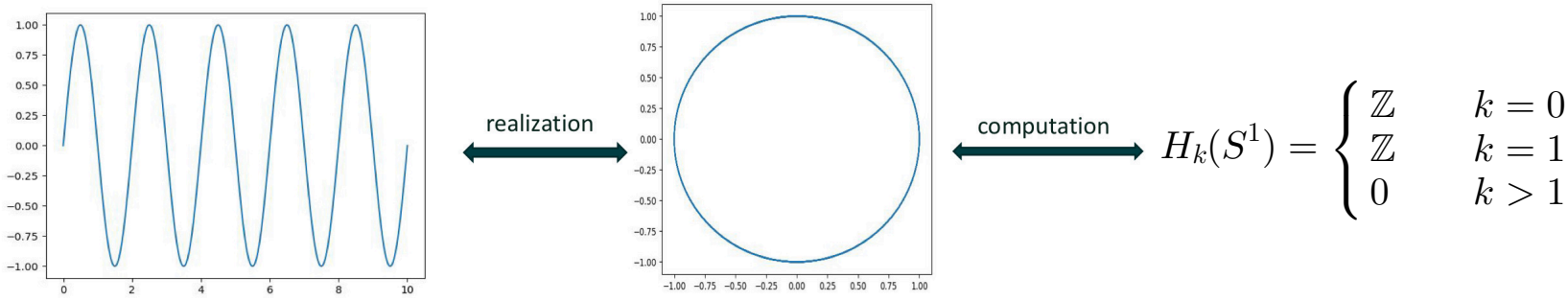

# Topological time series analysis

Let us make the assumption that sampled signals are distributed over a manifold (!) To topologically analyze time series, we then proceed as follows:

Step 1 Embed the data into a Euclidean space of suitable dimension;

Step 2 Compute the algebraic invariants for statistical inference.

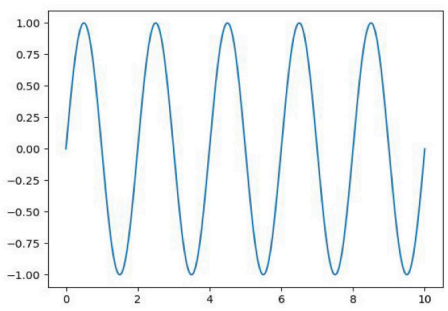

realization

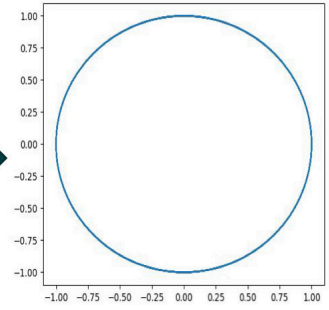

computation

$$H_k(S^1) = \begin{cases} \mathbb{Z} & k = 0 \\ \mathbb{Z} & k = 1 \\ 0 & k > 1 \end{cases}$$

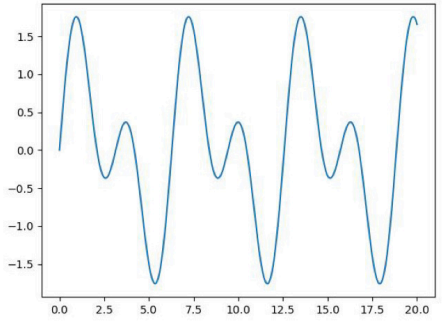

not an embedding

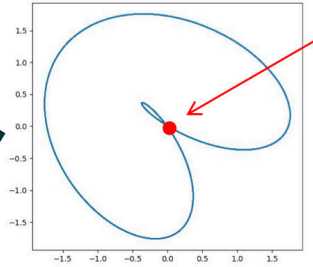

self-intersection

2D

# Topological time series analysis

Let us make the assumption that sampled signals are distributed over a manifold (!) To topologically analyze time series, we then proceed as follows:

Step 1 Embed the data into a Euclidean space of suitable dimension;

Step 2 Compute the algebraic invariants for statistical inference.

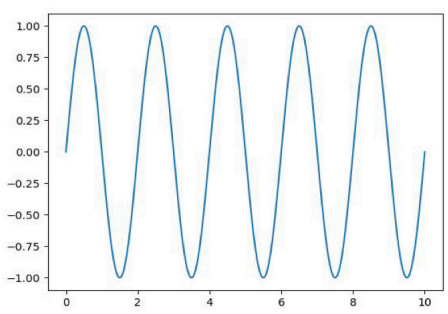

realization

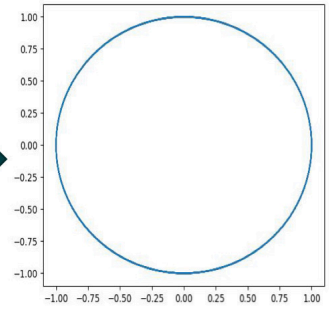

computation

$$H_k(S^1) = \begin{cases} \mathbb{Z} & k = 0 \\ \mathbb{Z} & k = 1 \\ 0 & k > 1 \end{cases}$$

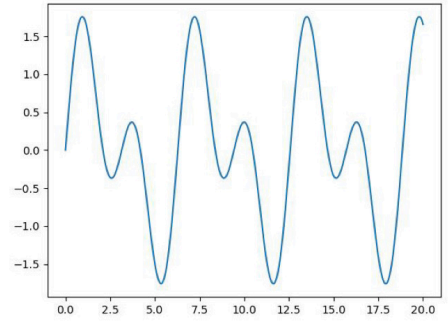

not an embedding

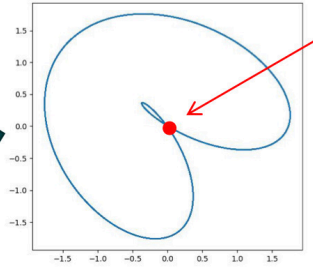

self-intersection

2D

a topological circle

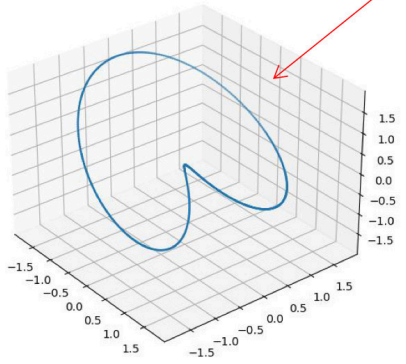

3D

an embedding (preserves topological information)

## Topological time series analysis

Let us make the assumption that sampled signals are distributed over a manifold (!) To topologically analyze time series, we then proceed as follows:

Step 1 Embed the data into a Euclidean space of suitable dimension;

Step 2 Compute the algebraic invariants for statistical inference.

Perea, *Topological time series analysis*, **Notices of the American Mathematical Society**, 2019.

Perea & Harer, *Sliding windows and persistence: An application of topological methods to signal analysis*, **Foundations of Computational Mathematics**, 2015.

# An application: detection of wheeze in medical science (pulmonology)

wheeze

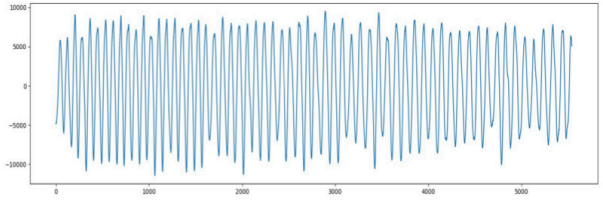


normal

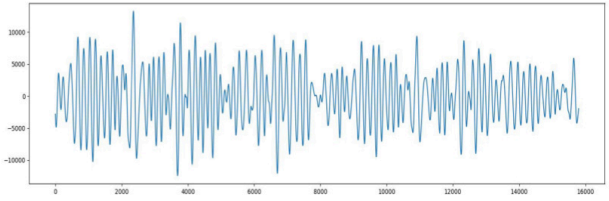


Original sound signals

# An application: detection of wheeze in medical science (pulmonology)

wheeze

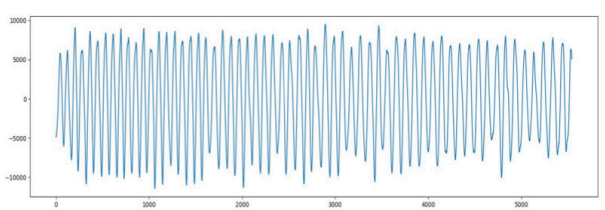

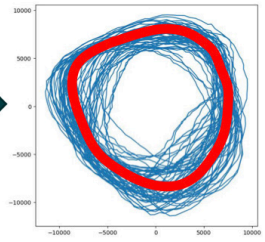

normal

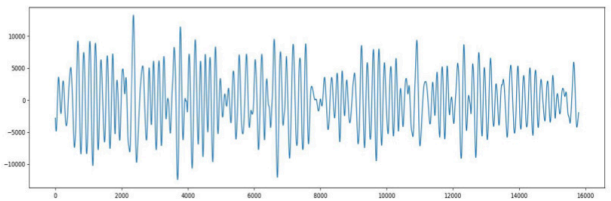

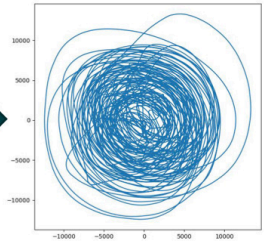

Original sound signals

Realized topological shapes embedded in 2D Euclidean space

# An application: detection of wheeze in medical science (pulmonology)

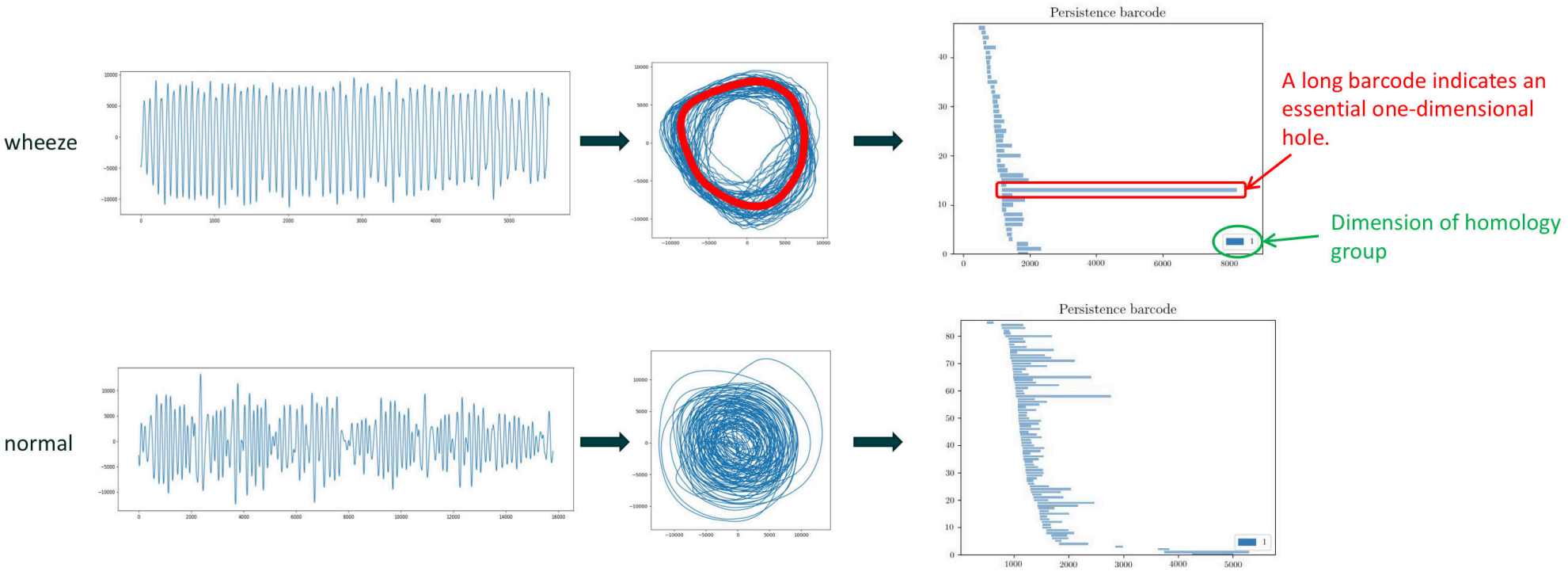


Original sound signals

Realized topological shapes embedded in 2D Euclidean space

Persistence barcodes as representations of the algebraic invariant (1D homology group)

Emrani, Gentimis, & Krim *Persistent homology of delay embeddings and its application to wheeze detection*, **IEEE Signal Processing Letters**, 2014.

# A pipeline for topological time series analysis

Time series data: $x_1, x_2, x_3, x_4, \ldots$

# A pipeline for topological time series analysis

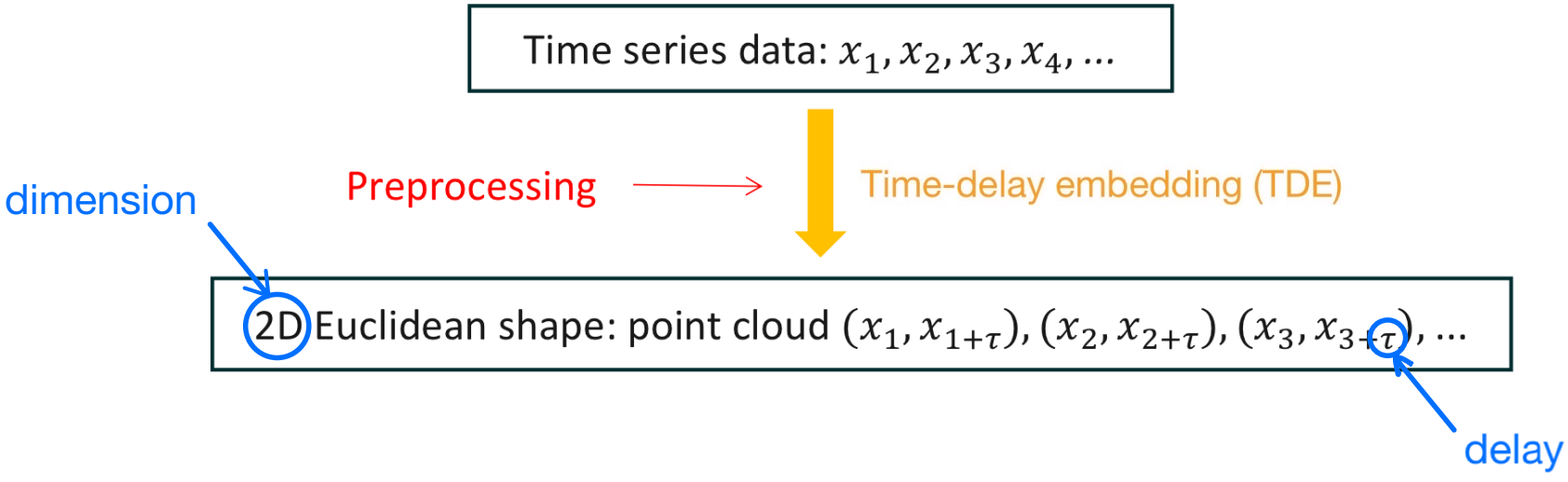

# A pipeline for topological time series analysis

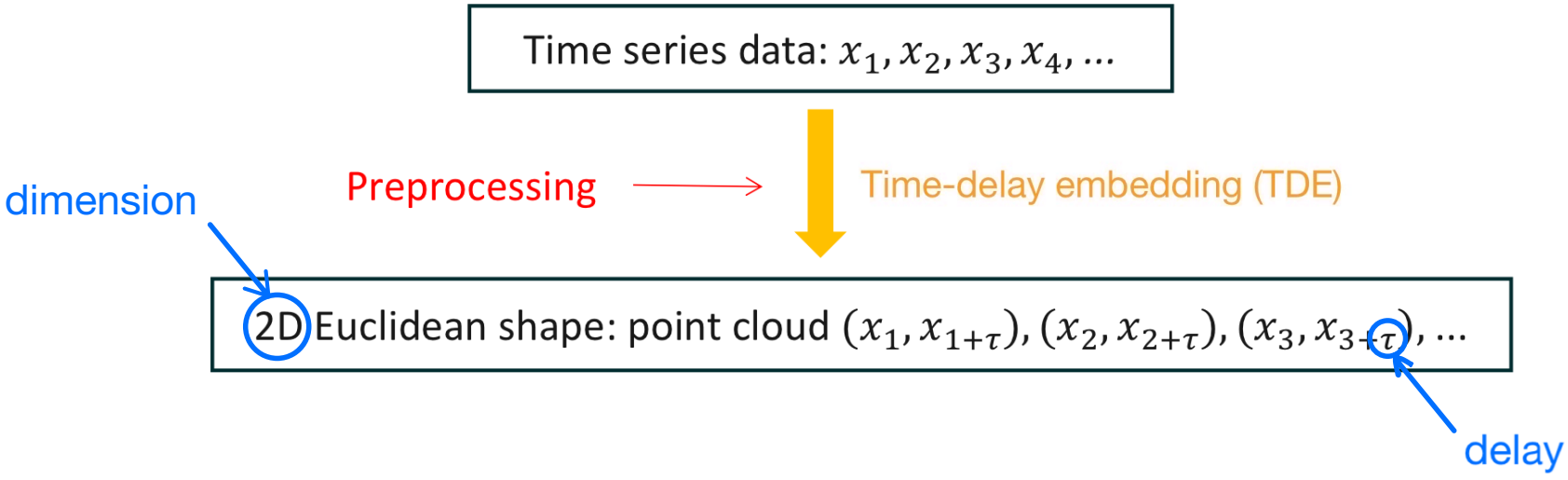


Euclidean embedding of time series data dates back to Takens's work on fluid turbulence.

Theorem (Takens 1981). Let $M$ be a compact manifold of dimension $n$. Given pairs $(\phi, y)$ with $\phi : M \to M$ a smooth diffeomorphism and $y : M \to \mathbb{R}$ a smooth function, it is a generic property that the map $\Phi_{(\phi, y)} : M \to \mathbb{R}^{2n+1}$ defined by

$$\Phi_{(\varphi,y)}(x) = \left(y(x), y(\varphi(x)), \ldots, y(\varphi^{2n}(x))\right)$$

is an embedding.

# A pipeline for topological time series analysis

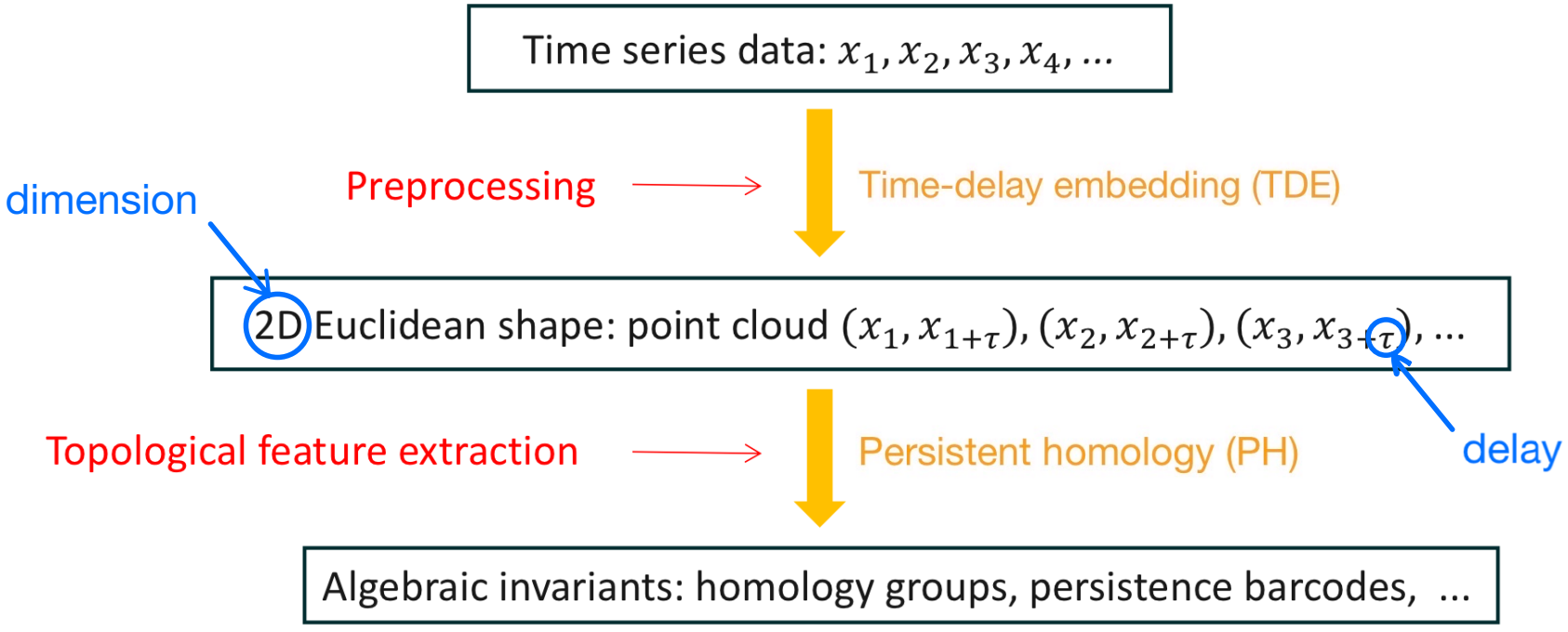

# A pipeline for topological time series analysis

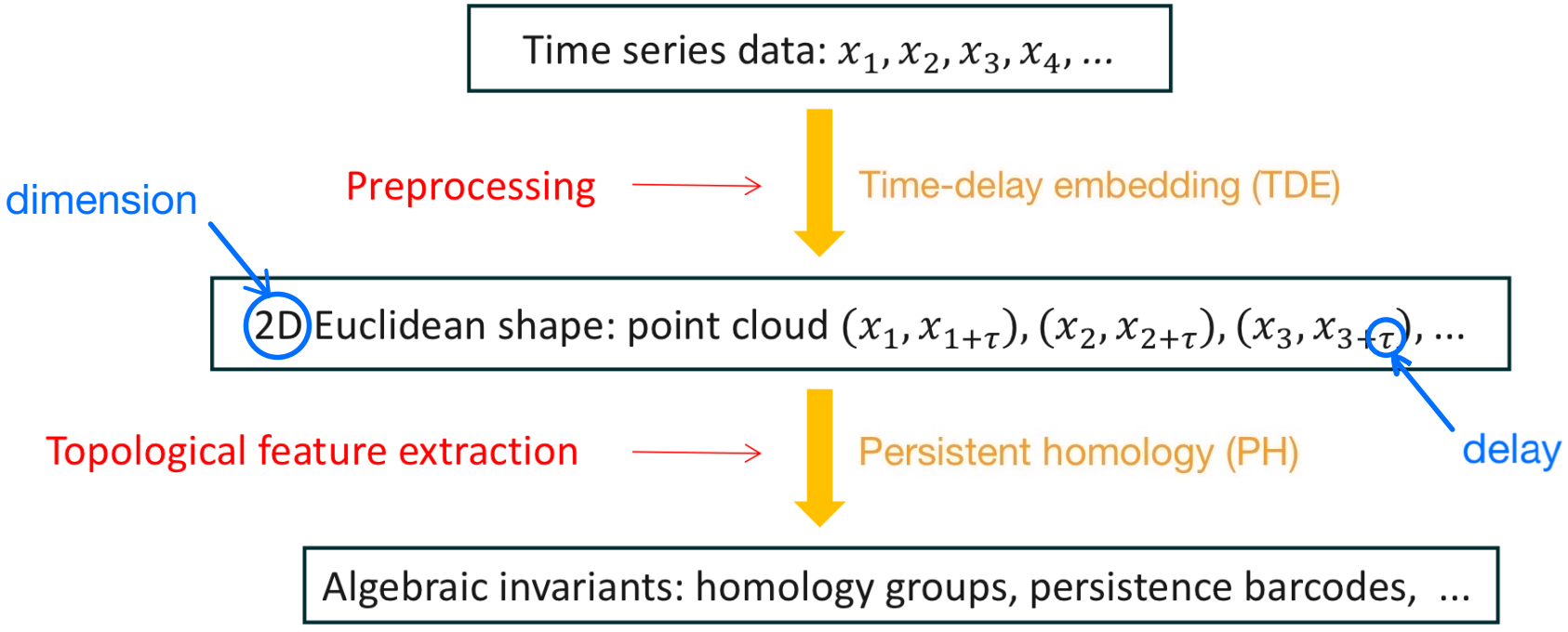


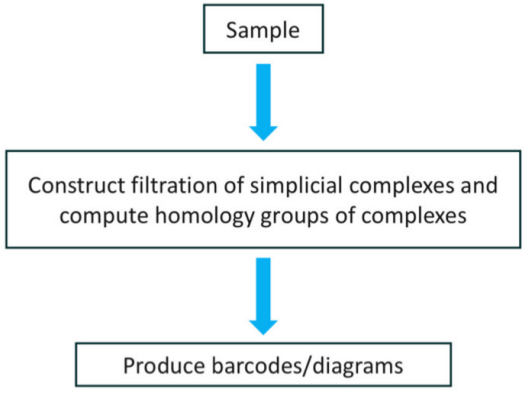


How filtration through varying distance measure reveals essential topological features

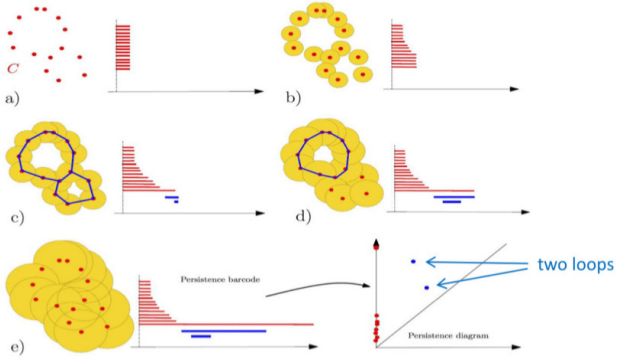

# A pipeline for topological time series analysis

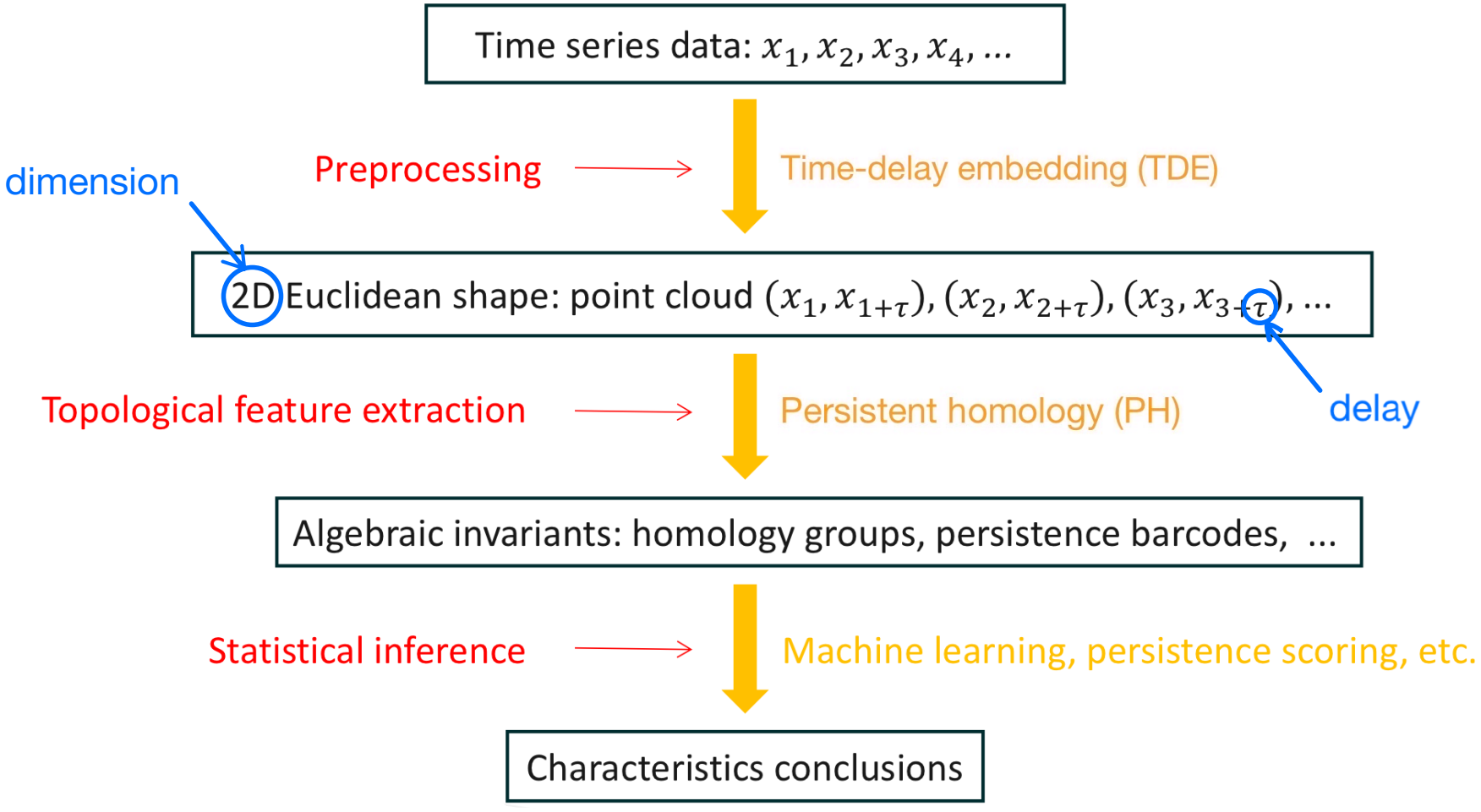

## Classification of speech signals

In consultation with Meng Yu of Tencent AI Lab, we applied topological methods to classify voiced/voiceless and vowel/consonant speech data

## Classification of speech signals

In consultation with Meng Yu of Tencent AI Lab, we applied topological methods to classify voiced/voiceless and vowel/consonant speech data, with motivations from industrial applications, including medical diagnosis, neurophysiology, speaker identification and other AI innovations.

## Classification of speech signals

In consultation with Meng Yu of Tencent AI Lab, we applied topological methods to classify voiced/voiceless and vowel/consonant speech data, with motivations from industrial applications, including medical diagnosis, neurophysiology, speaker identification and other AI innovations.

## Spectrograms

There are speech signal processing softwares for professional use.

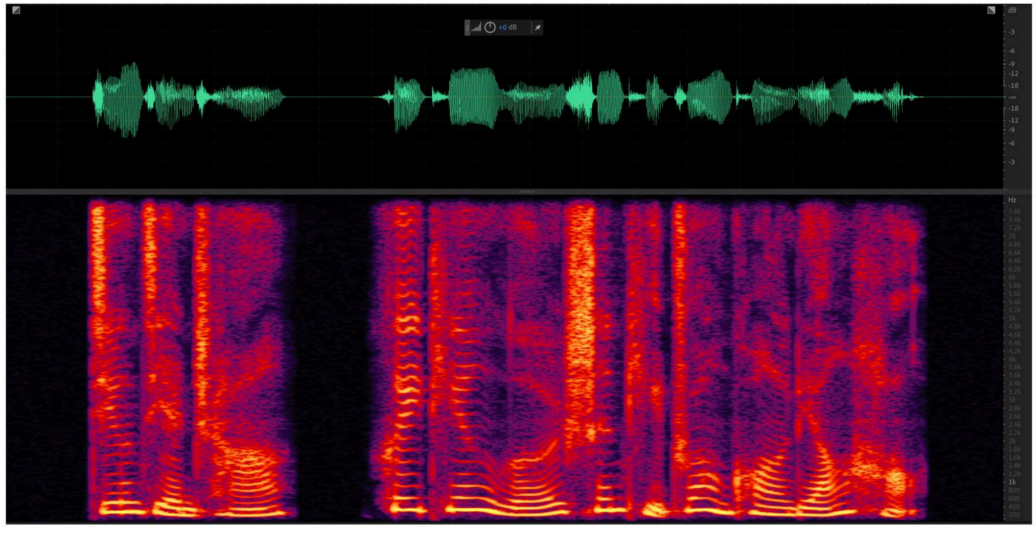

## Classification of speech signals

In consultation with Meng Yu of Tencent AI Lab, we applied topological methods to classify voiced/voiceless and vowel/consonant speech data, with motivations from industrial applications, including medical diagnosis, neurophysiology, speaker identification and other AI innovations.

## Spectrograms

There are speech signal processing softwares for professional use.

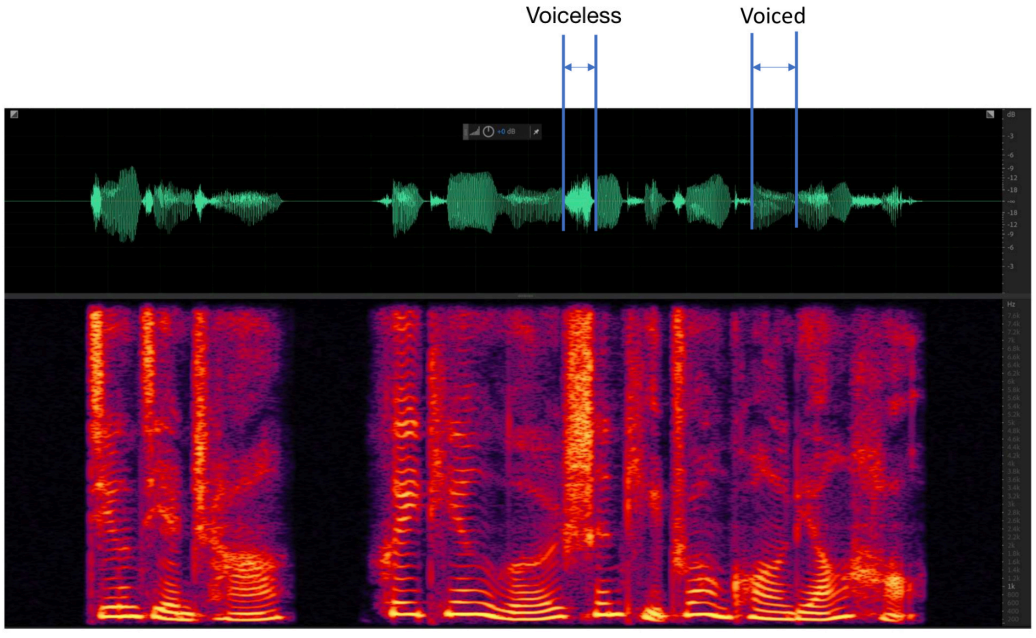

# Classification of speech signals

Sinusoid in time domain

## Voiced

[ŋ], [m], [n], [j], [l], [v], [ʒ], *etc.*

Harmonics in frequency domain

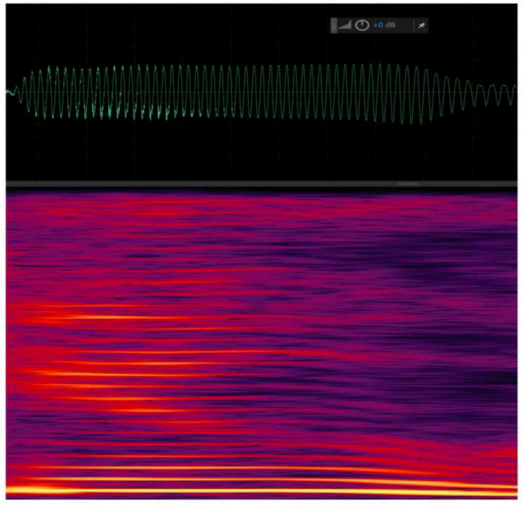

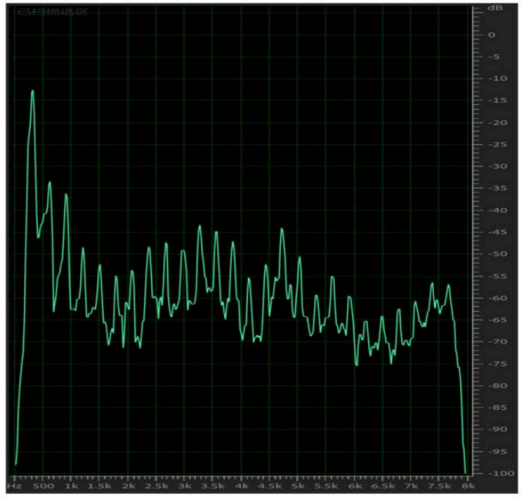

Time and Time-Frequency domain

Frequency response

Like a white noise

## Voiceless

[f], [k], [θ], [t], [s], [tʃ], *etc.*

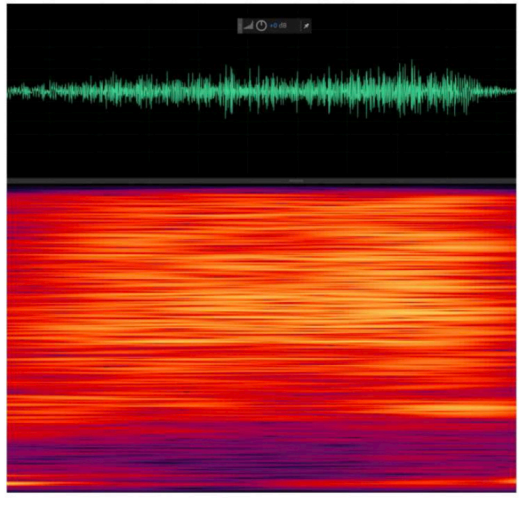

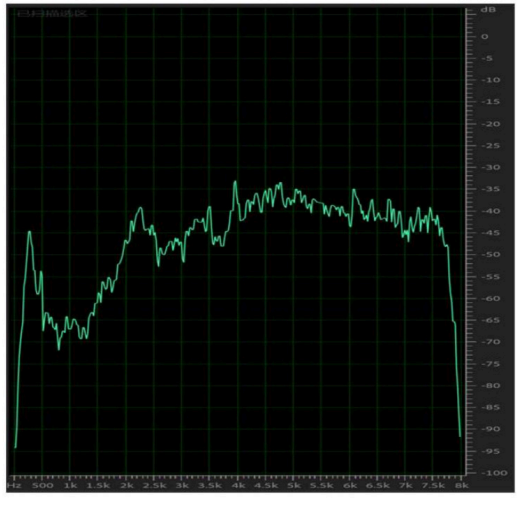

# Classification of speech signals

## Voiced

*exhibit periodic waveforms resulting from glottal vibrations*

Sinusoid in time domain

Harmonics in frequency domain

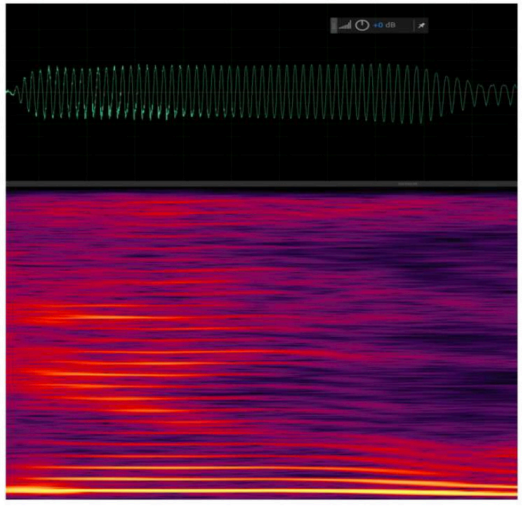

Time and Time-Frequency domain

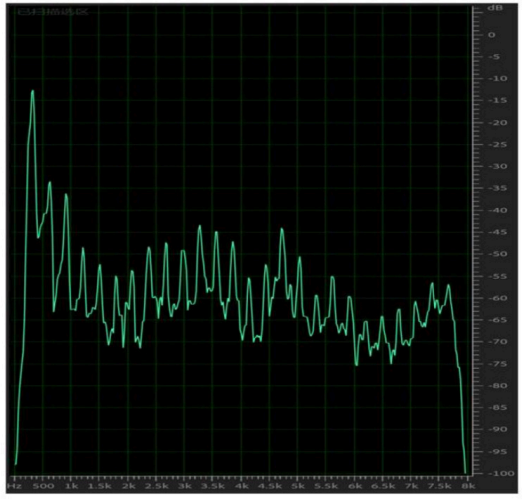

Frequency response

## Voiceless

*predominantly characterized by aperiodic, turbulence-induced noise*

Like a white noise

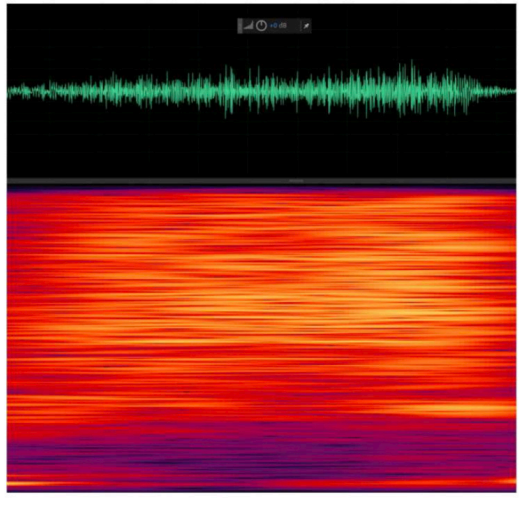

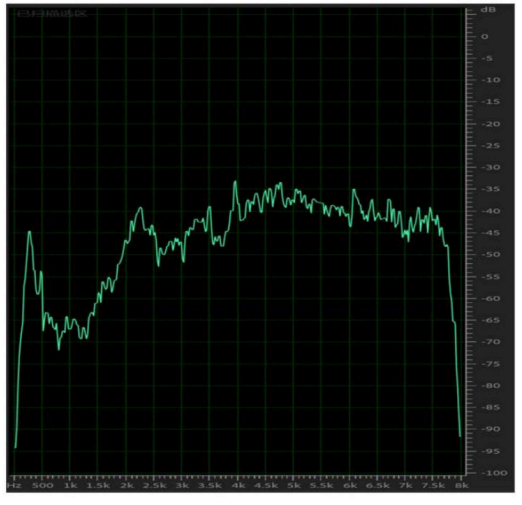

## Primary experiments combining topological features with ML models

Here is a flowchart for our method of TopCap:

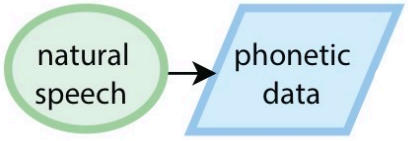

# Primary experiments combining topological features with ML models

Here is a flowchart for our method of TopCap:

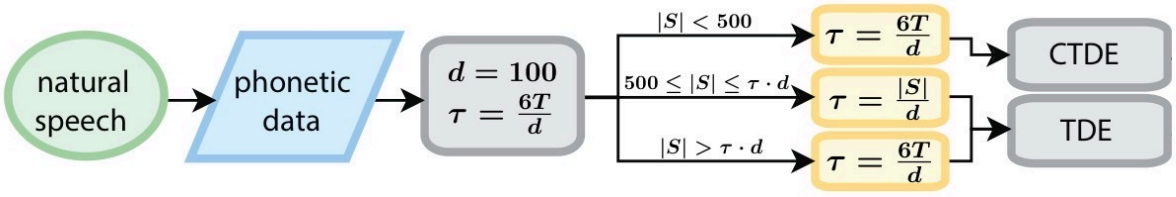

# Primary experiments combining topological features with ML models

Here is a flowchart for our method of TopCap:

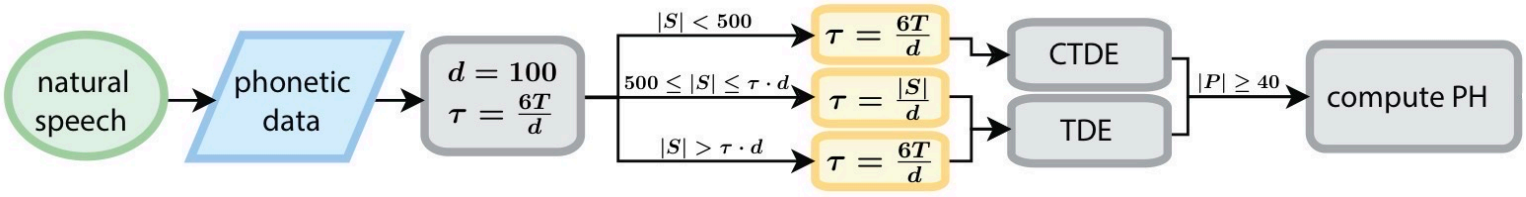

# Primary experiments combining topological features with ML models

Here is a flowchart for our method of TopCap:

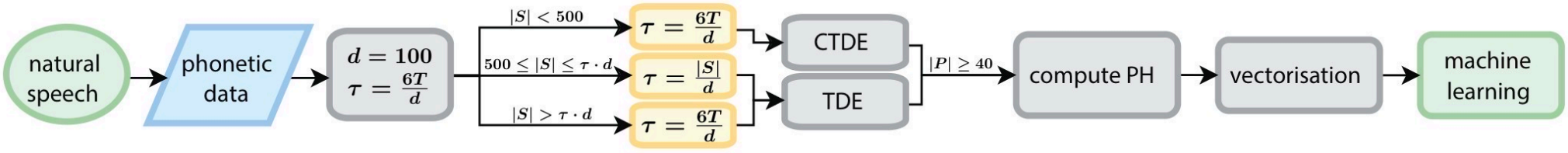

# Primary experiments combining topological features with ML models

Here is a flowchart for our method of TopCap:

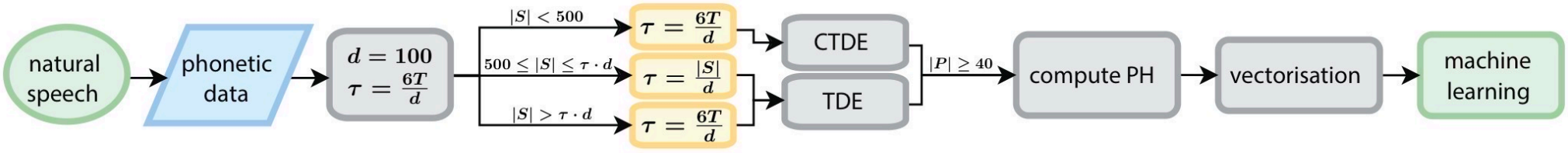


# Topological profiles for vowels and consonants

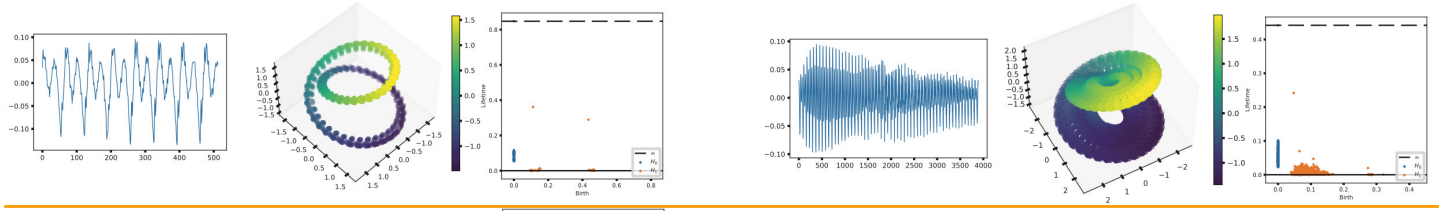

*vowels*

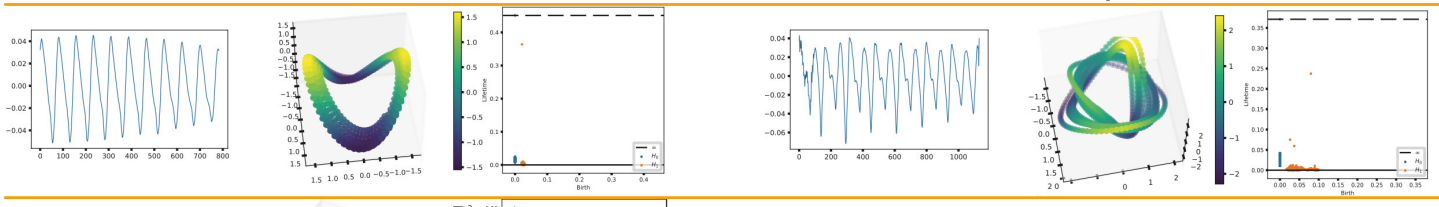

*voiced consonants*

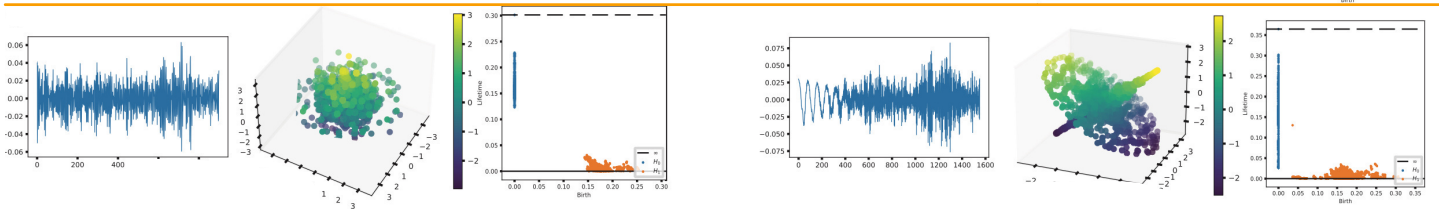

*voiceless consonants*

# Primary experiments combining topological features with ML models

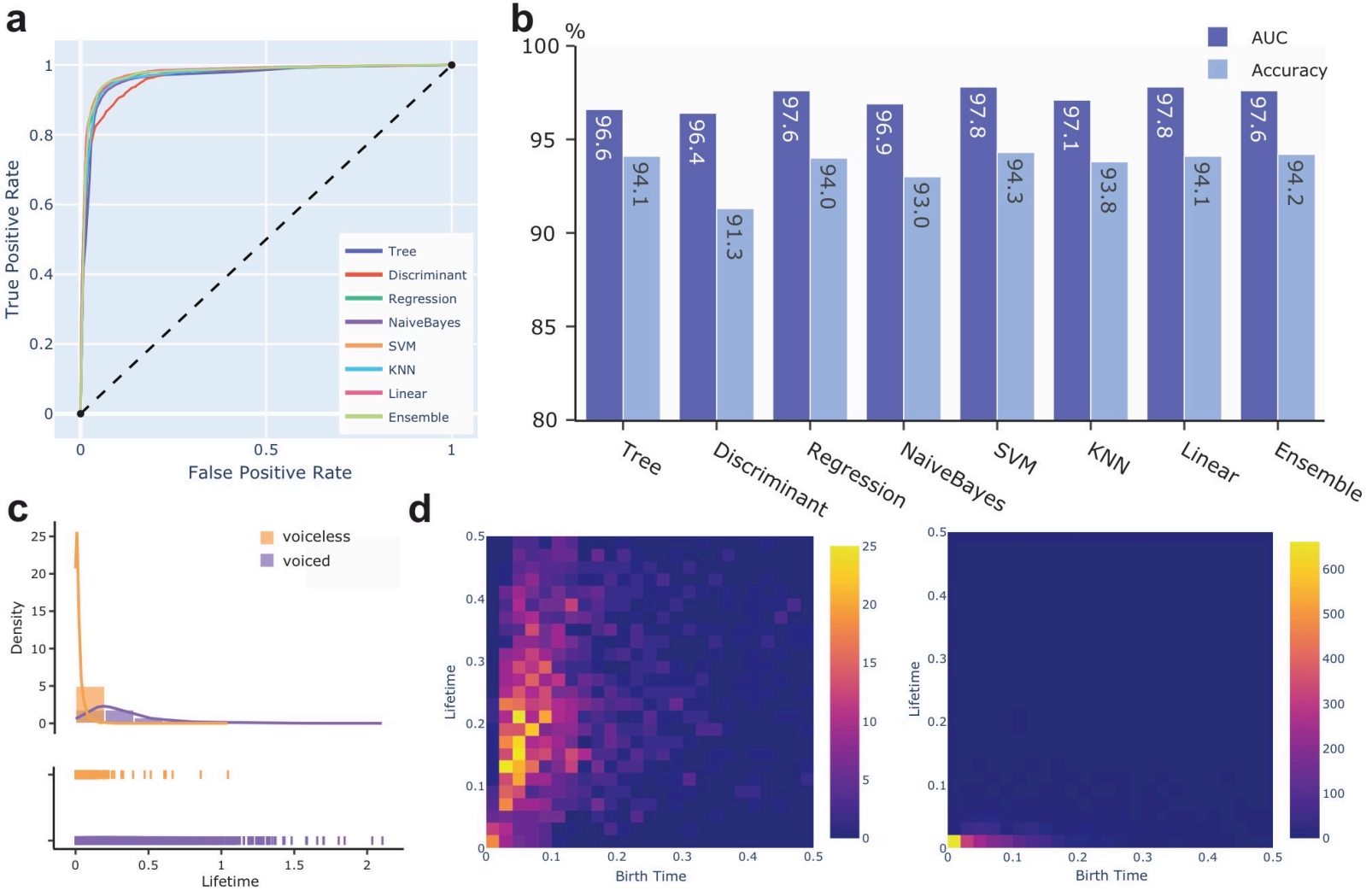


*Results of machine learning topological features*

# Primary experiments combining topological features with ML models

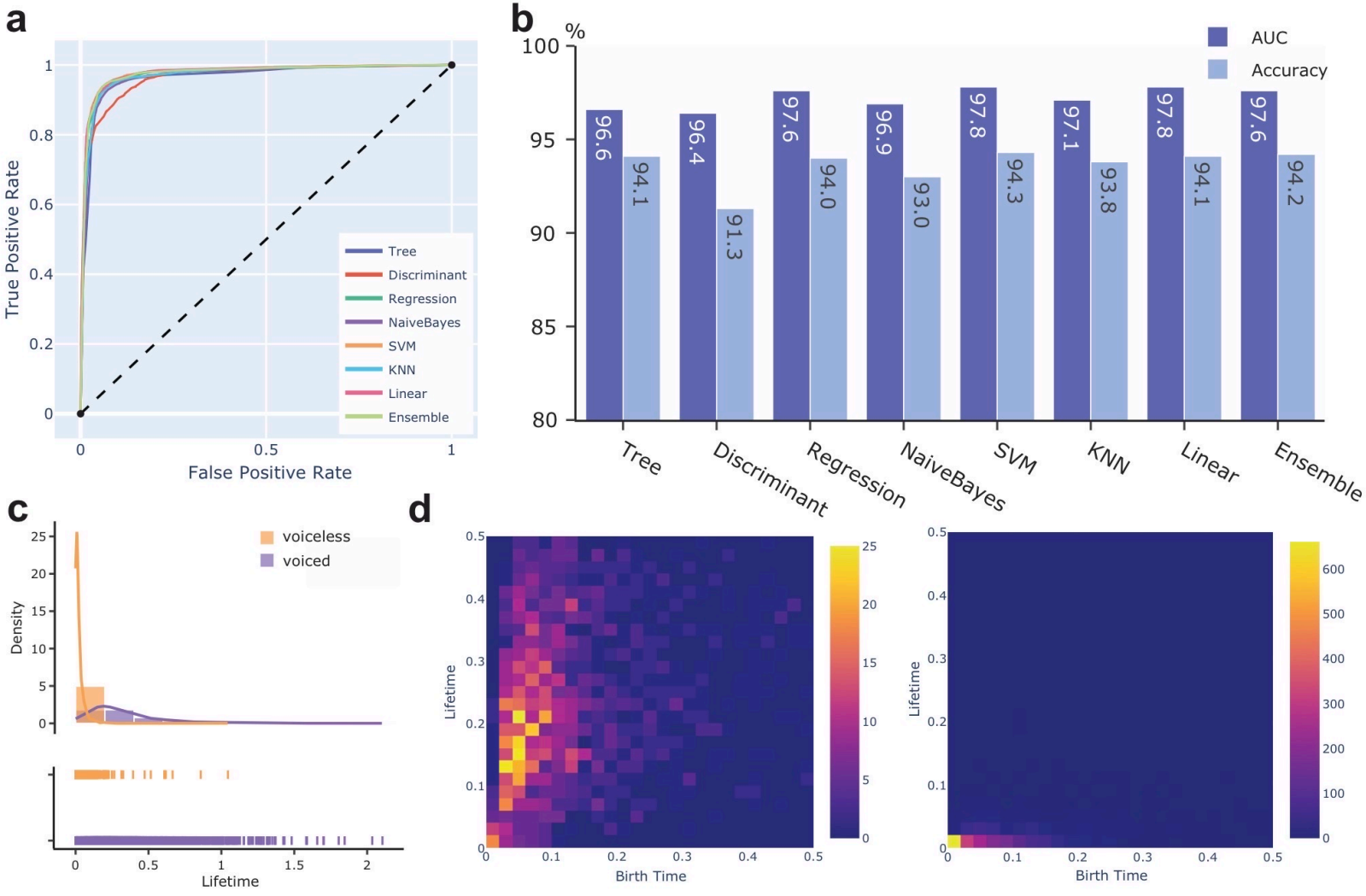


*Results of machine learning topological features*

***a**, Receiver operating characteristic curves of traditional machine learning algorithms.*

# Primary experiments combining topological features with ML models

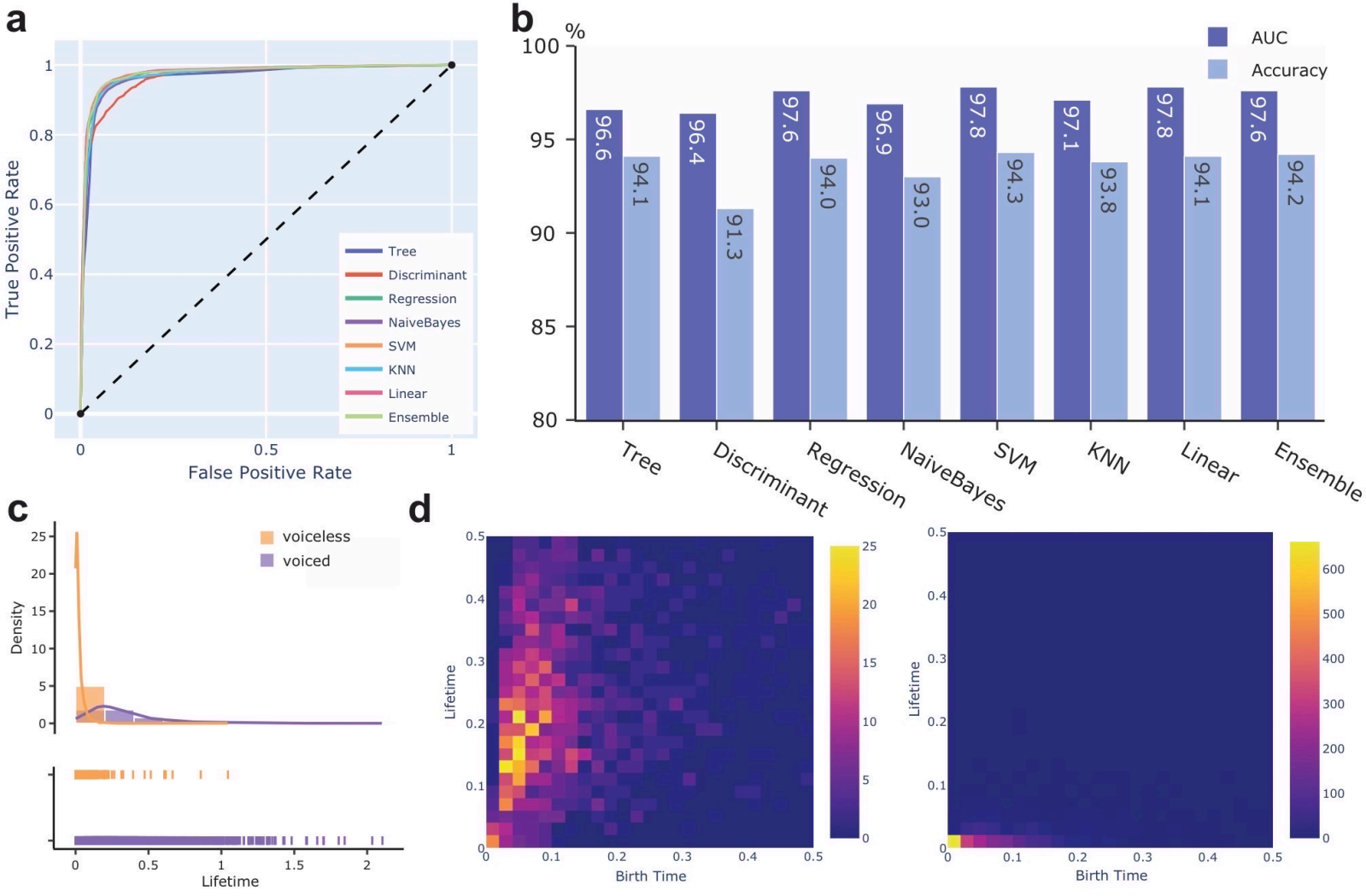


*Results of machine learning topological features*

***b**, Accuracy and area under the curve of each of these algorithms.*

# Primary experiments combining topological features with ML models

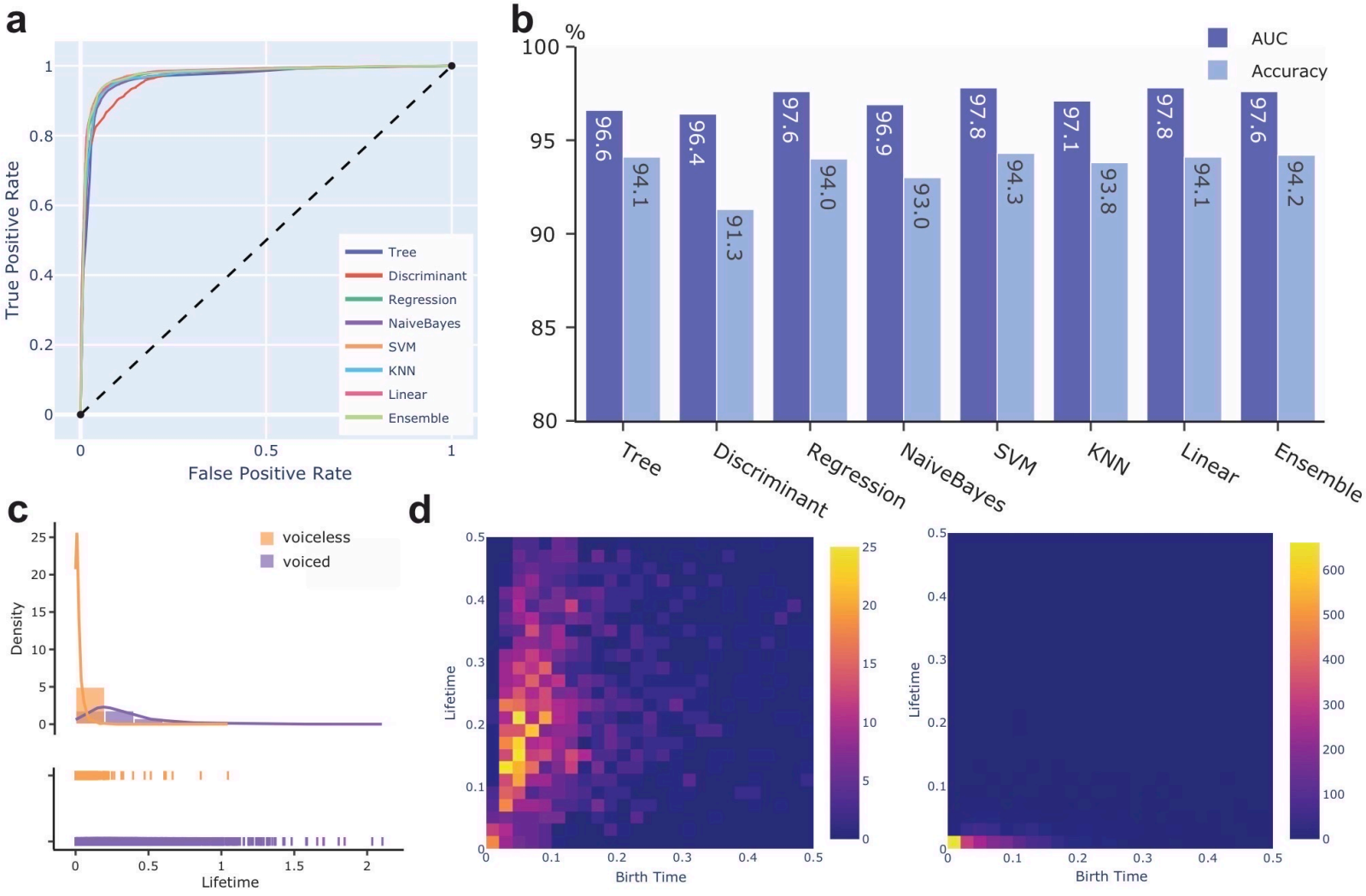


*Results of machine learning topological features*

***c**, Histograms of records represented by their PH-lifetime for voiced and voiceless consonants, together with kernel density estimation and rug plot. The distributions of maximal persistence can distinguish voiced and voiceless consonants.*

# Primary experiments combining topological features with ML models

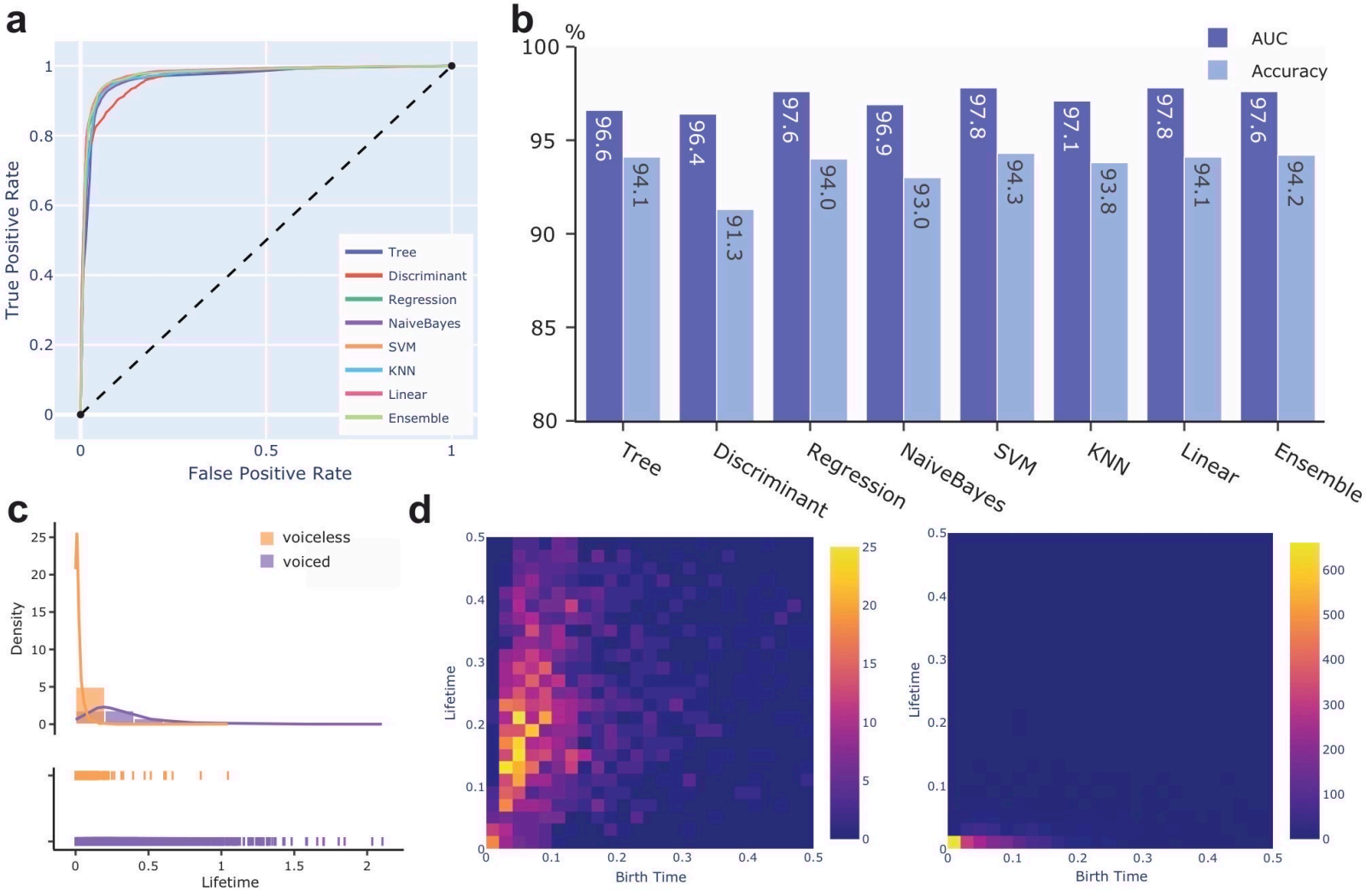


*Results of machine learning topological features*
***d**, Diagrams of records represented as (birth time, lifetime) for voiced consonants (left) and voiceless consonants (right), where voiced consonants exhibit higher birth time and lifetime. The color represents the density of points in each unit grid box.*

# Model comparison on benchmark datasets

| | ALLSSTAR corpora | | | | | Random samples | | |
|---|---|---|---|---|---|---|---|---|
| Small dataset | HT1 | HT2 | DHR | LPP | NWS | LJ | TIMIT | Libri |
| Number of phones | 3200 | 3000 | 3600 | 3800 | 1800 | 2000 | 2000 | 2000 |
| TopCap | 94.3 | 92.7 | 92.3 | 91.9 | 88.8 | 94.6 | 83.9 | 85.1 |
| MFCC–GRU | 93.3 | 92.2 | 93.2 | 91.4 | 89.8 | 86.0 | 70.5 | 79.0 |
| MFCC–Transformer | 96.0 | 93.9 | 94.2 | 92.4 | 94.4 | 92.0 | 96.3 | 87.5 |
| STFT–CNN-8 | 87.1 | 84.0 | 78.2 | 79.1 | 79.9 | 82.7 | 76.3 | 77.5 |
| STFT–CNN-16 | 96.7 | 95.1 | 94.4 | 92.1 | 94.0 | 95.6 | 89.4 | 88.7 |

| Large dataset | ALLSSTAR | LJSpeech | TIMIT | LibriSpeech |
|---|---|---|---|---|
| Number of phones | 21000 | 257000 | 42000 | 500000 |
| TopCap | 92.5 | 92.9 | 92.8 | 88.7 |
| MFCC–GRU | 93.9 | 96.2 | 97.4 | 91.0 |
| MFCC–Transformer | 93.7 | 96.9 | 97.6 | 92.1 |
| STFT–CNN-8 | 81.2 | 85.4 | 77.5 | 80.3 |
| STFT–CNN-16 | 94.6 | 96.3 | 91.4 | 90.6 |

*Accuracy rates % of TopCap on 8 small datasets and 4 large datasets stand in comparison with state-of-the-art methods.*

# Model comparison on benchmark datasets

| | ALLSSTAR corpora | | | | | Random samples | | |
|---|---|---|---|---|---|---|---|---|
| Small dataset | HT1 | HT2 | DHR | LPP | NWS | LJ | TIMIT | Libri |
| Number of phones | 3200 | 3000 | 3600 | 3800 | 1800 | 2000 | 2000 | 2000 |
| TopCap | 94.3 | 92.7 | 92.3 | 91.9 | 88.8 | 94.6 | 83.9 | 85.1 |
| MFCC–GRU | 93.3 | 92.2 | 93.2 | 91.4 | 89.8 | 86.0 | 70.5 | 79.0 |
| MFCC–Transformer | 96.0 | 93.9 | 94.2 | 92.4 | 94.4 | 92.0 | 96.3 | 87.5 |
| STFT–CNN-8 | 87.1 | 84.0 | 78.2 | 79.1 | 79.9 | 82.7 | 76.3 | 77.5 |
| STFT–CNN-16 | 96.7 | 95.1 | 94.4 | 92.1 | 94.0 | 95.6 | 89.4 | 88.7 |

| Large dataset | ALLSSTAR | LJSpeech | TIMIT | LibriSpeech |
|---|---|---|---|---|
| Number of phones | 21000 | 257000 | 42000 | 500000 |
| TopCap | 92.5 | 92.9 | 92.8 | 88.7 |
| MFCC–GRU | 93.9 | 96.2 | 97.4 | 91.0 |
| MFCC–Transformer | 93.7 | 96.9 | 97.6 | 92.1 |
| STFT–CNN-8 | 81.2 | 85.4 | 77.5 | 80.3 |
| STFT–CNN-16 | 94.6 | 96.3 | 91.4 | 90.6 |

*Accuracy rates % of TopCap on 8 small datasets and 4 large datasets stand in comparison with state-of-the-art methods. While MFCC–Transformer and STFT–CNN-16 generally outperform TopCap, it is important to note that TopCap exceeds the performance of MFCC–GRU (gated recurrent unit, which also uses advanced architecture) and STFT–CNN-8 (convolutional neural network, a smaller model than STFT–CNN-16) on small datasets.*

# Model comparison on benchmark datasets

| | ALLSSTAR corpora | | | | | Random samples | | |
|---|---|---|---|---|---|---|---|---|
| Small dataset | HT1 | HT2 | DHR | LPP | NWS | LJ | TIMIT | Libri |
| Number of phones | 3200 | 3000 | 3600 | 3800 | 1800 | 2000 | 2000 | 2000 |
| TopCap | 94.3 | 92.7 | 92.3 | 91.9 | 88.8 | 94.6 | 83.9 | 85.1 |
| MFCC–GRU | 93.3 | 92.2 | 93.2 | 91.4 | 89.8 | 86.0 | 70.5 | 79.0 |
| MFCC–Transformer | 96.0 | 93.9 | 94.2 | 92.4 | 94.4 | 92.0 | 96.3 | 87.5 |
| STFT–CNN-8 | 87.1 | 84.0 | 78.2 | 79.1 | 79.9 | 82.7 | 76.3 | 77.5 |
| STFT–CNN-16 | 96.7 | 95.1 | 94.4 | 92.1 | 94.0 | 95.6 | 89.4 | 88.7 |

| Large dataset | ALLSSTAR | LJSpeech | TIMIT | LibriSpeech |
|---|---|---|---|---|
| Number of phones | 21000 | 257000 | 42000 | 500000 |
| TopCap | 92.5 | 92.9 | 92.8 | 88.7 |
| MFCC–GRU | 93.9 | 96.2 | 97.4 | 91.0 |
| MFCC–Transformer | 93.7 | 96.9 | 97.6 | 92.1 |
| STFT–CNN-8 | 81.2 | 85.4 | 77.5 | 80.3 |
| STFT–CNN-16 | 94.6 | 96.3 | 91.4 | 90.6 |

*Accuracy rates % of TopCap on 8 small datasets and 4 large datasets stand in comparison with state-of-the-art methods. While MFCC–Transformer and STFT–CNN-16 generally outperform TopCap, it is important to note that TopCap exceeds the performance of MFCC–GRU (gated recurrent unit, which also uses advanced architecture) and STFT–CNN-8 (convolutional neural network, a smaller model than STFT–CNN-16) on small datasets. For larger datasets, TopCap generally does not match the performance of deep neural networks, primarily due to its use of simpler topological features and basic machine learning models.*

# Model comparison on benchmark datasets

| | ALLSSTAR corpora | | | | | Random samples | | |
|---|---|---|---|---|---|---|---|---|
| Small dataset | HT1 | HT2 | DHR | LPP | NWS | LJ | TIMIT | Libri |
| Number of phones | 3200 | 3000 | 3600 | 3800 | 1800 | 2000 | 2000 | 2000 |
| TopCap | 94.3 | 92.7 | 92.3 | 91.9 | 88.8 | 94.6 | 83.9 | 85.1 |
| MFCC–GRU | 93.3 | 92.2 | 93.2 | 91.4 | 89.8 | 86.0 | 70.5 | 79.0 |
| MFCC–Transformer | 96.0 | 93.9 | 94.2 | 92.4 | 94.4 | 92.0 | 96.3 | 87.5 |
| STFT–CNN-8 | 87.1 | 84.0 | 78.2 | 79.1 | 79.9 | 82.7 | 76.3 | 77.5 |
| STFT–CNN-16 | 96.7 | 95.1 | 94.4 | 92.1 | 94.0 | 95.6 | 89.4 | 88.7 |

| Large dataset | ALLSSTAR | LJSpeech | TIMIT | LibriSpeech |
|---|---|---|---|---|
| Number of phones | 21000 | 257000 | 42000 | 500000 |
| TopCap | 92.5 | 92.9 | 92.8 | 88.7 |
| MFCC–GRU | 93.9 | 96.2 | 97.4 | 91.0 |
| MFCC–Transformer | 93.7 | 96.9 | 97.6 | 92.1 |
| STFT–CNN-8 | 81.2 | 85.4 | 77.5 | 80.3 |
| STFT–CNN-16 | 94.6 | 96.3 | 91.4 | 90.6 |

*Accuracy rates % of TopCap on 8 small datasets and 4 large datasets stand in comparison with state-of-the-art methods. While MFCC–Transformer and STFT–CNN-16 generally outperform TopCap, it is important to note that TopCap exceeds the performance of MFCC–GRU (gated recurrent unit, which also uses advanced architecture) and STFT–CNN-8 (convolutional neural network, a smaller model than STFT–CNN-16) on small datasets. For larger datasets, TopCap generally does not match the performance of deep neural networks, primarily due to its use of simpler topological features and basic machine learning models. This limitation motivates the integration TopNN of topological features into neural networks.*

# Model comparison on benchmark datasets

| | ALLSSTAR corpora | | | | | Random samples | | |
|---|---|---|---|---|---|---|---|---|
| Small dataset | HT1 | HT2 | DHR | LPP | NWS | LJ | TIMIT | Libri |
| Number of phones | 3200 | 3000 | 3600 | 3800 | 1800 | 2000 | 2000 | 2000 |
| TopCap | 94.3 | 92.7 | 92.3 | 91.9 | 88.8 | 94.6 | 83.9 | 85.1 |
| MFCC–GRU | 93.3 | 92.2 | 93.2 | 91.4 | 89.8 | 86.0 | 70.5 | 79.0 |
| MFCC–Transformer | 96.0 | 93.9 | 94.2 | 92.4 | 94.4 | 92.0 | 96.3 | 87.5 |
| STFT–CNN-8 | 87.1 | 84.0 | 78.2 | 79.1 | 79.9 | 82.7 | 76.3 | 77.5 |
| STFT–CNN-16 | 96.7 | 95.1 | 94.4 | 92.1 | 94.0 | 95.6 | 89.4 | 88.7 |

| Large dataset | ALLSSTAR | LJSpeech | TIMIT | LibriSpeech |
|---|---|---|---|---|
| Number of phones | 21000 | 257000 | 42000 | 500000 |
| TopCap | 92.5 | 92.9 | 92.8 | 88.7 |
| MFCC–GRU | 93.9 | 96.2 | 97.4 | 91.0 |
| MFCC–Transformer | 93.7 | 96.9 | 97.6 | 92.1 |
| STFT–CNN-8 | 81.2 | 85.4 | 77.5 | 80.3 |
| STFT–CNN-16 | 94.6 | 96.3 | 91.4 | 90.6 |

*Accuracy rates % of TopCap on 8 small datasets and 4 large datasets stand in comparison with state-of-the-art methods. While MFCC–Transformer and STFT–CNN-16 generally outperform TopCap, it is important to note that TopCap exceeds the performance of MFCC–GRU (gated recurrent unit, which also uses advanced architecture) and STFT–CNN-8 (convolutional neural network, a smaller model than STFT–CNN-16) on small datasets. For larger datasets, TopCap generally does not match the performance of deep neural networks, primarily due to its use of simpler topological features and basic machine learning models. This limitation motivates the integration TopNN of topological features into neural networks. Overall, while TopCap may not achieve the highest performance across all benchmarks, it produces decent results.*

# Model comparison on benchmark datasets

| | ALLSSTAR corpora | | | | | Random samples | | |
|---|---|---|---|---|---|---|---|---|
| Small dataset | HT1 | HT2 | DHR | LPP | NWS | LJ | TIMIT | Libri |
| Number of phones | 3200 | 3000 | 3600 | 3800 | 1800 | 2000 | 2000 | 2000 |
| TopCap | 94.3 | 92.7 | 92.3 | 91.9 | 88.8 | 94.6 | 83.9 | 85.1 |
| MFCC–GRU | 93.3 | 92.2 | 93.2 | 91.4 | 89.8 | 86.0 | 70.5 | 79.0 |
| MFCC–Transformer | 96.0 | 93.9 | 94.2 | 92.4 | 94.4 | 92.0 | 96.3 | 87.5 |
| STFT–CNN-8 | 87.1 | 84.0 | 78.2 | 79.1 | 79.9 | 82.7 | 76.3 | 77.5 |
| STFT–CNN-16 | 96.7 | 95.1 | 94.4 | 92.1 | 94.0 | 95.6 | 89.4 | 88.7 |

| Large dataset | ALLSSTAR | LJSpeech | TIMIT | LibriSpeech |
|---|---|---|---|---|
| Number of phones | 21000 | 257000 | 42000 | 500000 |
| TopCap | 92.5 | 92.9 | 92.8 | 88.7 |
| MFCC–GRU | 93.9 | 96.2 | 97.4 | 91.0 |
| MFCC–Transformer | 93.7 | 96.9 | 97.6 | 92.1 |
| STFT–CNN-8 | 81.2 | 85.4 | 77.5 | 80.3 |
| STFT–CNN-16 | 94.6 | 96.3 | 91.4 | 90.6 |

*Advantages of TopCap:*

- ***Structural efficiency.*** *Neural network models require further feature extraction from input MFCC sequences or STFT spectrograms for classification tasks, necessitating a training process which lengthens with a growing dataset.*

# Model comparison on benchmark datasets

| | ALLSSTAR corpora | | | | | Random samples | | |
|---|---|---|---|---|---|---|---|---|
| Small dataset | HT1 | HT2 | DHR | LPP | NWS | LJ | TIMIT | Libri |
| Number of phones | 3200 | 3000 | 3600 | 3800 | 1800 | 2000 | 2000 | 2000 |
| TopCap | 94.3 | 92.7 | 92.3 | 91.9 | 88.8 | 94.6 | 83.9 | 85.1 |
| MFCC–GRU | 93.3 | 92.2 | 93.2 | 91.4 | 89.8 | 86.0 | 70.5 | 79.0 |
| MFCC–Transformer | 96.0 | 93.9 | 94.2 | 92.4 | 94.4 | 92.0 | 96.3 | 87.5 |
| STFT–CNN-8 | 87.1 | 84.0 | 78.2 | 79.1 | 79.9 | 82.7 | 76.3 | 77.5 |
| STFT–CNN-16 | 96.7 | 95.1 | 94.4 | 92.1 | 94.0 | 95.6 | 89.4 | 88.7 |

| Large dataset | ALLSSTAR | LJSpeech | TIMIT | LibriSpeech |
|---|---|---|---|---|
| Number of phones | 21000 | 257000 | 42000 | 500000 |
| TopCap | 92.5 | 92.9 | 92.8 | 88.7 |
| MFCC–GRU | 93.9 | 96.2 | 97.4 | 91.0 |
| MFCC–Transformer | 93.7 | 96.9 | 97.6 | 92.1 |
| STFT–CNN-8 | 81.2 | 85.4 | 77.5 | 80.3 |
| STFT–CNN-16 | 94.6 | 96.3 | 91.4 | 90.6 |

*Advantages of TopCap:*

- ***Structural efficiency.*** *Neural network models require further feature extraction from input MFCC sequences or STFT spectrograms for classification tasks, necessitating a training process which lengthens with a growing dataset. In contrast, TopCap mainly utilizes topology-based methods (TDE and PH) which are more straightforward for feature extraction.*

# Model comparison on benchmark datasets

| | ALLSSTAR corpora | | | | | Random samples | | |
|---|---|---|---|---|---|---|---|---|
| Small dataset | HT1 | HT2 | DHR | LPP | NWS | LJ | TIMIT | Libri |
| Number of phones | 3200 | 3000 | 3600 | 3800 | 1800 | 2000 | 2000 | 2000 |
| TopCap | 94.3 | 92.7 | 92.3 | 91.9 | 88.8 | 94.6 | 83.9 | 85.1 |
| MFCC–GRU | 93.3 | 92.2 | 93.2 | 91.4 | 89.8 | 86.0 | 70.5 | 79.0 |
| MFCC–Transformer | 96.0 | 93.9 | 94.2 | 92.4 | 94.4 | 92.0 | 96.3 | 87.5 |
| STFT–CNN-8 | 87.1 | 84.0 | 78.2 | 79.1 | 79.9 | 82.7 | 76.3 | 77.5 |
| STFT–CNN-16 | 96.7 | 95.1 | 94.4 | 92.1 | 94.0 | 95.6 | 89.4 | 88.7 |

| Large dataset | ALLSSTAR | LJSpeech | TIMIT | LibriSpeech |
|---|---|---|---|---|
| Number of phones | 21000 | 257000 | 42000 | 500000 |
| TopCap | 92.5 | 92.9 | 92.8 | 88.7 |
| MFCC–GRU | 93.9 | 96.2 | 97.4 | 91.0 |
| MFCC–Transformer | 93.7 | 96.9 | 97.6 | 92.1 |
| STFT–CNN-8 | 81.2 | 85.4 | 77.5 | 80.3 |
| STFT–CNN-16 | 94.6 | 96.3 | 91.4 | 90.6 |

*Advantages of TopCap:*

- ***Structural efficiency.*** *Neural network models require further feature extraction from input MFCC sequences or STFT spectrograms for classification tasks, necessitating a training process which lengthens with a growing dataset. In contrast, TopCap mainly utilizes topology-based methods (TDE and PH) which are more straightforward for feature extraction. Meanwhile, the topological fingerprints (e.g., maximal persistence) are strong enough to characterize phonemes effectively for our classification tasks.*

# Model comparison on benchmark datasets

| | ALLSSTAR corpora | | | | | Random samples | | |
|---|---|---|---|---|---|---|---|---|
| Small dataset | HT1 | HT2 | DHR | LPP | NWS | LJ | TIMIT | Libri |
| Number of phones | 3200 | 3000 | 3600 | 3800 | 1800 | 2000 | 2000 | 2000 |
| TopCap | 94.3 | 92.7 | 92.3 | 91.9 | 88.8 | 94.6 | 83.9 | 85.1 |
| MFCC–GRU | 93.3 | 92.2 | 93.2 | 91.4 | 89.8 | 86.0 | 70.5 | 79.0 |
| MFCC–Transformer | 96.0 | 93.9 | 94.2 | 92.4 | 94.4 | 92.0 | 96.3 | 87.5 |
| STFT–CNN-8 | 87.1 | 84.0 | 78.2 | 79.1 | 79.9 | 82.7 | 76.3 | 77.5 |
| STFT–CNN-16 | 96.7 | 95.1 | 94.4 | 92.1 | 94.0 | 95.6 | 89.4 | 88.7 |

| Large dataset | ALLSSTAR | LJSpeech | TIMIT | LibriSpeech |
|---|---|---|---|---|
| Number of phones | 21000 | 257000 | 42000 | 500000 |
| TopCap | 92.5 | 92.9 | 92.8 | 88.7 |
| MFCC–GRU | 93.9 | 96.2 | 97.4 | 91.0 |
| MFCC–Transformer | 93.7 | 96.9 | 97.6 | 92.1 |
| STFT–CNN-8 | 81.2 | 85.4 | 77.5 | 80.3 |
| STFT–CNN-16 | 94.6 | 96.3 | 91.4 | 90.6 |

*Advantages of TopCap:*

- ***Structural efficiency.*** *Neural network models require further feature extraction from input MFCC sequences or STFT spectrograms for classification tasks, necessitating a training process which lengthens with a growing dataset. In contrast, TopCap mainly utilizes topology-based methods (TDE and PH) which are more straightforward for feature extraction. Meanwhile, the topological fingerprints (e.g., maximal persistence) are strong enough to characterize phonemes effectively for our classification tasks. Therefore, TopCap gains higher efficiency, especially when handling larger datasets.*

# Model comparison on benchmark datasets

| | ALLSSTAR corpora | | | | | Random samples | | |
|---|---|---|---|---|---|---|---|---|
| Small dataset | HT1 | HT2 | DHR | LPP | NWS | LJ | TIMIT | Libri |
| Number of phones | 3200 | 3000 | 3600 | 3800 | 1800 | 2000 | 2000 | 2000 |
| TopCap | 94.3 | 92.7 | 92.3 | 91.9 | 88.8 | 94.6 | 83.9 | 85.1 |
| MFCC–GRU | 93.3 | 92.2 | 93.2 | 91.4 | 89.8 | 86.0 | 70.5 | 79.0 |
| MFCC–Transformer | 96.0 | 93.9 | 94.2 | 92.4 | 94.4 | 92.0 | 96.3 | 87.5 |
| STFT–CNN-8 | 87.1 | 84.0 | 78.2 | 79.1 | 79.9 | 82.7 | 76.3 | 77.5 |
| STFT–CNN-16 | 96.7 | 95.1 | 94.4 | 92.1 | 94.0 | 95.6 | 89.4 | 88.7 |

| Large dataset | ALLSSTAR | LJSpeech | TIMIT | LibriSpeech |
|---|---|---|---|---|
| Number of phones | 21000 | 257000 | 42000 | 500000 |
| TopCap | 92.5 | 92.9 | 92.8 | 88.7 |
| MFCC–GRU | 93.9 | 96.2 | 97.4 | 91.0 |
| MFCC–Transformer | 93.7 | 96.9 | 97.6 | 92.1 |
| STFT–CNN-8 | 81.2 | 85.4 | 77.5 | 80.3 |
| STFT–CNN-16 | 94.6 | 96.3 | 91.4 | 90.6 |

*Advantages of TopCap:*

- ***Structural efficiency.*** *Neural network models require further feature extraction from input MFCC sequences or STFT spectrograms for classification tasks, necessitating a training process which lengthens with a growing dataset. In contrast, TopCap mainly utilizes topology-based methods (TDE and PH) which are more straightforward for feature extraction. Meanwhile, the topological fingerprints (e.g., maximal persistence) are strong enough to characterize phonemes effectively for our classification tasks. Therefore, TopCap gains higher efficiency, especially when handling larger datasets. On a related note, deep learning methods, as a data-driven approach, require large amounts of data for training and generalization.*

# Model comparison on benchmark datasets

| | ALLSSTAR corpora | | | | | Random samples | | |
|---|---|---|---|---|---|---|---|---|
| Small dataset | HT1 | HT2 | DHR | LPP | NWS | LJ | TIMIT | Libri |
| Number of phones | 3200 | 3000 | 3600 | 3800 | 1800 | 2000 | 2000 | 2000 |
| TopCap | 94.3 | 92.7 | 92.3 | 91.9 | 88.8 | 94.6 | 83.9 | 85.1 |
| MFCC–GRU | 93.3 | 92.2 | 93.2 | 91.4 | 89.8 | 86.0 | 70.5 | 79.0 |
| MFCC–Transformer | 96.0 | 93.9 | 94.2 | 92.4 | 94.4 | 92.0 | 96.3 | 87.5 |
| STFT–CNN-8 | 87.1 | 84.0 | 78.2 | 79.1 | 79.9 | 82.7 | 76.3 | 77.5 |
| STFT–CNN-16 | 96.7 | 95.1 | 94.4 | 92.1 | 94.0 | 95.6 | 89.4 | 88.7 |

| Large dataset | ALLSSTAR | LJSpeech | TIMIT | LibriSpeech |
|---|---|---|---|---|
| Number of phones | 21000 | 257000 | 42000 | 500000 |
| TopCap | 92.5 | 92.9 | 92.8 | 88.7 |
| MFCC–GRU | 93.9 | 96.2 | 97.4 | 91.0 |
| MFCC–Transformer | 93.7 | 96.9 | 97.6 | 92.1 |
| STFT–CNN-8 | 81.2 | 85.4 | 77.5 | 80.3 |
| STFT–CNN-16 | 94.6 | 96.3 | 91.4 | 90.6 |

*Advantages of TopCap:*

- ***Structural efficiency.*** *Neural network models require further feature extraction from input MFCC sequences or STFT spectrograms for classification tasks, necessitating a training process which lengthens with a growing dataset. In contrast, TopCap mainly utilizes topology-based methods (TDE and PH) which are more straightforward for feature extraction. Meanwhile, the topological fingerprints (e.g., maximal persistence) are strong enough to characterize phonemes effectively for our classification tasks. Therefore, TopCap gains higher efficiency, especially when handling larger datasets. On a related note, deep learning methods, as a data-driven approach, require large amounts of data for training and generalization. In contrast, comparing the upper and lower halves of the above table, we see that TopCap achieves equally good performance on relatively small datasets.*

# Model comparison on benchmark datasets

| | ALLSSTAR corpora | | | | | Random samples | | |
|---|---|---|---|---|---|---|---|---|
| Small dataset | HT1 | HT2 | DHR | LPP | NWS | LJ | TIMIT | Libri |
| Number of phones | 3200 | 3000 | 3600 | 3800 | 1800 | 2000 | 2000 | 2000 |
| TopCap | 94.3 | 92.7 | 92.3 | 91.9 | 88.8 | 94.6 | 83.9 | 85.1 |
| MFCC–GRU | 93.3 | 92.2 | 93.2 | 91.4 | 89.8 | 86.0 | 70.5 | 79.0 |
| MFCC–Transformer | 96.0 | 93.9 | 94.2 | 92.4 | 94.4 | 92.0 | 96.3 | 87.5 |
| STFT–CNN-8 | 87.1 | 84.0 | 78.2 | 79.1 | 79.9 | 82.7 | 76.3 | 77.5 |
| STFT–CNN-16 | 96.7 | 95.1 | 94.4 | 92.1 | 94.0 | 95.6 | 89.4 | 88.7 |

| Large dataset | ALLSSTAR | LJSpeech | TIMIT | LibriSpeech |
|---|---|---|---|---|
| Number of phones | 21000 | 257000 | 42000 | 500000 |
| TopCap | 92.5 | 92.9 | 92.8 | 88.7 |
| MFCC–GRU | 93.9 | 96.2 | 97.4 | 91.0 |
| MFCC–Transformer | 93.7 | 96.9 | 97.6 | 92.1 |
| STFT–CNN-8 | 81.2 | 85.4 | 77.5 | 80.3 |
| STFT–CNN-16 | 94.6 | 96.3 | 91.4 | 90.6 |

*Advantages of TopCap:*

- ***Interpretability.*** *Neural networks are often referred to as black boxes due to their low explainability and interpretability, which makes it challenging to understand the mechanism of feature extraction and effectively improve a model for classification. However, TopCap offers a white-box method for visualizing features of time series data, which gives insight to the intrinsic properties and nuanced differences within the data, enabling us to better understand and improve the model.*

# Model comparison on benchmark datasets

| | ALLSSTAR corpora | | | | | Random samples | | |
|---|---|---|---|---|---|---|---|---|
| Small dataset | HT1 | HT2 | DHR | LPP | NWS | LJ | TIMIT | Libri |
| Number of phones | 3200 | 3000 | 3600 | 3800 | 1800 | 2000 | 2000 | 2000 |
| TopCap | 94.3 | 92.7 | 92.3 | 91.9 | 88.8 | 94.6 | 83.9 | 85.1 |
| MFCC–GRU | 93.3 | 92.2 | 93.2 | 91.4 | 89.8 | 86.0 | 70.5 | 79.0 |
| MFCC–Transformer | 96.0 | 93.9 | 94.2 | 92.4 | 94.4 | 92.0 | 96.3 | 87.5 |
| STFT–CNN-8 | 87.1 | 84.0 | 78.2 | 79.1 | 79.9 | 82.7 | 76.3 | 77.5 |
| STFT–CNN-16 | 96.7 | 95.1 | 94.4 | 92.1 | 94.0 | 95.6 | 89.4 | 88.7 |

| Large dataset | ALLSSTAR | LJSpeech | TIMIT | LibriSpeech |
|---|---|---|---|---|
| Number of phones | 21000 | 257000 | 42000 | 500000 |
| TopCap | 92.5 | 92.9 | 92.8 | 88.7 |
| MFCC–GRU | 93.9 | 96.2 | 97.4 | 91.0 |
| MFCC–Transformer | 93.7 | 96.9 | 97.6 | 92.1 |
| STFT–CNN-8 | 81.2 | 85.4 | 77.5 | 80.3 |
| STFT–CNN-16 | 94.6 | 96.3 | 91.4 | 90.6 |

*Advantages of TopCap:*

- ***Computational speed.*** *Neural networks involve time-consuming training process, even with GPU acceleration. For instance, on the TIMIT dataset, a full training cycle of 15 epochs can take approximately 30 minutes with GPU parallelization.*

# Model comparison on benchmark datasets

| | ALLSSTAR corpora | | | | | Random samples | | |
|---|---|---|---|---|---|---|---|---|
| Small dataset | HT1 | HT2 | DHR | LPP | NWS | LJ | TIMIT | Libri |
| Number of phones | 3200 | 3000 | 3600 | 3800 | 1800 | 2000 | 2000 | 2000 |
| TopCap | 94.3 | 92.7 | 92.3 | 91.9 | 88.8 | 94.6 | 83.9 | 85.1 |
| MFCC–GRU | 93.3 | 92.2 | 93.2 | 91.4 | 89.8 | 86.0 | 70.5 | 79.0 |
| MFCC–Transformer | 96.0 | 93.9 | 94.2 | 92.4 | 94.4 | 92.0 | 96.3 | 87.5 |
| STFT–CNN-8 | 87.1 | 84.0 | 78.2 | 79.1 | 79.9 | 82.7 | 76.3 | 77.5 |
| STFT–CNN-16 | 96.7 | 95.1 | 94.4 | 92.1 | 94.0 | 95.6 | 89.4 | 88.7 |

| Large dataset | ALLSSTAR | LJSpeech | TIMIT | LibriSpeech |
|---|---|---|---|---|
| Number of phones | 21000 | 257000 | 42000 | 500000 |
| TopCap | 92.5 | 92.9 | 92.8 | 88.7 |
| MFCC–GRU | 93.9 | 96.2 | 97.4 | 91.0 |
| MFCC–Transformer | 93.7 | 96.9 | 97.6 | 92.1 |
| STFT–CNN-8 | 81.2 | 85.4 | 77.5 | 80.3 |
| STFT–CNN-16 | 94.6 | 96.3 | 91.4 | 90.6 |

*Advantages of TopCap:*

- ***Computational speed.*** *Neural networks involve time-consuming training process, even with GPU acceleration. For instance, on the TIMIT dataset, a full training cycle of 15 epochs can take approximately 30 minutes with GPU parallelization. In contrast, TopCap bypasses the need for iterative training and achieves significantly faster computation. TopCap performs lightweight machine learning with negligible runtime overhead, completing both feature extraction and classification in just 2 minutes when utilizing 16-thread CPU parallelization.*

# Model comparison on benchmark datasets

| | ALLSSTAR corpora | | | | | Random samples | | |
|---|---|---|---|---|---|---|---|---|
| Small dataset | HT1 | HT2 | DHR | LPP | NWS | LJ | TIMIT | Libri |
| Number of phones | 3200 | 3000 | 3600 | 3800 | 1800 | 2000 | 2000 | 2000 |
| TopCap | 94.3 | 92.7 | 92.3 | 91.9 | 88.8 | 94.6 | 83.9 | 85.1 |
| MFCC–GRU | 93.3 | 92.2 | 93.2 | 91.4 | 89.8 | 86.0 | 70.5 | 79.0 |
| MFCC–Transformer | 96.0 | 93.9 | 94.2 | 92.4 | 94.4 | 92.0 | 96.3 | 87.5 |
| STFT–CNN-8 | 87.1 | 84.0 | 78.2 | 79.1 | 79.9 | 82.7 | 76.3 | 77.5 |
| STFT–CNN-16 | 96.7 | 95.1 | 94.4 | 92.1 | 94.0 | 95.6 | 89.4 | 88.7 |

| Large dataset | ALLSSTAR | LJSpeech | TIMIT | LibriSpeech |
|---|---|---|---|---|
| Number of phones | 21000 | 257000 | 42000 | 500000 |
| TopCap | 92.5 | 92.9 | 92.8 | 88.7 |
| MFCC–GRU | 93.9 | 96.2 | 97.4 | 91.0 |
| MFCC–Transformer | 93.7 | 96.9 | 97.6 | 92.1 |
| STFT–CNN-8 | 81.2 | 85.4 | 77.5 | 80.3 |
| STFT–CNN-16 | 94.6 | 96.3 | 91.4 | 90.6 |

*Advantages of TopCap:*

- ***Computational speed.*** *Neural networks involve time-consuming training process, even with GPU acceleration. For instance, on the TIMIT dataset, a full training cycle of 15 epochs can take approximately 30 minutes with GPU parallelization. In contrast, TopCap bypasses the need for iterative training and achieves significantly faster computation. TopCap performs lightweight machine learning with negligible runtime overhead, completing both feature extraction and classification in just 2 minutes when utilizing 16-thread CPU parallelization. TopCap's efficiency advantage comes from avoiding gradient-based optimization and using computationally cheaper topologically derived features, along with a highly parallelizable pipeline. These make it significantly faster and more scalable especially for large datasets or real-time applications.*

# From topological data analysis to topological deep learning

## From topological data analysis to topological deep learning

Motivated by the work of Carlsson and colleagues, we have been investigating analogous questions for speech signals

## From topological data analysis to topological deep learning

Motivated by the work of Carlsson and colleagues, we have been investigating analogous questions for speech signals, with the additional tool of time-delay embedding for turning time series data to point clouds in Euclidean spaces

## From topological data analysis to topological deep learning

Motivated by the work of Carlsson and colleagues, we have been investigating analogous questions for speech signals, with the additional tool of time-delay embedding for turning time series data to point clouds in Euclidean spaces, as well as spectrograms as their imagery representations.

## From topological data analysis to topological deep learning

Motivated by the work of Carlsson and colleagues, we have been investigating analogous questions for speech signals, with the additional tool of time-delay embedding for turning time series data to point clouds in Euclidean spaces, as well as spectrograms as their imagery representations.

- For phonetic data, linguists created a charted “distribution space” of vowels:

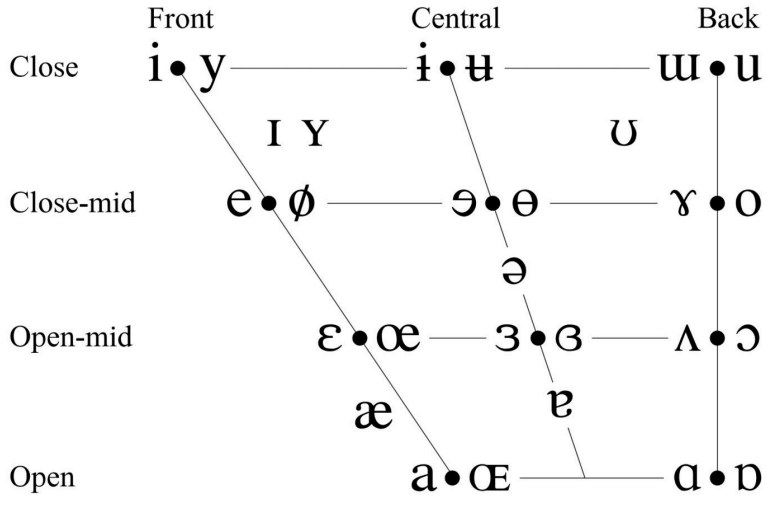

## From topological data analysis to topological deep learning

Motivated by the work of Carlsson and colleagues, we have been investigating analogous questions for speech signals, with the additional tool of time-delay embedding for turning time series data to point clouds in Euclidean spaces, as well as spectrograms as their imagery representations.

- For phonetic data, linguists created a charted “distribution space” of vowels:

The vertical axis of the chart denotes vowel height. Vowels pronounced with the tongue lowered are at the bottom and raised are at the top.

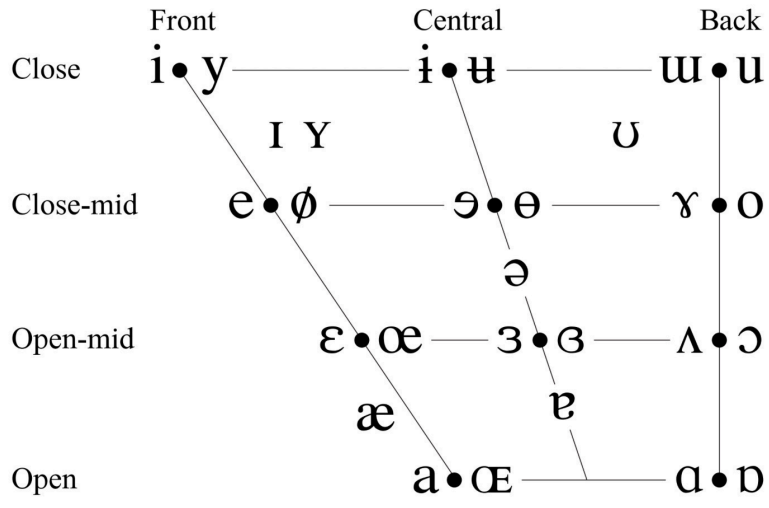

## From topological data analysis to topological deep learning

Motivated by the work of Carlsson and colleagues, we have been investigating analogous questions for speech signals, with the additional tool of time-delay embedding for turning time series data to point clouds in Euclidean spaces, as well as spectrograms as their imagery representations.

- For phonetic data, linguists created a charted “distribution space” of vowels:

The vertical axis of the chart denotes vowel height. Vowels pronounced with the tongue lowered are at the bottom and raised are at the top. The horizontal axis of the chart denotes vowel backness. Vowels with the tongue moved towards the front of the mouth are in the left of the chart, while those with the tongue moved to the back are I placed in right.

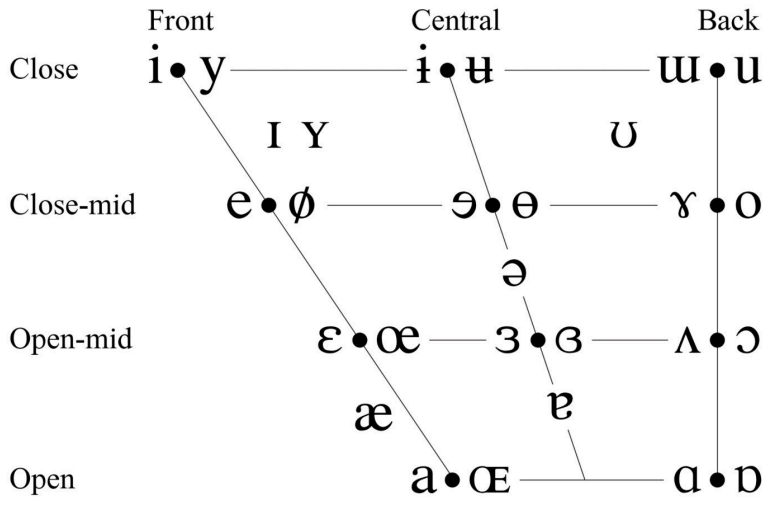

## From topological data analysis to topological deep learning

Motivated by the work of Carlsson and colleagues, we have been investigating analogous questions for speech signals, with the additional tool of time-delay embedding for turning time series data to point clouds in Euclidean spaces, as well as spectrograms as their imagery representations.

- For phonetic data, linguists created a charted “distribution space” of vowels:

The vertical axis of the chart denotes vowel height. Vowels pronounced with the tongue lowered are at the bottom and raised are at the top. The horizontal axis of the chart denotes vowel backness. Vowels with the tongue moved towards the front of the mouth are in the left of the chart, while those with the tongue moved to the back are I placed in right. The last parameter is whether the lips are rounded. At each given spot, vowels on the right and left are rounded and unrounded, respectively.

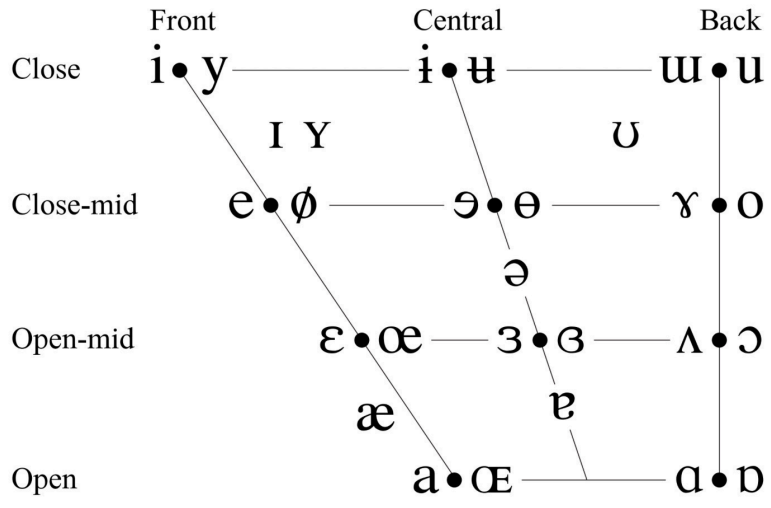

## From topological data analysis to topological deep learning

Motivated by the work of Carlsson and colleagues, we have been investigating analogous questions for speech signals, with the additional tool of time-delay embedding for turning time series data to point clouds in Euclidean spaces, as well as spectrograms as their imagery representations.

- For phonetic data, linguists created a charted “distribution space” of vowels.
- A main goal remains to use topological methods to reveal a distribution space for speech (and audio) data

## From topological data analysis to topological deep learning

Motivated by the work of Carlsson and colleagues, we have been investigating analogous questions for speech signals, with the additional tool of time-delay embedding for turning time series data to point clouds in Euclidean spaces, as well as spectrograms as their imagery representations.

- For phonetic data, linguists created a charted “distribution space” of vowels.

- A main goal remains to use topological methods to reveal a distribution space for speech (and audio) data, even a digraph on it modeling the complex network of speech-signal sequences

## From topological data analysis to topological deep learning

Motivated by the work of Carlsson and colleagues, we have been investigating analogous questions for speech signals, with the additional tool of time-delay embedding for turning time series data to point clouds in Euclidean spaces, as well as spectrograms as their imagery representations.

- For phonetic data, linguists created a charted “distribution space” of vowels.

- A main goal remains to use topological methods to reveal a distribution space for speech (and audio) data, even a digraph on it modeling the complex network of speech-signal sequences, and apply these topological inputs for smarter learning.

## From topological data analysis to topological deep learning

Motivated by the work of Carlsson and colleagues, we have been investigating analogous questions for speech signals, with the additional tool of time-delay embedding for turning time series data to point clouds in Euclidean spaces, as well as spectrograms as their imagery representations.

- For phonetic data, linguists created a charted “distribution space” of vowels.
- A main goal remains to use topological methods to reveal a distribution space for speech (and audio) data, even a digraph on it modeling the complex network of speech-signal sequences, and apply these topological inputs for smarter learning.
- In a related direction, based on TopCap, we developed topology-enhanced neural networks.

## From topological data analysis to topological deep learning

Motivated by the work of Carlsson and colleagues, we have been investigating analogous questions for speech signals, with the additional tool of time-delay embedding for turning time series data to point clouds in Euclidean spaces, as well as spectrograms as their imagery representations.

- For phonetic data, linguists created a charted “distribution space” of vowels.
- A main goal remains to use topological methods to reveal a distribution space for speech (and audio) data, even a digraph on it modeling the complex network of speech-signal sequences, and apply these topological inputs for smarter learning.
- In a related direction, based on TopCap, we developed topology-enhanced neural networks.
- Moreover, we exploited the reduced symmetry of spectrograms and designed topological convolutional layers for deep learning speech data.

# Topology-enhanced neural networks

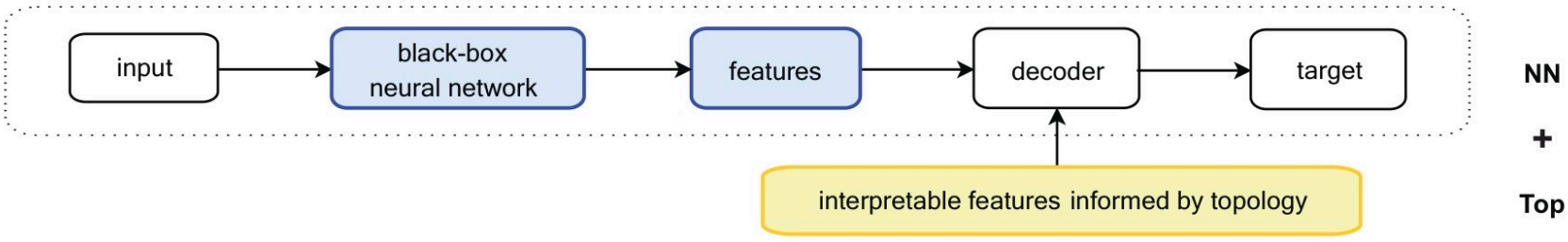


*A generic flow chart for enhancing neural networks with topological features*

# Topology-enhanced neural networks

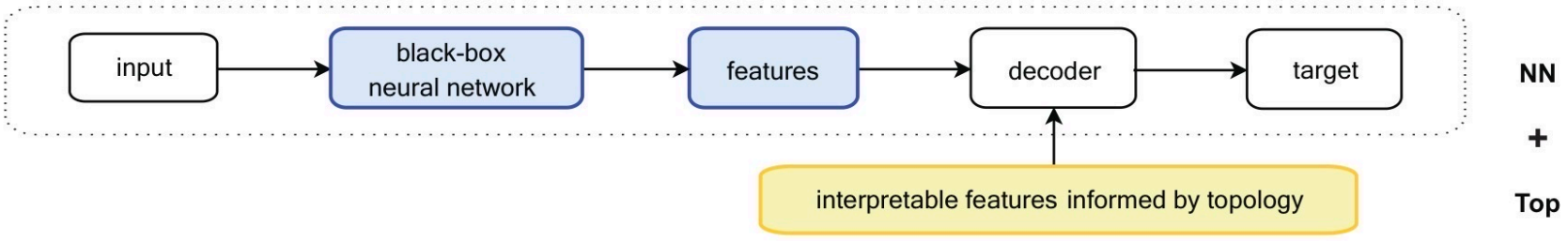


*A generic flow chart for enhancing neural networks with topological features*

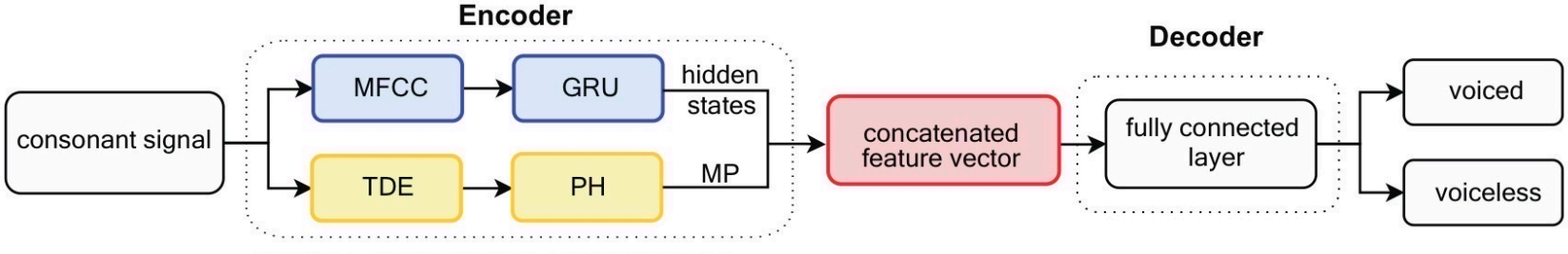


*Architecture of a specific TopNN, concatenating GRU and TopCap features*

# Topology-enhanced neural networks

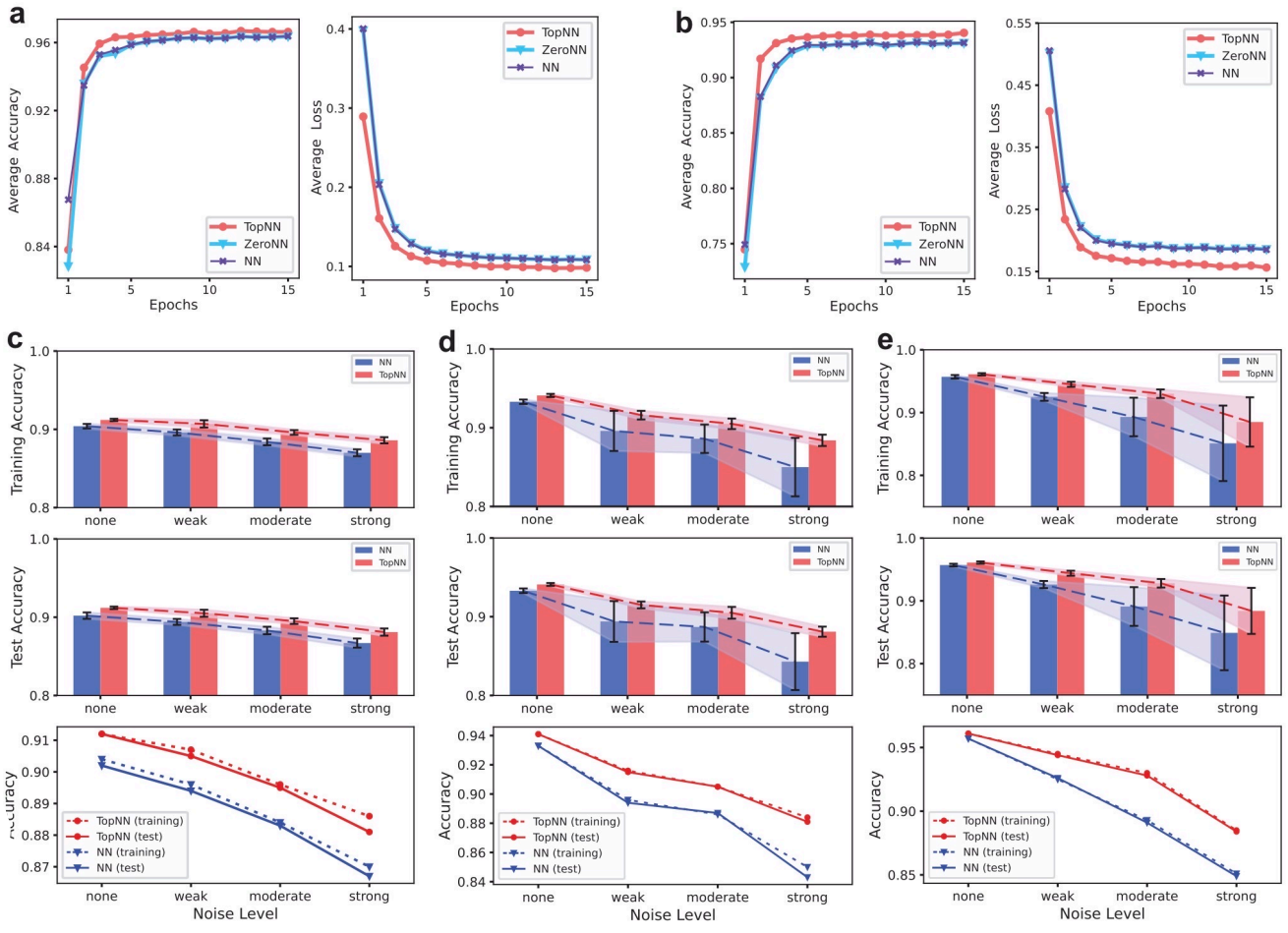


*Visual analytics of experiments with TopNN*

# Topology-enhanced neural networks

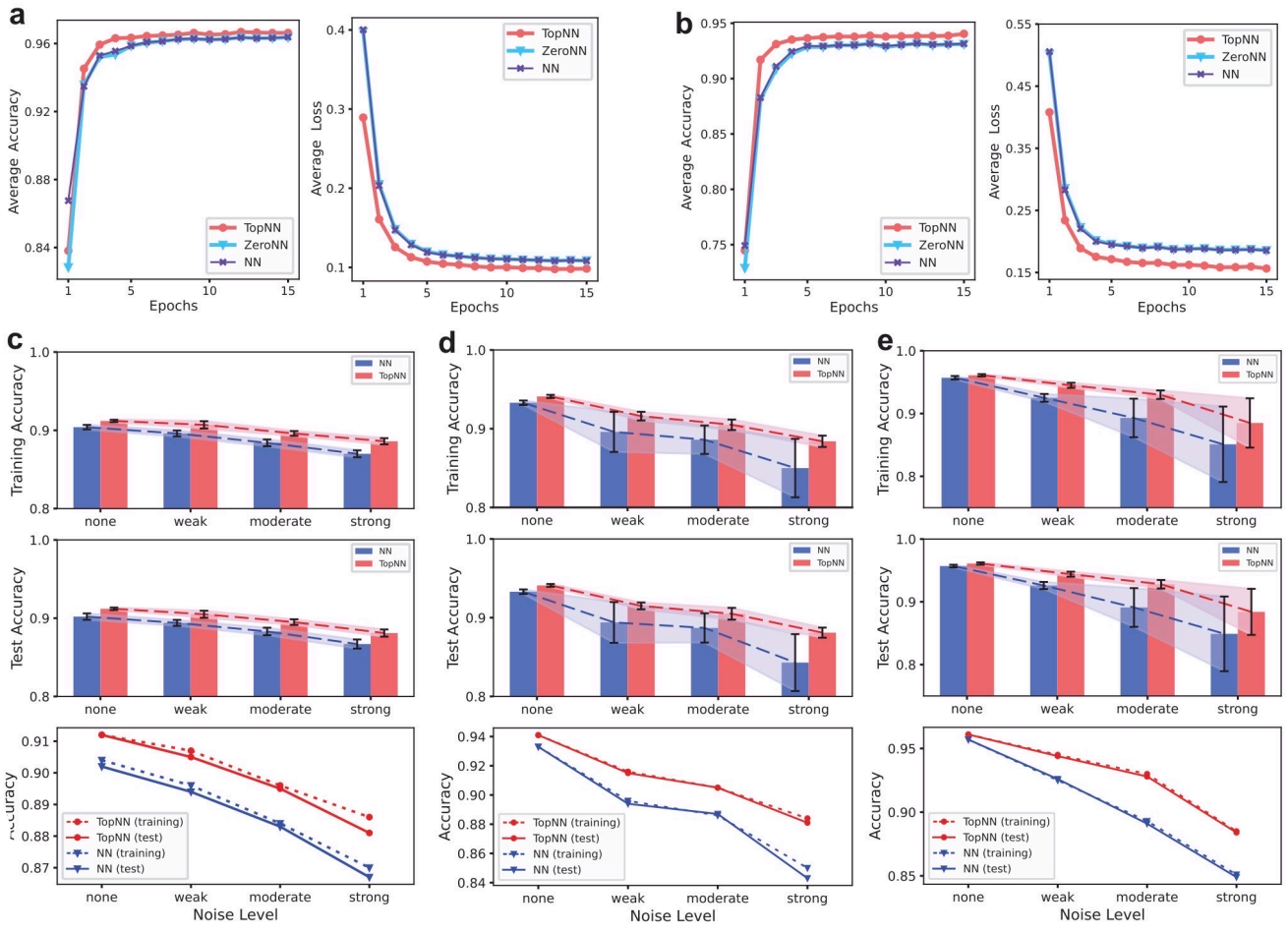


*Visual analytics of experiments with TopNN*
***a**, Training curves of TopNN, ZeroNN (NN features concatenated with null topological feature, as a sanity check), and NN on 36000 original speech data from the TIMIT dataset.*

# Topology-enhanced neural networks

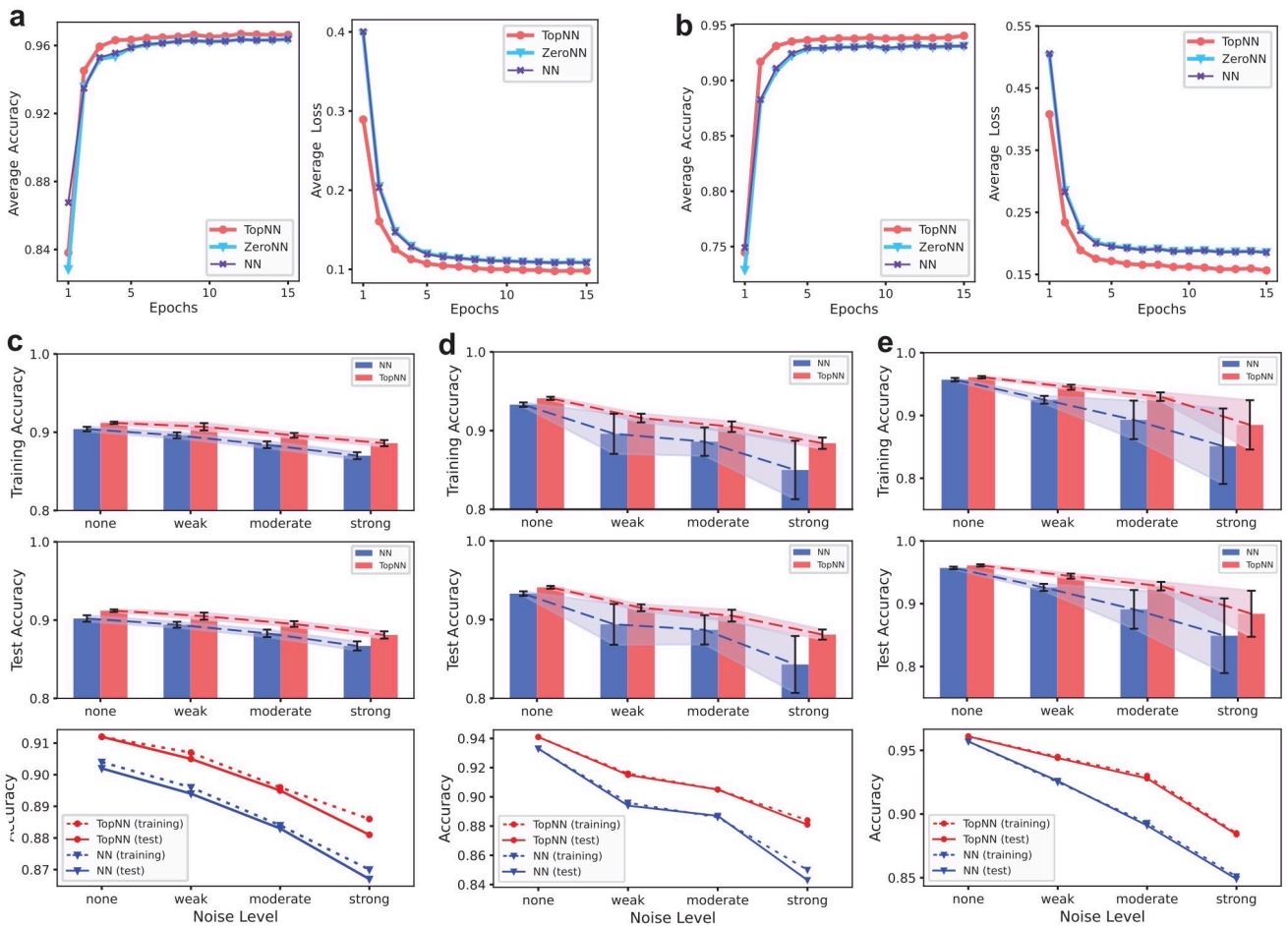


*Visual analytics of experiments with TopNN*
***a**, Training curves of TopNN, ZeroNN (NN features concatenated with null topological feature, as a sanity check), and NN on 36000 original speech data from the TIMIT dataset. They demonstrate that TopNN has higher accuracy and faster convergence in loss function than ZeroNN and NN.*

# Topology-enhanced neural networks

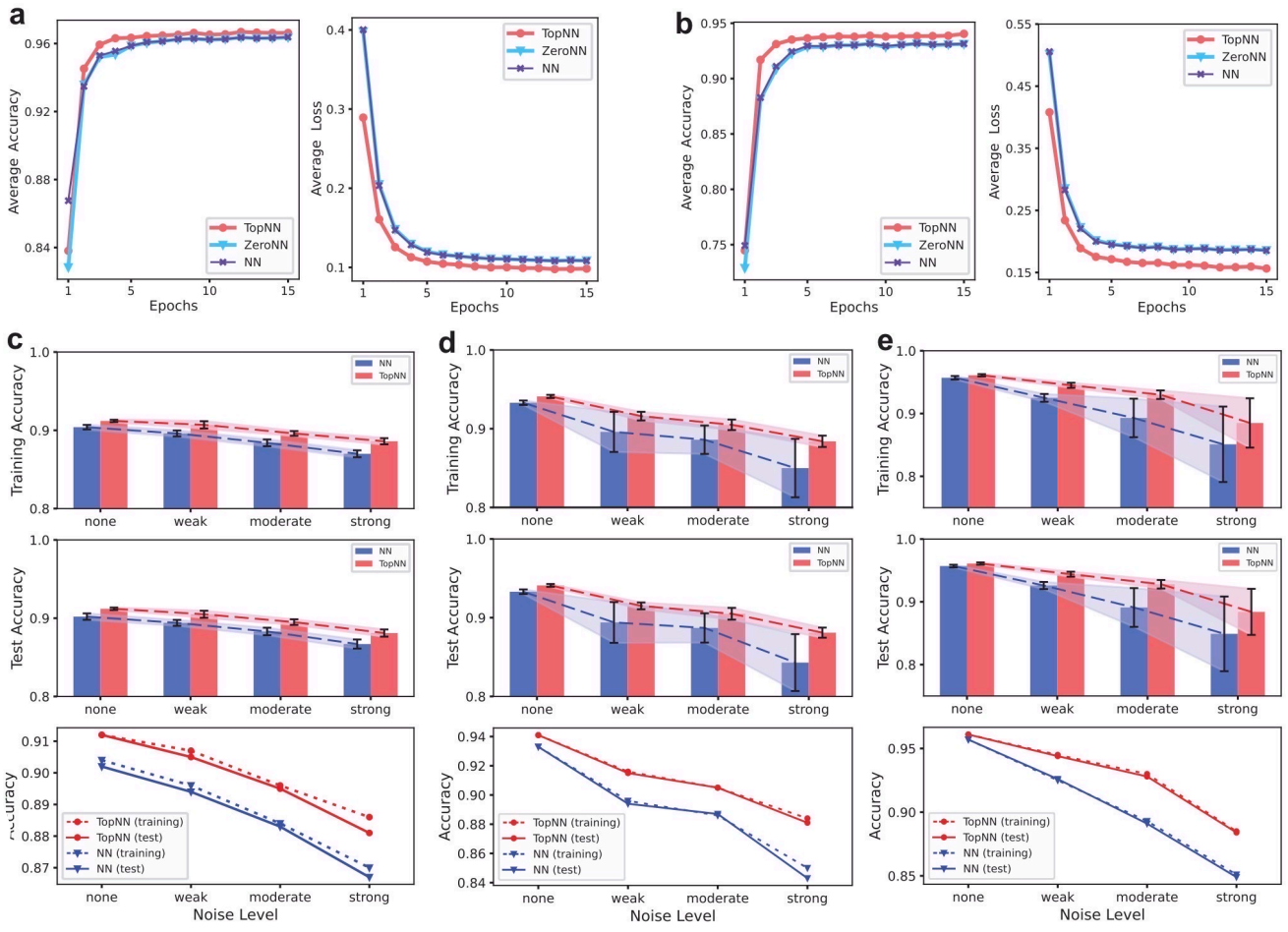


*Visual analytics of experiments with TopNN*
***b**, Training curves of TopNN, ZeroNN, and NN with the same set up as in **a** and including noise (signal-to-noise ratio = 5dB).*

# Topology-enhanced neural networks

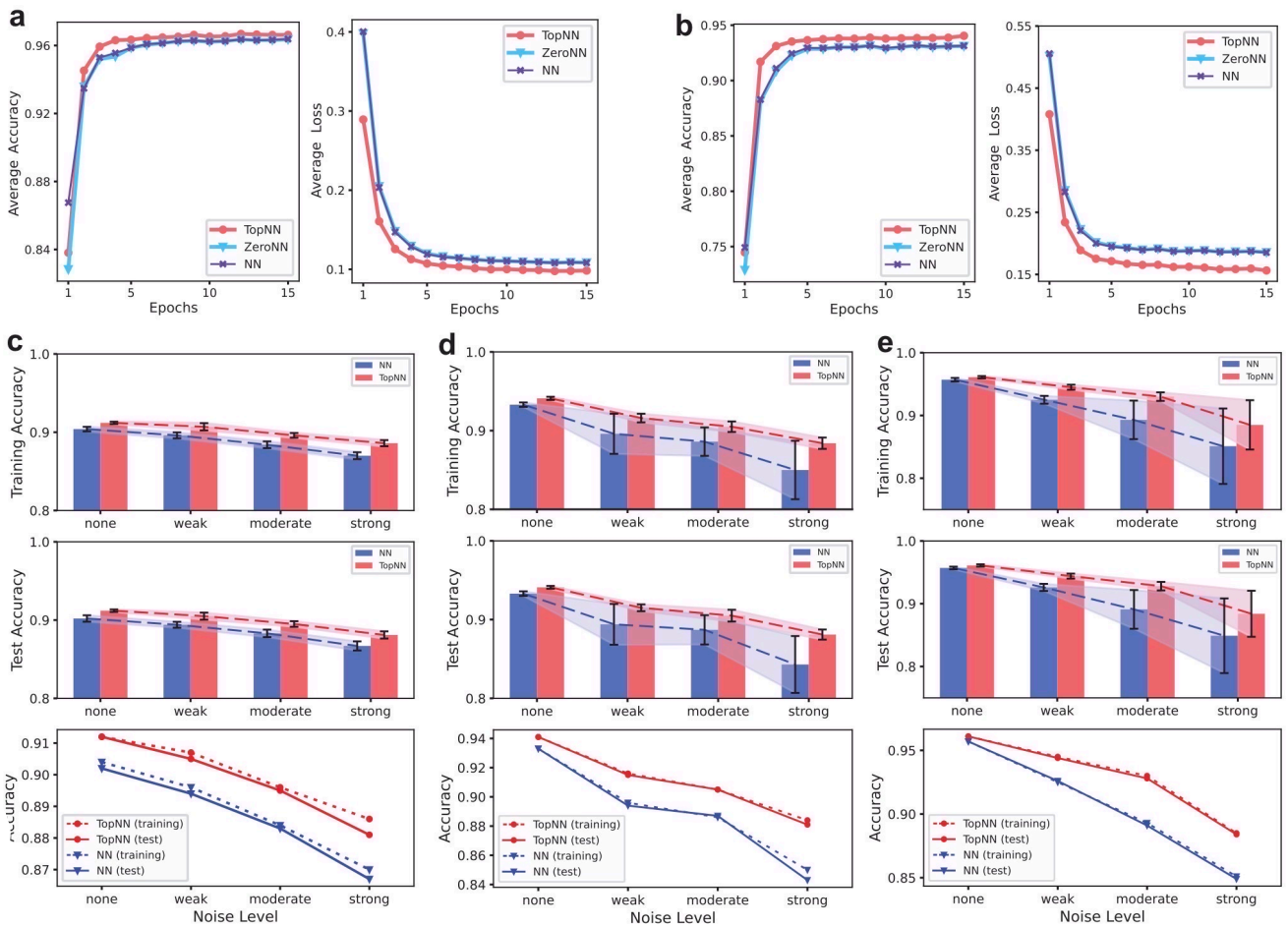


*Visual analytics of experiments with TopNN*
***b**, Training curves of TopNN, ZeroNN, and NN with the same set up as in **a** and including noise (signal-to-noise ratio = 5dB). With Gaussian white noise added, TopNN's improvement in accuracy and loss decrease are more prominent compared with the results in **a**.*

# Topology-enhanced neural networks

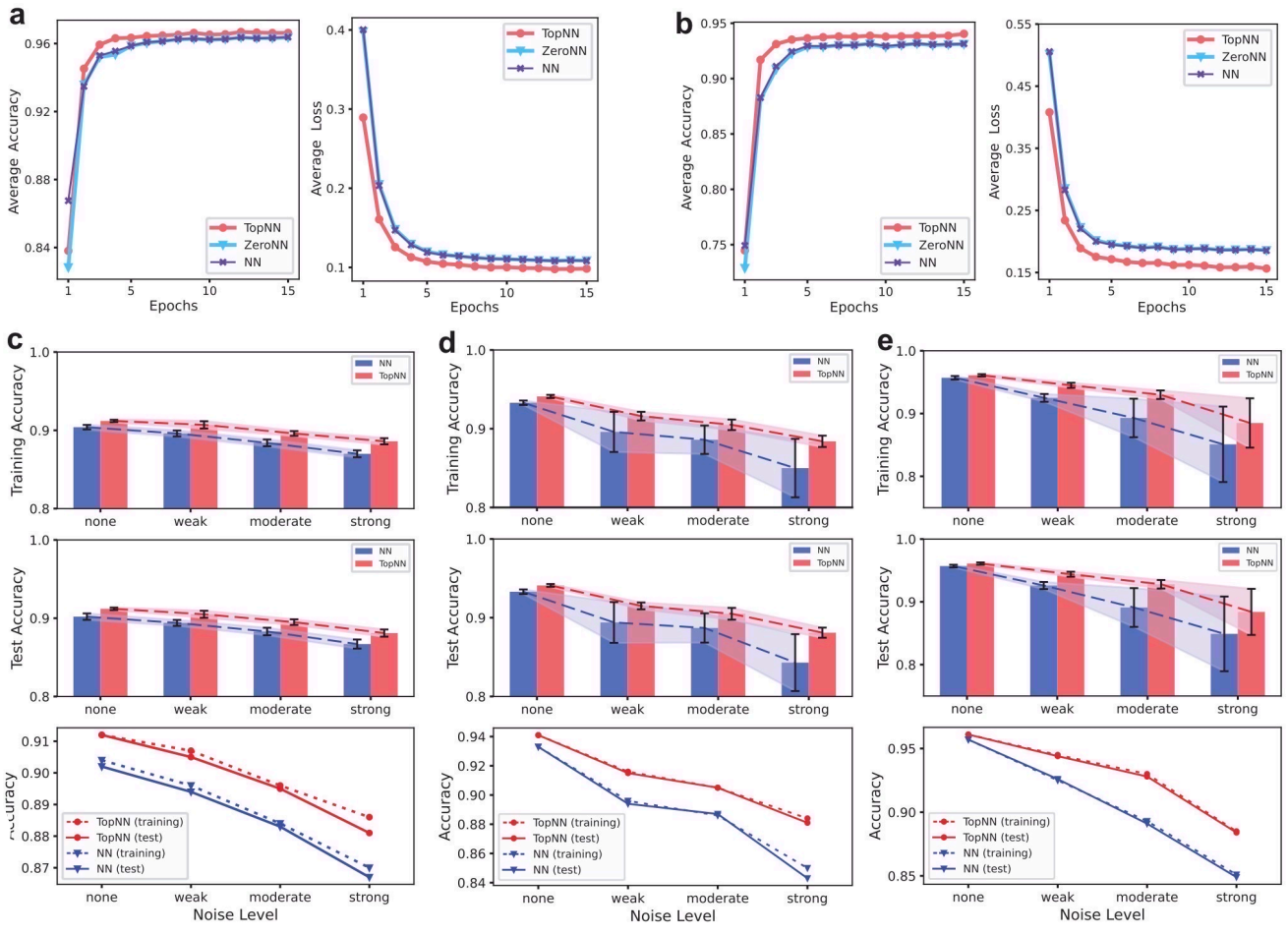


*Visual analytics of experiments with TopNN*
***c**, **d**, and **e**, Comprehensive performance comparison and noise robustness analysis of TopNN and NN based on training and test accuracy rates with the large datasets ALLSSTAR, LJSpeech, and TIMIT, respectively.*

# Topology-enhanced neural networks

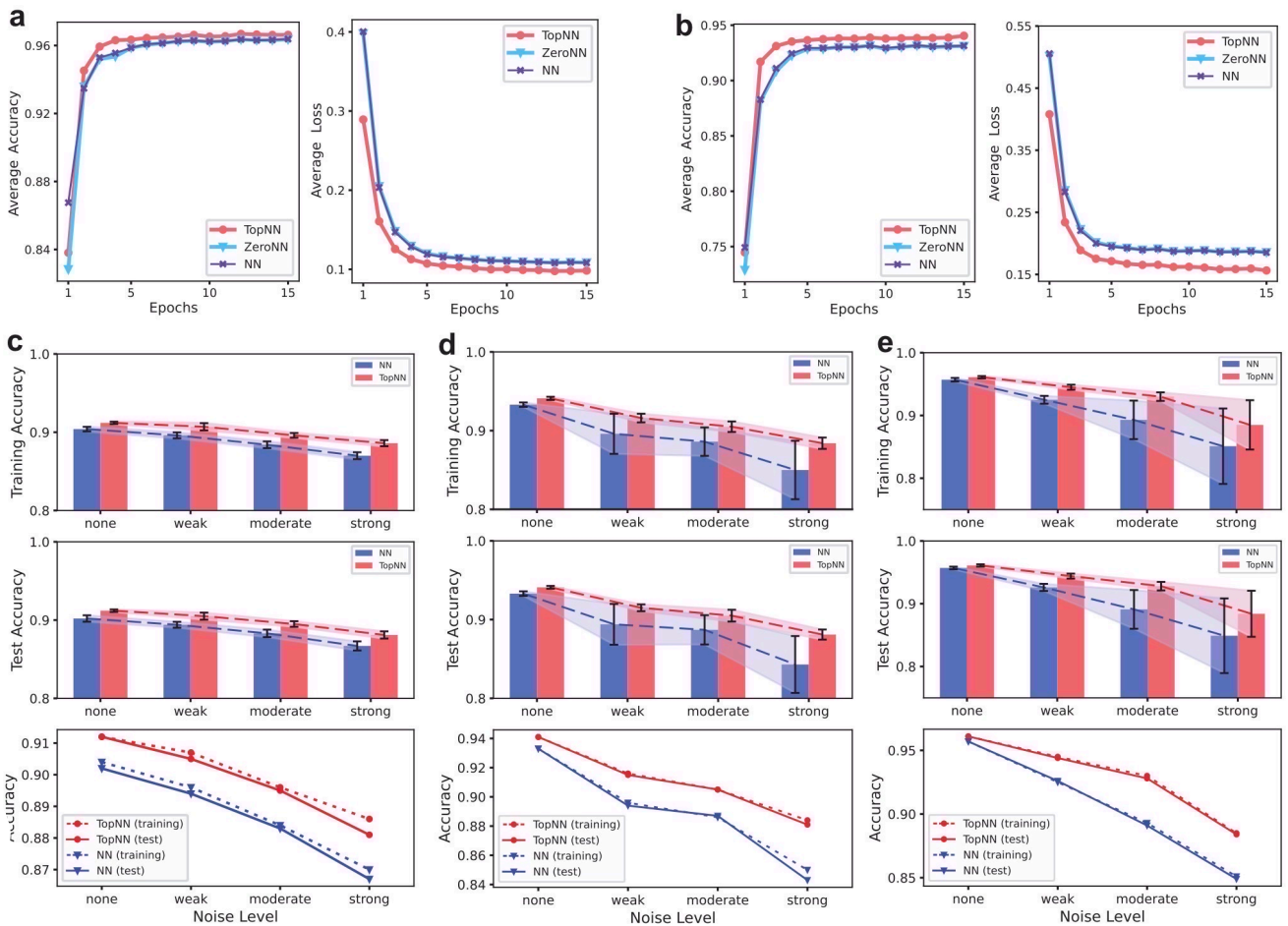


*Visual analytics of experiments with TopNN*
***c**, **d**, and **e**, Comprehensive performance comparison and noise robustness analysis of TopNN and NN based on training and test accuracy rates with the large datasets ALLSSTAR, LJSpeech, and TIMIT, respectively. Noise levels include none, weak (SNR = 10dB), moderate (SNR = 5dB), and strong (SNR = 0dB).*

# Topology-enhanced neural networks

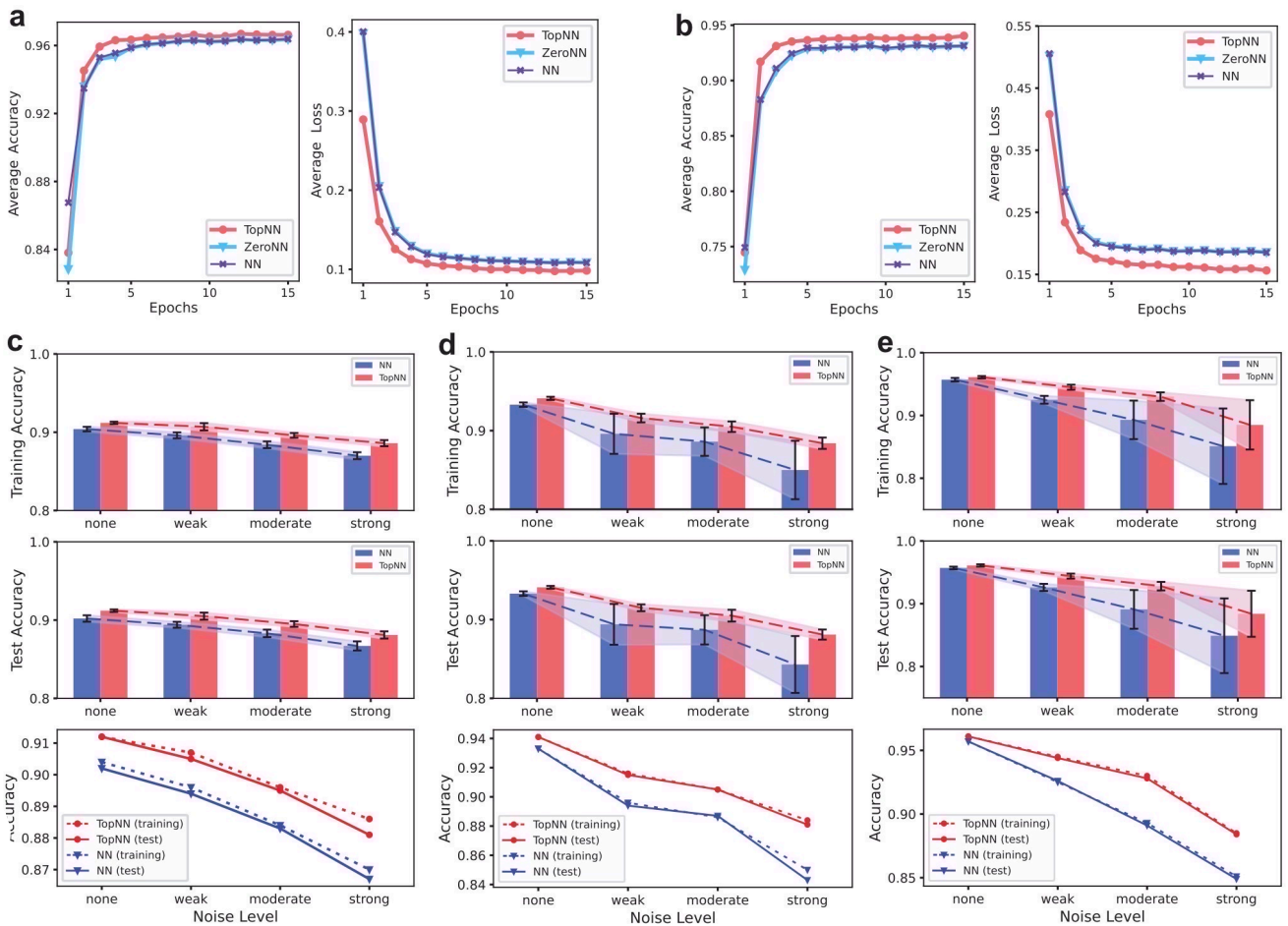


*Visual analytics of experiments with TopNN*
***c**, **d**, and **e**, Comprehensive performance comparison and noise robustness analysis of TopNN and NN based on training and test accuracy rates with the large datasets ALLSSTAR, LJSpeech, and TIMIT, respectively. Noise levels include none, weak (SNR = 10dB), moderate (SNR = 5dB), and strong (SNR = 0dB). In all three figures, TopNN achieves higher accuracy and is more robust against noise than NN.*

## Topology-informed convolution kernels for speech recognition

We defined a notion of *contrast* for 3 x 3 convolution kernels that process spectrograms, and introduced rigid constraints (unit norm and zero-sum of column vectors) to define a space *V* of kernels.

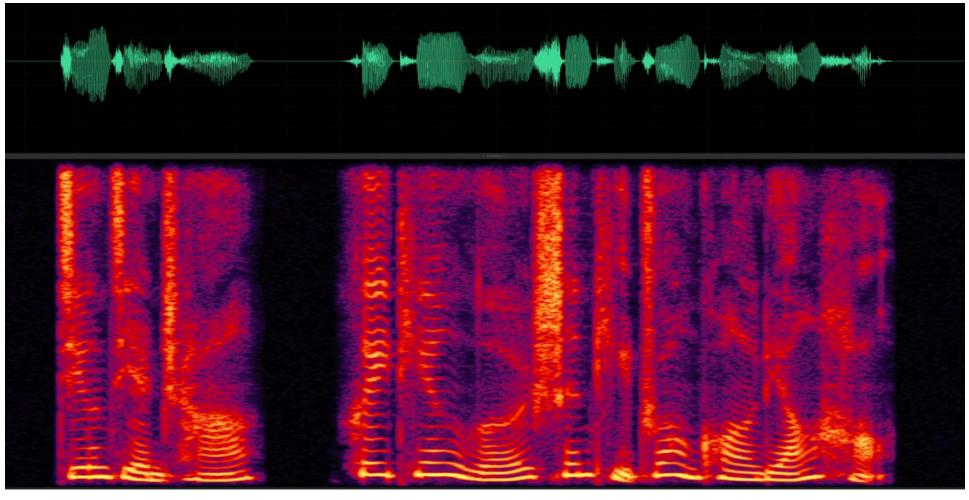

## Topology-informed convolution kernels for speech recognition

We defined a notion of *contrast* for 3 x 3 convolution kernels that process spectrograms, and introduced rigid constraints (unit norm and zero-sum of column vectors) to define a space $V$ of kernels. We showed that $V$ is homeomorphic to $S^5$ and that the natural SO(3)-action on $V$ induces a quotient space $B$ that is homeomorphic to a disk $D^2$.

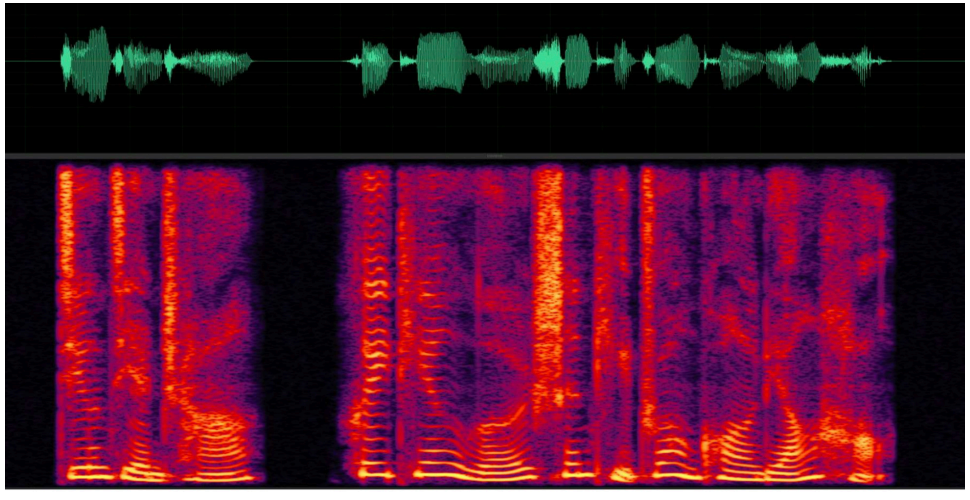

## Topology-informed convolution kernels for speech recognition

We defined a notion of *contrast* for 3 x 3 convolution kernels that process spectrograms, and introduced rigid constraints (unit norm and zero-sum of column vectors) to define a space $V$ of kernels. We showed that $V$ is homeomorphic to $S^5$ and that the natural SO(3)-action on $V$ induces a quotient space $B$ that is homeomorphic to a disk $D^2$. We then defined untrained Orthogonal Filter (OF) layer with convolution kernels informed by this topology.

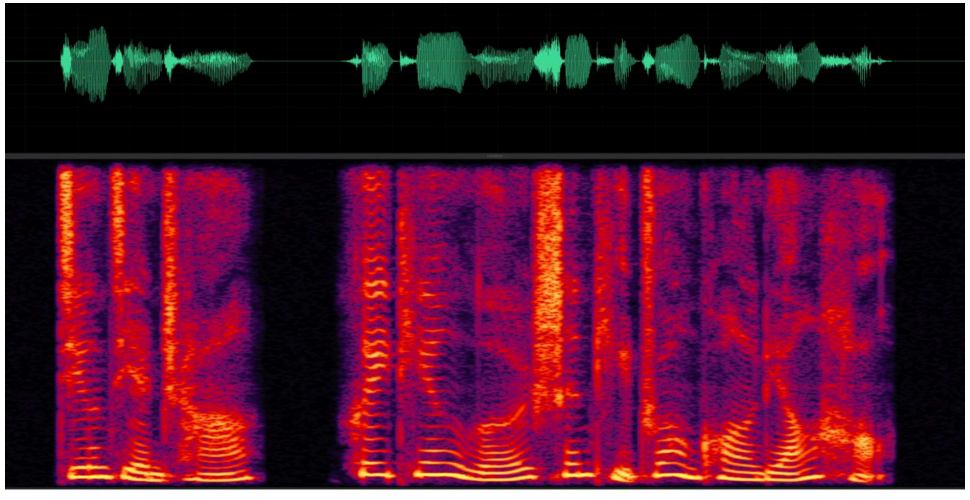

# Topology-informed convolution kernels for speech recognition

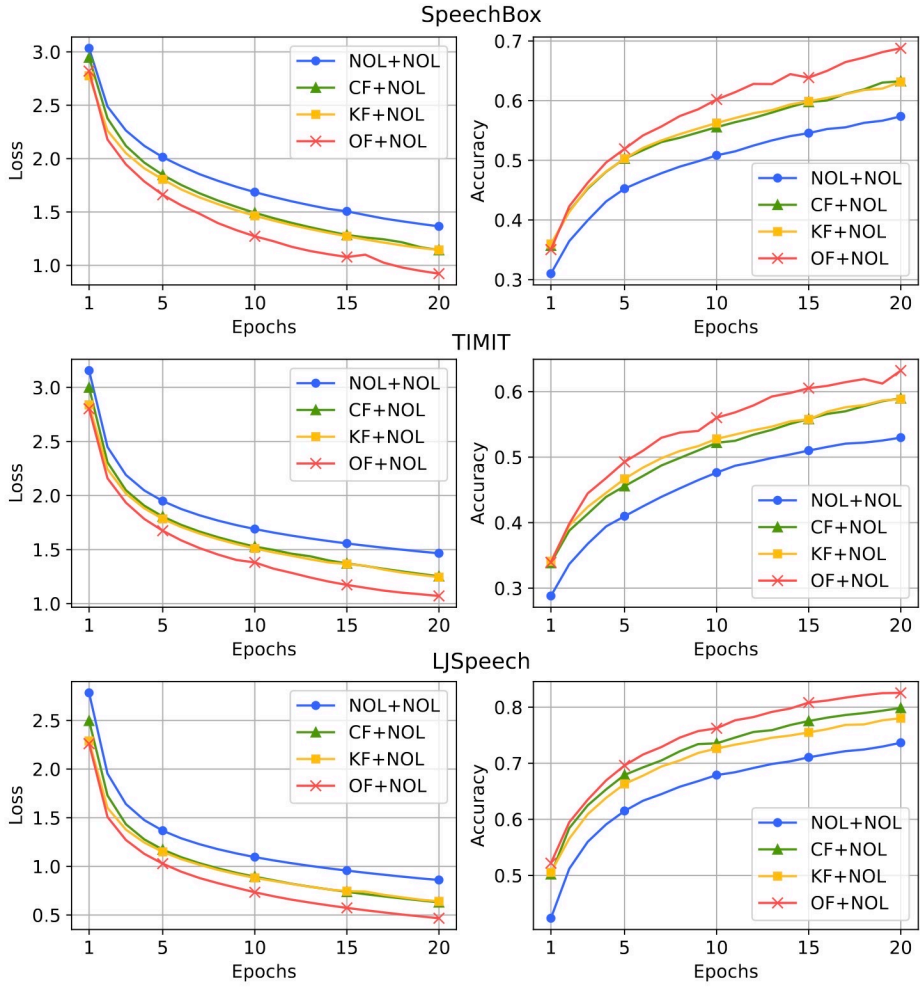


*Comparisons of normal (NOL), Love, Filippenko, Maroulas, & Carlsson's circle filter (CF) and Klein-bottle filter (KF), and our orthogonal filter (OF) convolutional layers for phoneme classification tasks via loss and accuracy on datasets SpeechBox, TIMIT, and LJSpeech*

# Topology-informed convolution kernels for speech recognition

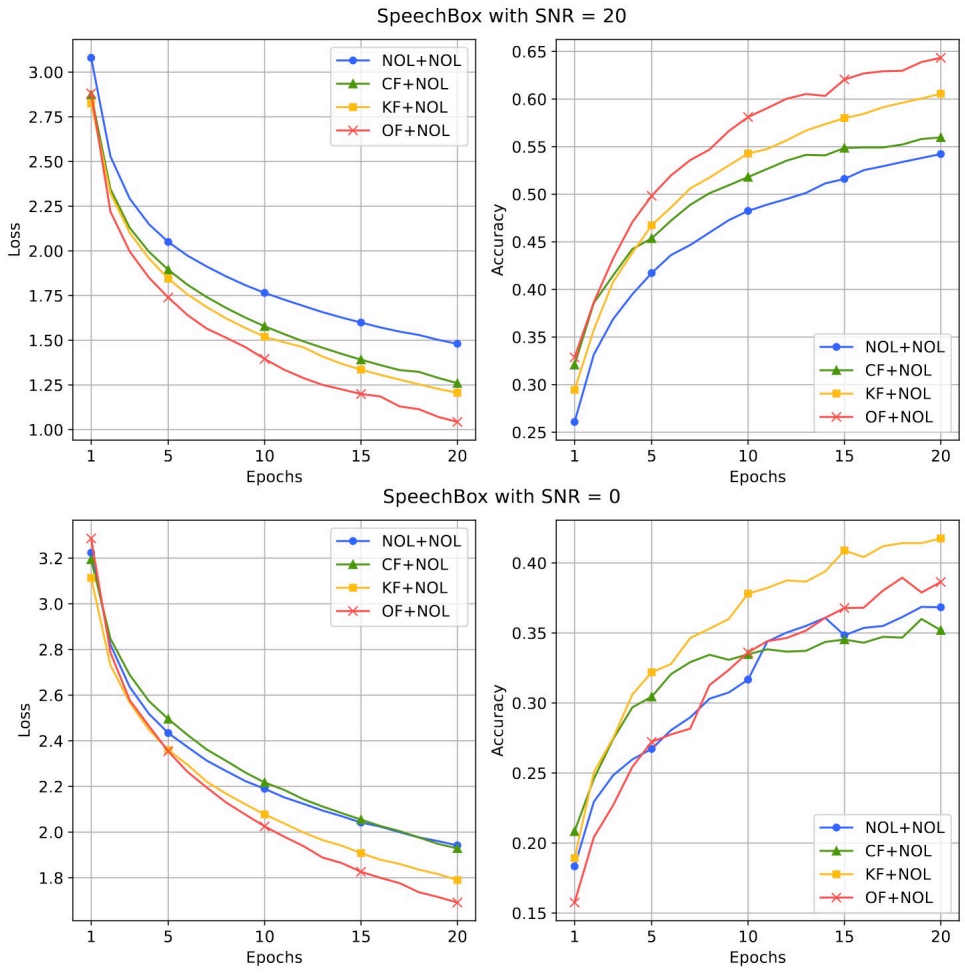


*Comparisons with noise added*
*Our proposed OF layer enables superior performance in phoneme recognition, particularly in low-noise scenarios.*

# Topology-informed convolution kernels for speech recognition

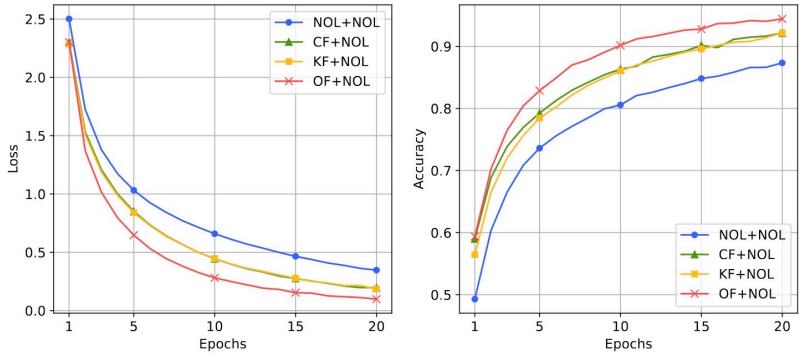


*Comparison for word classification on SpeechCommands*

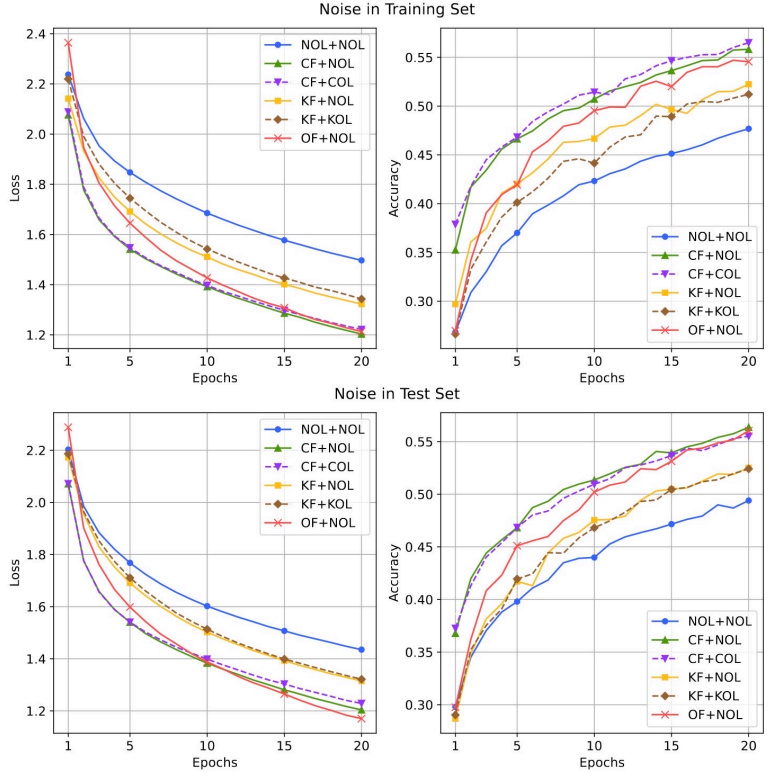


*Comparisons for image classification on CIFAR10*

## Outlook

**Questions:**

- Will deep learning speech (and audio) signals artificially, with topological input, help understand the mechanism of human auditory perception?

## Outlook

**Questions:**

- Will deep learning speech (and audio) signals artificially, with topological input, help understand the mechanism of human auditory perception?

- Analogous experiments with A1 through computational topology?

## Outlook

**Questions:**

- Will deep learning speech (and audio) signals artificially, with topological input, help understand the mechanism of human auditory perception?
- Analogous experiments with A1 through computational topology?
- Further experiments and modeling with V1?

## Outlook

**Questions:**

- Will deep learning speech (and audio) signals artificially, with topological input, help understand the mechanism of human auditory perception?
- Analogous experiments with A1 through computational topology?
- Further experiments and modeling with V1? Topological robustness vs. visual plasticity?

## Outlook

**Questions:**

- Will deep learning speech (and audio) signals artificially, with topological input, help understand the mechanism of human auditory perception?
- Analogous experiments with A1 through computational topology?
- Further experiments and modeling with V1? Topological robustness vs. visual plasticity?

**Related work:**


- Chen, Lin, & Yan, *The Gestalt computational model by persistent homology*, **Vision Research** 2025.

## Outlook

**Questions:**

- Will deep learning speech (and audio) signals artificially, with topological input, help understand the mechanism of human auditory perception?
- Analogous experiments with A1 through computational topology?
- Further experiments and modeling with V1? Topological robustness vs. visual plasticity?

**Related work:**


- Chen, Lin, & Yan, *The Gestalt computational model by persistent homology*, **Vision Research** 2025.
- Reise, Fernández [https://ximenafernandez.github.io], Dominguez, & Harrington, *Topological fingerprints for audio identification*, **SIAM Journal on Mathematics of Data Science** 2024.

*Thank you.*